A Physiological Role for Hypothalamic Proopiomelanocortin in the Intrinsic Regulation of Locomotor Activity and Stress

By

Jessica Michelle Adams

A dissertation submitted in partial fulfillment
of the requirements for the degree of
Doctor of Philosophy
(Neuroscience)
in the University of Michigan
2015

Doctoral Committee:

Professor Malcolm J. Low, Chair
Professor Jill B. Becker
Assistant Professor David Paul Olson
Professor Leslie Satin
Professor Audrey F. Seasholtz

“It is what we know already that often prevents us from learning.”

- Claude Bernard

In memory of Veronica Otero-Corchon

Acknowledgements

I would first like to acknowledge and thank my mentor, Malcolm Low. He has shown me by his example how to be a thoughtful scientist, created a laboratory environment in which I could flourish, and given me the freedom to pursue the questions that I was interested in. Furthermore, he has always been a patient teacher and has taught me a great deal about how to craft meaningful experiments and carefully interpret results.

I would also like to thank the many members of the lab past and present. Veronica Oter-Corchon, Daniel Lam, Miho Yamashita, Aaron Mercer, Kavaljit Chhabra, Graham Jones, and Elisa Na were always available as a sounding board for ideas, to help troubleshoot techniques, or to suggest new experiments. I am also especially indebted to Jared Goldberg, Courtney Attard and Eva Yokosawa for all of the mice breeding and colony maintenance work that they did for me. I want to extend special thanks to Samantha Spierling, a very talented undergraduate who worked with me for 2 years and some of whose work is presented here.

I have been lucky enough to have other mentors in addition to Malcolm, and I would like to thank each member of my dissertation committee as well as the director of the Neuroscience Program, Ed Stuenkel, for their encouragement and advice.

Finally, I want to thank my parents and my sister, my boyfriend and all of my friends. You have returned me to sanity again and again.

Table of Contents

List of Tables

List of Figures

Chapter 1: Introduction

Proopiomelanocortin (POMC) is a pre-propeptide encoded by the *Pomc* gene, which is expressed predominantly in the hypothalamus and pituitary (1-3). The POMC propeptide is subsequently cleaved by processing enzymes in a tissue-specific manner, yielding multiple bioactive peptides (Figure 1.1). In anterior pituitary corticotrophs, POMC is processed into adrenocorticotropic hormone (ACTH) and released into the bloodstream where it regulates glucocorticoid (GC) production and release from the adrenal glands (2,3). Peripheral ACTH is also critical for proper adrenal gland development and is a major signaling molecule in the hypothalamic-pituitary-adrenal (HPA) stress axis (4). In the hypothalamus, *Pomc* is expressed in a small group of ~3,000 neurons in the arcuate nucleus (Arc) (5). There, the POMC propeptide is processed into ACTH, as well as α- and γ-melanocyte stimulating hormone (MSH), and the opioid β-endorphin (2,3). Together, ACTH and α- and γ-MSH are referred to as the melanocortins, as these peptides activate downstream melanocortin receptors. There are five known melanocortin receptors, Mc1r-Mc5r, which are all G-protein coupled receptors. Mc1r is expressed in the skin and is involved in pigmentation, and Mc5r is expressed in exocrine glands. Mc2r, also known as the ACTH receptor, is expressed in the adrenal cortex where it is necessary for ACTH signaling in the HPA axis. Mc3r and Mc4r are primarily expressed in the central nervous system (CNS) (6,7).

The *Pomc*, *Mc3r*, and *Mc4r* genes are conserved in all major groups of jawed vertebrates, and POMC-expressing neuronal cell bodies are restricted to the hypothalamus and brain stem in

cartilaginous and bony fishes as well as tetrapods including mammals (8,9). Such strong evolutionary conservation highlights the important physiological role of POMC. Due to their proximity to the median eminence, POMC neurons are uniquely situated to receive peripheral signals via blood-borne molecules (10,11). Indeed, the discovery that direct injection of melanocortins into the brain inhibited both spontaneous and drug-induced feeding in rats (12) suggested that POMC neurons may sense and respond to signals of nutritional status. In the past 30 years, a great deal of research has focused on unraveling how melanocortins control both food intake and energy expenditure. Immense progress has been made in this field, and has been extensively reviewed elsewhere (6,13-16). Some of these studies have revealed that POMC plays a critical role in physiological processes other than energy balance, including the cardiovascular and immune systems (17,18). Here, I will briefly describe the classical working model of the melanocortin system as well as highlight some of the exciting tools, techniques and ideas that have been generated recently to study the physiological role of POMC in the brain (Section I). I will then provide a detailed discussion of two slightly less well-studied roles of CNS melanocortins: Regulation of locomotor activity (Section II) and interaction with the HPA stress axis (Section III).

I. The neural melanocortin system

A. Classical model

In addition to POMC, an endogenous melanocortin receptor competitive antagonist, agouti-related peptide (AGRP), is produced in a separate small group of adjacent neurons in the

Arc (19,20). Collectively, POMC and AGRP neurons, their projecting fibers, target neurons expressing Mc3r or Mc4r, and a second small group of *Pomc*-expressing neurons in the brain stem, define the neural melanocortin system (21,22) (Figure 1.2). Through a combination of studies using pharmacological manipulation, genetic knockout mouse models, and electrophysiological recordings, an early model of how the melanocortin system regulates energy homeostasis was formed.

The early "yin/yang" model suggested that feeding and energy expenditure are directly controlled via two peptides, α-MSH and AGRP, acting on melanocortin receptors throughout the brain. POMC and AGRP neurons send projections to cells expressing either Mc3r, important for energy partitioning, or Mc4r, controlling food intake and energy expenditure. α-MSH-induced activation of melanocortin receptors decreases food intake and increases energy expenditure, and AGRP antagonizes these effects. *Pomc*-KO and *Mc4r*-KO mice are morbidly obese and hyperphagic, whereas *Mc3r*-KO mice have increased fat mass, and *Agrp*-KO mice have no metabolic phenotype (23-29).

Circulating nutrients and hormones can both directly and indirectly modulate these neurons. Early studies focused on leptin, an adipocyte-derived hormone. Circulating leptin levels are a direct proxy for an animal's energy stores, and leptin activates POMC neurons and increases *Pomc* mRNA levels while inhibiting AGRP neurons and decreasing *Agrp* mRNA levels directly via the long form of the leptin receptor (LepRb), which is expressed on both cell types (5,30-35). Leptin signaling also depolarizes POMC neurons via activation of TRPC channels (36). Furthermore, leptin depolarizes POMC neurons through reduction of an inhibitory tone from AGRP neurons conveyed by both neuropeptide Y (NPY) and γ-aminobutyric acid

(GABA) (5). In addition to leptin, POMC and AGRP neurons are now known to also respond to insulin, estrogen, ghrelin, glucose and fatty acids in an opposing manner (37-46).

Conditional genetic knockouts have been generated to further parse how the two networks of melanocortin neurons drive energy homeostasis. *Pomc*-Cre and *Agrp*-Cre mice were generated and crossed with strains engineered to contain floxed alleles of other genes of interest, resulting in specific deletion or re-expression of that gene in only POMC or AGRP neurons (47,48). These studies have begun to identify how specific hormones directly affect each cell population and, for example, suggested a direct role for POMC neurons in the anorectic response to leptin, estrogen, and serotonin (47,49,50). However, these results should be interpreted with caution as it was also recently discovered that *Pomc* is expressed transiently during development in neurons that later go on to become AGRP or kisspeptin neurons, and thus *Pomc*-Cre may be active during development in these cells (51-53).

B. Recent discoveries

The dual peptide model of melanocortin action has held up well, and recent technological advances have yielded further exciting findings [for review, see (54-56)]. *In vivo* calcium imaging has shown that POMC and AGRP neurons respond rapidly to sensory food cues even before ingestion, and that the response varies with nutritional state and depends on the palatability of the food presented (57,58). Thus, in addition to long-term integration of nutritional signals and control of homeostasis, the melanocortin system appears to be dynamically regulated by sensory stimuli and may be directly involved in food-seeking behavior.

POMC and AGRP neurons usually, but not always, project to the same nuclei, suggesting a possible role for each peptide independently of the other (59,60). For years there has been disagreement in the field as to whether Mc4r is constitutively active and therefore if AGRP acts as a competitive antagonist or an inverse agonist at this receptor (61). The signaling cascade downstream of Mc4r activation has now been more extensively studied. Recent experiments suggest that not only can Mc4r couple to multiple G-proteins and therefore signal via a wide variety of downstream signaling cascades, it can also act independently of G-proteins to modulate the gating of potassium channels. Furthermore, AGRP can selectively activate specific pathways and act as a biased agonist (62,63).

Agrp-KO mice have no metabolic phenotype, as mentioned above, but postnatal ablation of AGRP neurons resulted in rapid starvation (29,64,65), which initially suggested developmental compensation in the knockout model. Surprisingly, though, an additional and clever series of neuronal ablation studies identified that the starvation was independent of melanocortin signaling and was mediated in part by the fast neurotransmitter GABA (66-68). Further, opto-and chemo-genetic activation of AGRP neurons led to immediate and voracious hyperphagia, also independent of melanocortin signaling (69-71). Additional genetic and pharmacological experiments revealed that GABA and NPY released by AGRP neurons each play a critical role in this immediate feeding behavior, whereas AGRP can mediate feeding on a longer time scale (71-73).

Opto- and chemogenetic activation of POMC neurons inhibited food intake as predicted. Although based on pharmacological experiments this effect might be expected to occur within a few hours, constant activation of POMC neurons for 24 hours was necessary before there was any measurable difference from controls in food intake or body weight (69,74). Conversely,

chemogenetic inhibition of POMC neurons did not measurably increase food intake until it had occurred for 24 hours (72). The decrease in food intake upon POMC neuron activation was likely due to the release of POMC-derived peptides and the activation of melanocortin receptors, since no change in food intake was observed when the experiments were performed in mice overexpressing a melanocortin antagonist (69). POMC neurons can also express glutamate or GABA but the functional significance is not yet clear (75,76). Preliminary studies have indicated that there are two types of neuromodulator release sites, one that releases a combination of neurotransmitters and peptides at conventional synapses and other extra-synaptic sites that only release peptides (77).

In light of these exciting new discoveries, it is worth re-examining what has been revealed about the neural melanocortin system's roles in non-feeding behavior as well. In this chapter, I will review studies in the literature using genetic knockout models and/or administration of melanocortin pharmacological agents that have implicated the neural melanocortin system in the regulation of locomotor activity and the HPA axis.

II. Locomotor activity

Energy from consumed food is either used, stored or excreted, and the balance between caloric intake and energy expenditure determines body weight. The three main components of energy expenditure are basal metabolic rate, the thermic effect of food, and physical activity (78). Physical activity levels vary greatly between individuals and are to some extent biologically determined, although many of the genes and pathways involved have not yet been identified (79).

Physical activity can be divided into two categories: Obligatory for survival, such as searching for food and avoiding predators, or discretionary. According to a broader definition, obligatory activity falls under "spontaneous" or "nonexercise" activities that are associated with daily life, whereas discretionary activities are often considered voluntary exercise (80). In humans, many activities lie along a spectrum between these two categories and fall into a gray area that makes categorization difficult.

There is a tight negative relationship between body weight and activity levels in both humans and rodents (78,81). Often, obesity is assumed to be secondary to low physical activity levels, and increasing voluntary exercise is a common first approach to losing body weight in obese individuals. However, compensatory decreases in spontaneous activity can occur upon increased levels of voluntary exercise, as total energy expenditure varies little day-to-day whether or not a person exercises (80). On the other hand, it is equally possible that low physical activity levels are a result of obesity. Although both spontaneous and voluntary activity levels are believed to be controlled by multifaceted and likely extensively overlapping networks in the brain, very little is understood about either. Furthermore, the relationship between obesity and activity levels is complex and deserves further study, making the use of animal models imperative.

Laboratory rodents live in a tightly controlled environment with access to only certain types of behavior, and the definitions of spontaneous versus voluntary activities have become tied to specific measurement protocols. Standard rodent housing affords the opportunity for only spontaneous activity, which is measured in a home cage or home cage-like environment using infrared beams, force plates or video analysis, and includes locomotor activity as well as grooming and rearing (78). Differences in levels of spontaneous home cage activity are believed

to be representative of intrinsic differences between individuals in the tendency to be physically active. On the other hand, introduction of a running wheel into the standard cage has been argued to be representative of voluntary exercise (80). Although spontaneous and voluntary physical activity levels, as thus defined, tend to positively correlate across strains, treatment groups and genotypes, there is ample evidence that access to a running wheel amplifies activity levels and engages reward pathways (82).

There are some reports that neural circuits involved in feeding can also regulate physical activity levels. In keeping with the catabolic and anabolic roles of POMC and AGRP, respectively, one might hypothesize that POMC-derived peptides would increase activity levels whereas AGRP would decrease them. Here, I will review the literature suggesting a role for the neural melanocortin system in control of both spontaneous as well as voluntary activity levels. Furthermore, caloric restriction induces a unique behavior termed food anticipatory activity whereby an animal displays increased locomotor behavior immediately before it receives a daily allotment of food, and the melanocortin system has also been implicated in this behavior.

A. Spontaneous locomotor activity

Pharmacological studies in rats have in general supported the suggestion that POMC peptides activate, whereas AGRP inhibits, spontaneous physical activity levels. Acute i.c.v. injection of either α-MSH or ACTH dose-dependently increased home-cage grooming, locomotion and rearing in male rats for up to 9 hours (83). On the other hand, a single i.c.v. injection of AGRP decreased spontaneous home cage locomotion in male rats for up to three

days (84). Chronic i.c.v. treatment with a synthetic melanocortin antagonist similarly decreased spontaneous locomotion in male rats (85).

Evidence from genetic knockout models has generally supported these conclusions, but interpretation has been difficult because of the obesity in these models. Thus, *Pomc*-KO mice may be expected to have decreased locomotor activity as a direct result of the lack of POMC, but they are also morbidly obese which may itself affect activity levels. Separating the primary genetic insult from resulting obesity is not a simple task. Indeed, obese mice of both sexes lacking *Pomc* specifically in the Arc exhibited markedly decreased spontaneous locomotion which was completely normalized by reactivation of the *Pomc* gene in adulthood, concomitant with a return to normal body weight (34,86). Postnatal ablation of ArcPOMC neurons also significantly reduced spontaneous locomotor activity in association with increased body weight (74). In both of these studies, changes in activity levels were assumed to be secondary to body weight changes but this was not directly studied.

Several strains of *Mc3r*-KO mice have been generated, all of which have normal body weight but increased adiposity. In the first strain described, males were found to have normal spontaneous home cage locomotor activity, whereas females showed somewhat decreased activity (27). In the next strain generated, only males were characterized, and they exhibited normal spontaneous home cage locomotor activity (87,88). In a more recently described reactivateable *Mc3r*-KO mouse, the knockouts showed a slight decrease in spontaneous locomotor activity, but sex was not reported (89). *Mc4r*-KO mice are obese and both sexes exhibited decreased spontaneous locomotor activity (28,90). Interestingly, there is one report that young, pre-obese male *Mc4r*-KO mice had the same spontaneous locomotor activity as wildtype controls, suggesting that in this model, low locomotor activity may be secondary to obesity (91).

Agrp-KO mice of both sexes were initially described as having normal spontaneous locomotor activity (29), but further investigation revealed a late-onset hyperlocomotion in male *Agrp*-KO mice associated with a lean phenotype (92). This phenotype agrees with the pharmacological studies suggesting that AGRP inhibits spontaneous locomotion. In contrast, chemogenetic activation of AGRP neurons significantly increased spontaneous locomotor activity in mice of both sexes, but only in the fasted state (70,93). This effect could be mediated by NPY or GABA rather than AGRP, as one study suggested (93), or it could indicate that the role of the neural melanocortin system in control of locomotor activity may be differentially regulated by nutritional state.

Taken together, the reports of home cage activity of the knockout mouse lines described above suggest that the melanocortin system may not play a primary role in spontaneous locomotor levels, but that the obesity in these models may lead to decreased activity. However, this conclusion has not been thoroughly tested and there is evidence that the melanocortin system does regulate activity in other genetic mouse strains. O*b/ob* mice are a unique model in that they are morbidly obese but the brain perceives a state of starvation due to lack of leptin. These mice as well as mice lacking leptin receptor (LepR) displayed low spontaneous home cage locomotion. Systemic or i.c.v. infusion of leptin dose-dependently increased, although did not totally rescue, home cage activity of male *ob/ob* mice, but did not affect activity in wildtype controls (94,95). The effect of leptin on locomotor activity in *ob/ob* mice in these experiments occurred prior to any measurable decrease in body weight and suggested a primary role for leptin in the central control of locomotion in an otherwise hypoleptinemic animal.

Unilateral virus-mediated reactivation of LepR in the Arc of male *Lepr*-null mice almost completely normalized spontaneous locomotor activity while having little impact on body weight

and food intake (96). Genetic restoration of LepR limited to POMC neurons of male mice had the same phenotypic effect as whole Arc rescue, suggesting that POMC neurons in the Arc are sufficient for this leptin-induced increase of locomotor activity (97). However, as mentioned above, the *Pomc*-Cre mouse line used to generate these results has been shown to transiently express *Pomc* during development in neurons that differentiate into non-POMC neurons, so these results should be interpreted with caution. A study using a complementary approach suggested that Arc AGRP neurons are also leptin-responsive locomotion-inducing neurons. In this study, LepR was deleted in male mice only from AGRP neurons or in both POMC and AGRP neurons, and a similar decrease in home cage locomotor activity was observed in both transgenic groups (98). Conversely, mice with constitutive activation of Stat3 signaling (one of the major downstream pathways of LepR) specifically in AGRP neurons, but not POMC neurons, showed increased spontaneous locomotor activity (99). In this study sex was not reported.

Together these data suggest that leptin signaling onto either POMC or AGRP neurons may lead to increased spontaneous locomotor activity in some mouse models independent of changes in body weight. Signals other than leptin may also mediate spontaneous physical activity levels via the melanocortin system. For example, male mice lacking insulin receptor in the whole hypothalamus are lean and hypolocomotive. Re-expression of insulin receptor in only POMC neurons, but not AGRP neurons, rescued the locomotor activity levels of these mice (100). Possible involvement of the melanocortin system in the locomotor effects of other peripheral and central signals is still being explored. However, as alluded to earlier, exploring these pathways by utilizing knockout mice should be carefully controlled and interpreted, as deletion of a major nutritional signal will likely change the perceived nutritional status of the animal and thus could affect behavioral responses.

B. Voluntary wheel running activity

Although some controversy surrounds the use of running wheels as a rodent model for voluntary exercise, it is currently the best model available. Most laboratory mice and rats readily run on wheels provided in the home cage, although some strains show more intrinsic running activity than others. As mentioned above, spontaneous home cage locomotion and amount of running wheel activity are roughly correlated across strains. In some animals, the introduction of a running wheel can intensify total activity levels as evidenced by increased food intake or the development of a negative energy balance. In others, a compensatory decrease in spontaneous home cage activity can occur and total energy expended in physical activity remains unchanged (101). There is a huge level of individual, sex, strain and species variability in the behavioral response to a running wheel.

Although some argue that wheel running may be a stereotypical behavior induced by the unnatural environment of laboratory cages, there is extensive evidence that rodents find wheel running rewarding. Indeed, even wild mice ran extensively on wheels provided in their natural environment (102). Rats showed conditioned place preference for the environment paired with a previous running episode and they lever pressed for access to a wheel. Wheel running has been shown to decrease motivation for food and drugs such as amphetamines, while conversely food deprivation increased lever pressing for both cocaine and access to a running wheel. Additionally, running in a wheel is known to activate neural circuitry associated with reward. Therefore, running wheel activity, though correlated with spontaneous activity, likely does not reflect solely the tendency to be physically active but is also related to motivation and reward. Intriguingly, some of the same brain regions seem to be involved in controlling both appetite and

reward, and these areas are activated by wheel running. The neurobiological mechanisms regulating running wheel activity levels are almost completely unknown, but the dopaminergic system tops the list of candidates (103).

POMC and AGRP neurons are known to lie upstream of various regions of the dopaminergic system, including the ventral tegmental area and the nucleus accumbens, which abundantly express Mc3r and Mc4r, respectively (104,105). As such, the melanocortin system has been suggested to play a role in the rewarding effects of not only food but also alcohol and drugs of abuse. That body of literature is outside of the scope of this review, but in general, POMC peptides are believed to decrease the rewarding value of food and alcohol reward but increase drug reward whereas AGRP does the opposite. However, there are reports published that conflict with each of these conclusions. Thus the interaction of the neural melanocortin system with the reward system is complex and likely varies for different rewarding stimuli.

To my knowledge, no groups have reported differences in running wheel behavior after acute or chronic injections of melanocortin pharmacological agents. Rather, genetic knockout models have been used. As with spontaneous home cage activity, the obesity of these models can complicate the studies. Obese, neural-specific *Pomc*-KO male mice exhibited approximately half the amount of running wheel activity as wildtype controls (106). Perplexingly, *Mc3r*-KO male mice have been described as running either the same amount as, or significantly less than, wildtype controls by the same group of researchers (26,87-89). Young, preobese *Mc4r*-KO mice of both sexes showed the same voluntary running wheel activity levels as wildtype (107). When male *Mc4r*-KO mice were housed with a running wheel from an early age, they ran the same distance as wildtype controls over the course of an 8-week study and, although still slightly heavier than wildtype, fat mass, insulin, and leptin levels were normalized (108,109).

Together these studies suggest that POMC signaling via Mc3r and/or Mc4r plays either a negligible role or no role in direct regulation of voluntary wheel running behavior, and that any decrease in running amount seen in these genetic knockout models is secondary to development of obesity. However, more complete studies need to be performed, and there is at least one piece of evidence to the contrary. Older, slightly obese male rats that were administered a viral vector overexpressing *Pomc* showed increased running wheel activity. These rats also lost weight, but the control pair-fed group of rats lost the same amount of body weight and showed no change in wheel running activity (110). Furthermore, studies of running wheel activity in mice with altered *Agrp* expression have not been reported to my knowledge.

C. Food anticipatory activity

The light-dark cycle is an important entrainment cue for behavior and physiology. Both spontaneous home cage locomotor activity and voluntary running wheel activity occur almost exclusively during the night in laboratory rodents, which are nocturnal. However, when laboratory rodents are given access to a restricted amount of food for only a few hours during the day time, a new rhythm is created. Two hallmarks of this new rhythm are food anticipatory activity (FAA), or a marked rise in locomotor activity levels 2-3 hours before presentation of food, as well as a coinciding rise in corticosterone. These new rhythms suggest the presence of a food entrainable oscillator that is independent of the light-dark oscillator.

The search for the location and mechanism of the food entrainable oscillator using lesion studies and genetic knockout models has been reviewed elsewhere (111,112). Some studies have suggested that hypothalamic regions involved in feeding and energy expenditure may also be

involved in FAA. This phenomenon has not been well-studied as it relates to the neural melanocortin system. If FAA is driven by hunger, one might argue that AGRP, being an orexigenic hormone, might increase FAA while POMC might do the opposite. Along these lines, mice lacking leptin exhibit increased FAA and administration of leptin blocks FAA (95).

To my knowledge, FAA has not been studied in genetic knockout models of either *Pomc* or *Agrp*, but *Mc4r*-KO mice have been reported to have normal FAA (87). On the other hand, and contrary to the above hypothesis, male *Mc3r*-KO mice exhibited decreased FAA as measured both by home cage activity and running wheel activity (87). These results suggest that, although melanocortin signaling is not necessary for FAA, it may play a modulatory role on its amplitude. On the other hand, further studies suggested that the decreased FAA reported in *Mc3r*-KO mice may be due to an impairment in their ability to adjust to a new schedule because FAA levels are only lower than wildtype for the first two weeks of scheduled food restriction (88,113). In this case, melanocortins may be involved only in the acquisition but not the expression of FAA.

D. Concluding remarks

In synthesizing the results of all of the above-mentioned studies, one may conclude that the neural melanocortin system likely does not play a primary role in the control of locomotor activity. However, to my mind, the lack of consistent protocols, data collection methods and data reporting methods has left this conclusion questionable. Many of the studies mentioned were not designed as thorough examinations of physical activity but merely reported locomotor activity as part of a broad panel of energy expenditure assays. Additionally, and unfortunately, researchers

have often considered home cage activity and wheel running activity interchangeably and only reported one or the other. Thus a specific change in either spontaneous or voluntary activity levels could have been overlooked. Some groups even use activity in a short time frame upon exposure to a novel environment (e.g. open field test) as representative of spontaneous activity, but behavior in these situations is more directly related to anxiety or stress, does not correlate with either spontaneous or voluntary locomotor activity levels, and was not mentioned here. Furthermore, the relationship between obesity and locomotion needs to be investigated more thoroughly.

III. Hypothalamic-pituitary-adrenal stress axis

The HPA axis is the endocrine arm of the body's response to stress, which is broadly defined as any real or perceived threat to homeostasis and encompasses a broad range of psychological and physiological stimuli. The primary mediators of the HPA response are corticotropin-releasing hormone (CRH) and arginine vasopressin (AVP), which are synthesized in the paraventricular nucleus of the hypothalamus (PVH) (Figure 1.3). CRH and AVP are released from axon terminals in the median eminence, enter the hypophyseal portal system and bind to CRH receptor 1 and AVP receptor 1b, respectively, on corticotrophs in the anterior pituitary. CRH and AVP act synergistically to stimulate production and release of ACTH, which enters the bloodstream and binds to melanocortin 2 receptors (Mc2r) on the adrenal cortex. Mc2r activation stimulates synthesis and release of glucocorticoids (GCs), which act on glucocorticoid receptors (GR) throughout the body to increase energy mobilization, inhibit growth, suppress the immune and reproductive systems, and potentiate the other arm of the stress response mediated

by the sympathetic nervous system (114). In addition to its important role in the stress response, the HPA axis is diurnally regulated whereby a daily rise in GCs occurs at the beginning of the active cycle. At low concentrations, such as in the diurnal nadir, GCs can also signal via the high-affinity mineralocorticoid receptor (MR).

Critically, dysregulation of the HPA axis, usually presenting as a chronic elevation in GCs, is associated with neuropsychiatric diseases such as depression as well as diabetes and metabolic syndrome (115,116). GCs provide negative feedback to the HPA axis at the level of the pituitary as well as directly at the PVH (117). Additionally, the PVH receives and integrates signals from various brain regions, including the brainstem, limbic regions such as the amygdala and hippocampus, as well as other hypothalamic nuclei. Some of these sites stimulate the PVH upon exposure to a stressor while some mediate GC-regulated negative feedback (118,119). The complex system controlling HPA activation can become dysregulated due to increased central drive or decreased negative feedback, which are difficult if not impossible to distinguish from each other. Although there are several lines of evidence suggesting extensive crosstalk of the neural melanocortin system and the HPA axis, results have often been contradictory or difficult to interpret and the precise interaction between the two systems has not been defined.

A. The melanocortin system is downstream of the HPA axis

Stress is believed to affect feeding behavior in two distinct ways, and the neural melanocortin system has been implicated in both. An acute stressor results in a rapid decrease in food intake which is known as stress-induced anorexia, whereas chronically elevated GCs are believed to induce food intake, specifically of palatable or high-energy food (120,121).

1. Stress-induced anorexia

Pharmacological studies have indicated that CRH signaling in the brain is necessary for stress-induced anorexia (122), and several lines of evidence suggest that the neural melanocortin system may be downstream. Within 30 minutes of onset of a stressor, POMC neurons were activated and *Pomc* mRNA levels were increased (123-125). Furthermore, administration of a melanocortin receptor antagonist before the stressor ameliorated or eliminated stress-induced anorexia, suggesting a role for the melanocortins in this phenomenon (123,126-128). There are known direct projections from the PVH to ArcPOMC neurons as well as known relays through other candidate nuclei such as the ventromedial hypothalamus (VMH) (60). Glutamatergic neurons in the VMH express CRH receptors and project to the Arc. Injection with a CRH agonist into the VMH increased *Pomc* mRNA in the Arc and decreased feeding, suggesting a possible indirect route by which POMC neurons are activated by stress (129).

However, these data are merely correlative. If melanocortin signaling was necessary for stress-induced anorexia, one would predict that genetic models of melanocortin deficiency would not exhibit the anorectic response. Contrary to this hypothesis, mice that ectopically express the melanocortin receptor antagonist agouti in the brain, although in general are hyperphagic, exhibit an exaggerated anorectic response to stress (130). In agreement with this, we have observed the same phenomenon in mice that lack *Pomc* specifically from the Arc (unpublished observation). Thus the role of melanocortins in stress-induced anorexia is still controversial and under investigation.

2. Glucocorticoid-induced feeding

A direct orexigenic role for GCs is supported by reports that adrenalectomy induces anorexia (131) whereas sub-chronic i.c.v. infusion of GCs into adrenally intact animals increases food intake and body weight (132). Indeed, many genetic and pharmacologically-induced rodent models of obesity exhibit marked hypercorticosteronemia (133). One of the most extensively-studied examples is the *ob/ob* mouse, which genetically lacks the hormone leptin (134). *Ob/ob* mice have increased basal and stress-induced plasma corticosterone (135-137), and adrenalectomy normalizes food intake and reduces body weight (138,139). Similar studies on other obesity models have led to the conclusion that GCs are necessary for these obesity syndromes (140,141).

A role for the neural melanocortin system in GC-induced feeding has been suggested. *Ob/ob* mice have elevated *Agrp* mRNA levels, which are reduced by adrenalectomy (138). Transgenic mice overexpressing *Crh* exhibit increased GCs and food intake associated with increased *Agrp* levels (142). In adrenal-deficient mice and following adrenalectomy in rats, hypothalamic *Agrp* mRNA levels were markedly decreased and AGRP neurons were less excitable, both of which were reversed by GC administration (143-147). Surprisingly, *Pomc* mRNA levels in the rat hypothalamus were also markedly decreased following adrenalectomy, and chronic GC replacement returned these levels to normal (146,148-150). This is in marked contrast to the inhibitory effect of GCs on *Pomc* transcription in the anterior pituitary (151). These data suggest that GCs can increase both hypothalamic *Agrp* and *Pomc* and suggest that a role for melanocortins in GC-induced feeding may be complex.

GC-induced feeding is itself a rather complicated and controversial topic. Notably, *ob/ob* mice, along with other hypercorticosteronemic genetic models of obesity and rats chronically administered GCs, are also hyperinsulinemic (132,152). Furthermore, adrenalectomy in normal rodents also decreases insulin levels (143). A series of studies on adrenalectomized, insulin-deficient rats suggest that the interaction of GCs and insulin determines both how much and what type of food is consumed (153). Differentiating the specific roles and interactions of GCs and insulin has proven extremely challenging. Some researchers have concluded that GCs are permissive, but not causative, for hyperphagic obesity (154). Nonetheless, taken together the above-mentioned studies suggest that the melanocortin system can be regulated by GCs. Most, if not all, POMC and AGRP neurons express GR, suggesting that this effect could be direct, although this has not been well-studied (155,156).

B. The melanocortin system is upstream of the HPA axis

Obesity is associated with hyperactivation of the HPA axis. Although elevated GCs are often viewed as causative in the development of obesity, it is also plausible that energy status and the pathways involved in feeding and energy homeostasis could affect the HPA axis (157).

1. Pharmacological studies

Preliminary evidence that energy pathways affect the HPA axis came from rats treated neonatally with monosodium glutamate, which lesions the arcuate nucleus (158). The hypothalamus and anterior pituitary of MSG-treated rats are hyperresponsive to a variety of

stimuli, and specifically MSG-treated rats exhibited elevated ACTH and GCs both basally and following stress (159,160). Together with the fact that *ob/ob* mice exhibit the same phenotype, the MSG studies suggest that a leptin-responsive Arc population of neurons exhibits a net inhibitory effect on the HPA axis. Both POMC and AGRP neurons project directly to the PVH as well as to candidate relay nuclei such as the amygdala and the bed nucleus of the stria terminalis (60). Chronic implantation of an ACTH pellet into the median eminence, but not the pituitary, decreased corticosterone in rats (161), and ACTH and α-MSH dose-dependently decreased CRH release from hypothalamic slices *in vitro* (162,163). Furthermore, endogenous α-MSH inhibited activation of the HPA axis induced by interleukin-1β injection (164,165). Additionally, melanocortin signaling must be intact for rescue of elevated GCs caused by induction of diabetes (166). Thus, activation of melanocortin receptors can inhibit the HPA axis.

However, and in stark contrast to the studies mentioned above, acute i.c.v. injection of ACTH, α-MSH or the synthetic Mc3r/Mc4r agonist melanotan II (MTII) have been shown to increase plasma GCs as well as exaggerate the HPA response to stress (167-171). Approximately 20% of CRH neurons express Mc4r, and i.c.v. MTII or α-MSH increased *Crh* mRNA levels in the PVH, suggesting a direct route of activation of the HPA axis by melanocortins (170,172). Furthermore, administration of the Mc3r/Mc4r antagonist HS014 attenuated the rise in GCs following acute stress (128,173). Surprisingly, intra-PVH injection of either NDP-MSH, a long-acting α-MSH analogue, or AGRP led to equal rises in plasma ACTH and GCs, in contrast to the opposite effect that these two peptides have on feeding and energy balance (174). These studies suggest that acute activation of the entire melanocortin system can activate the HPA axis.

There are problems inherent in each approach to understanding the cross-talk of the melanocortin and HPA systems. MSG treatment has been shown to not only lesion the Arc but

also affect the VMH and suprachiasmatic nucleus (175). As in any pharmacological study, dosage and potency of the drugs administered is of tantamount importance to consider. Indeed, one study found that although a fairly "standard" dose of α-MSH administered i.c.v. increased plasma GC levels, a dose ten times lower actually inhibited the HPA response to an immunological stressor (165). The specific drug used also matters crucially as some synthetic melanocortin agonists are much more potent than endogenous ligands. All too often, these considerations are not tested and could lead to the discrepant results described here.

2. Genetic studies

One approach to probe the role of endogenous melanocortins in the HPA axis is to examine genetically engineered mouse models. *Agrp*-KO mice, as mentioned above, have no metabolic phenotype, which suggests either developmental compensation or a predominant role for other neuromodulators produced by AGRP neurons (29). In keeping with the relative lack of abnormal phenotype, *Agrp*-KO mice have normal basal GC levels (176). Postnatal ablation of AGRP neurons, which led to anorexia, did not affect GC levels as measured 48 hours after ablation (64). Further, although some CRH neurons express Mc4r, no synaptic connectivity of these neurons with AGRP neurons could be detected (73). Most studies, including all chemo- and opto-genetic studies of AGRP neurons published thus far, either did not measure or did not report any readout of HPA function. Thus although what has been reported does not absolutely exclude a role for endogenous AGRP in regulation of the HPA axis, there is as of yet no direct evidence that it has one.

The HPA axis of both *Mc3r*-KO and *Mc4r*-KO mice has not been well characterized beyond the report of normal basal GCs at the diurnal nadir (25,27). Similarly, *Mc4r*-KO rats have unchanged basal plasma GCs both at the diurnal nadir and peak, but they show a reduced HPA response to restraint stress (177). This suggests that the mouse knockout models of the melanocortin receptors may also have a non-obvious HPA phenotype.

The use of genetic mouse models to explore a role for neuronal POMC in regulation of the stress axis has been complicated by the critical role of peripheral POMC in the HPA axis. A gain of function approach was to transgenically overexpress only the N-terminal portion of the *Pomc* gene that includes α- and γ-MSH. These mice had normal basal plasma GCs but had significantly lower GCs than controls when challenged with a high-fat diet, suggesting that under metabolic challenge α-MSH can inhibit the HPA axis (178).

Two *Pomc*-KO mouse strains have been generated by separate laboratories (23,24). The adrenal glands do not develop properly postnatally secondary to the absence of circulating ACTH, and *Pomc*-KO mice have no measurable circulating GCs either basally or upon stimulation by a stressor (4,179). Similarly, postnatal POMC ablation leads to destruction of the corticotrophs and complete loss of GCs (64,180). In an effort to separate the role of POMC in the pituitary versus the hypothalamus, one group specifically ablated hypothalamic POMC neurons via stereotaxic injection and reported a decrease in fasting GC levels (74). Similar to AGRP, I could not find data reporting any HPA axis changes in mice that had POMC neurons chemo- or optogenetically activated or inhibited.

To specifically study the role of POMC in the hypothalamus, the Low laboratory crossed *Pomc*-KO mice with mice engineered to carry a transgene directing *Pomc* expression only to pituitary cells but not to neurons, effectively creating a neuron-specific *Pomc*-KO (181). In this

model, the diurnal rhythm of GCs was preserved but corticosterone levels were elevated over controls (181). This was associated with increased area of the adrenal cortex and increased mRNA levels of *Crh* in the PVH (182). These data suggested a role for hypothalamic POMC in inhibition of the HPA axis, but presence of the *Pomc*-KO allele was associated with development of late-onset pituitary adenomas, complicating the interpretations. Additionally, opioids are known to have an inhibitory role on the HPA axis, and β-endorphin is one of the cleavage products of the POMC propeptide (183). However, the HPA axis of β-endorphin-KO mice was completely normal, leading me to believe that any HPA phenotype in neural-*Pomc*-KO mice is due to loss of melanocortin signaling (184).

C. Concluding remarks

The relationship between the neural melanocortin system and the HPA axis is extremely complex and warrants further investigation. Although it has not been definitively proven, the neural melanocortin system could be directly and immediately activated by a stressor and play a role in stress-induced anorexia. On the other hand, melanocortins could be dysregulated by chronically high GCs and lead to excessive feeding behavior. Further, there is evidence that the melanocortin system could activate or inhibit the HPA axis. It is likely that the specific pathway activated could depend on the type and timing of the stressor as well as the physiological state of the organism. Much more work will be needed to unravel the precise interplay between the neural melanocortin system and the HPA axis.

IV. Conclusions and Future Directions

The neural melanocortin system has been shown to play a critical role in feeding behavior, energy expenditure, energy partitioning, cardiovascular health, the immune system, and sexual function. Here I have reviewed some accumulating evidence that it may also be involved in the regulation of locomotion and in control of the HPA stress axis. Overall, the consensus in the field currently is that neural melanocortins may induce locomotor activity via Mc3r specifically in cases of food restriction but otherwise are not critically and directly involved in physical activity levels. Additionally, although there is evidence that melanocortins could inhibit the HPA axis, the preponderance of evidence suggests that, at least acutely, they stimulate it.

Most of the studies probing these roles have measured behavior or physiology after administration of exogenous melanocortin ligands or in the melanocortin receptor knockout animals. A large and missing piece of the puzzle is the phenotypic characterization of a mouse model that selectively lacks endogenous neural melanocortin agonists. The Low and Rubinstein laboratories have identified two upstream enhancer regions necessary to drive *Pomc* expression specifically in the Arc (185). Upon insertion of a neomycin resistance cassette into this enhancer region, *Pomc* expression is completely ablated in the Arc but left intact in the pituitary (86) (Figure 1.4). These Arc*Pomc*-KO mice phenocopy the previously generated neuron-specific *Pomc*-KO mice described above in that they are morbidly obese due to a combination of hyperphagia and reduced energy expenditure, but no Arc*Pomc*-KO mouse has been observed to develop pituitary tumors.

Systematic characterization of spontaneous home cage locomotor activity and voluntary wheel running activity in obese Arc*Pomc*-KO mice and weight-matched knockouts will help to definitively prove whether and how POMC controls activity levels. Further, calorically restricted, weight-matched knockouts will provide an ideal opportunity to study the role of POMC in food anticipatory activity (See Chapter 2). An in-depth examination of the HPA axis of this novel genetic model will also help to identify the role and mechanism of ArcPOMC in the regulation of the HPA axis (See Chapter 3). One shortcoming of many previously-published reports is that only one sex is studied and, sometimes, sex is not even reported. Sex affects physiology and behavior and is especially relevant in the study of every aspect of neuroendocrinology. Therefore, in this report, we have studied each sex separately and speculate on the mechanism and significance of identified sex differences.

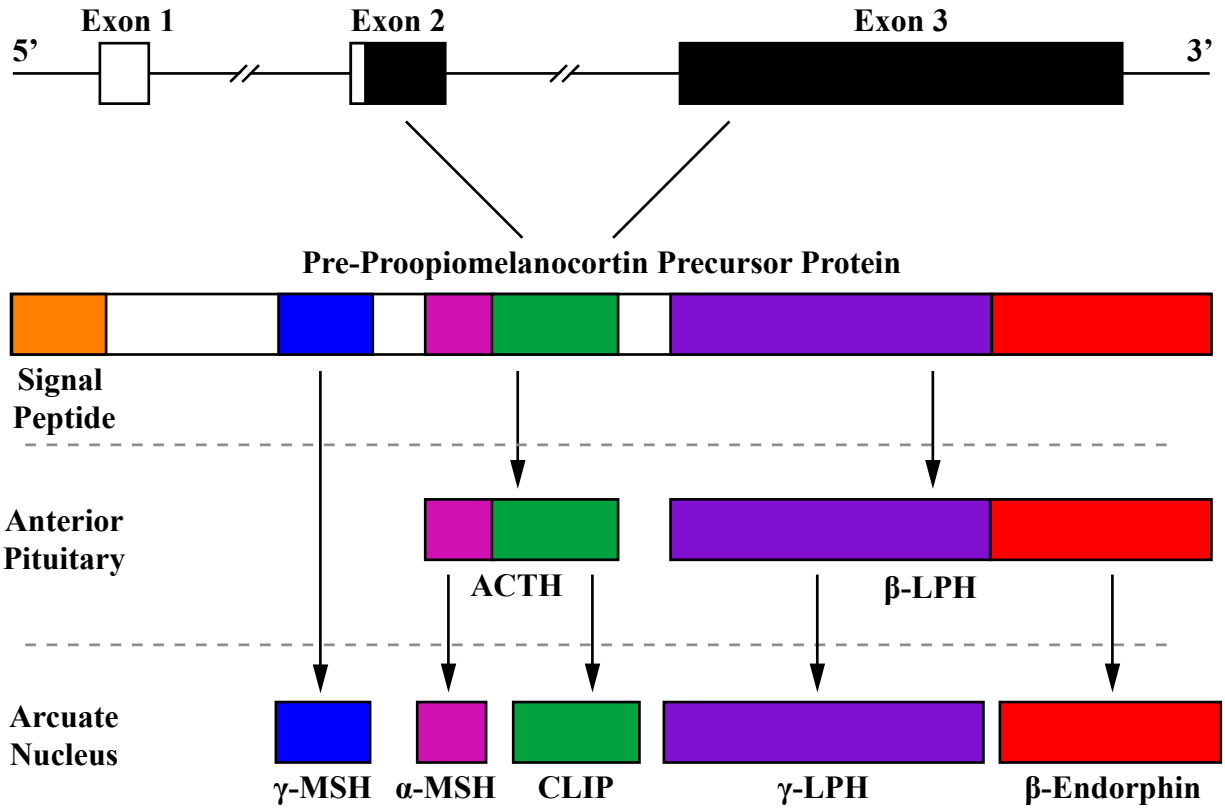

Figure 1.1: Proopiomelanocortin peptide processing in the anterior pituitary and arcuate nucleus. ACTH: adrenocorticotropic hormone; LPH: lipotropic hormone; MSH: melanocyte-stimulating hormone; CLIP: corticotropin-like intermediate peptide.

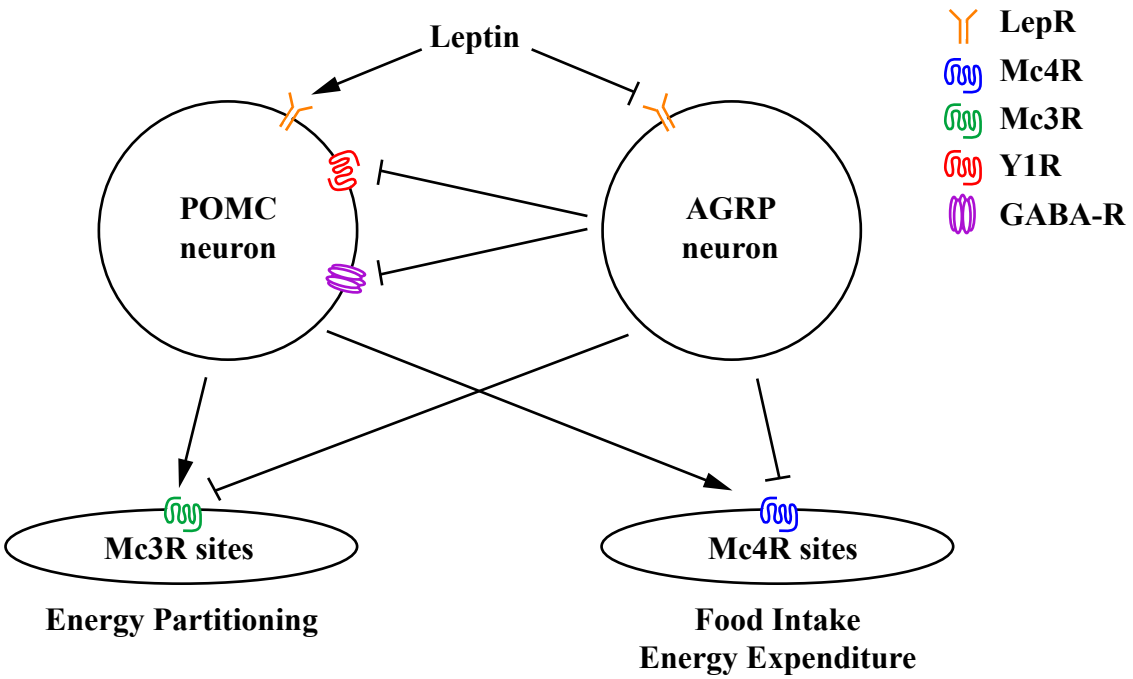

Figure 1.2: Classic model of the neural melanocortin system. LepR: Leptin receptor; POMC: Proopiomelanocortin; AGRP: Agouti-related peptide; Mc3r: Melanocortin-3 receptor; Mc4r: Melanocortin-4 receptor; Y1r: Neuropeptide Y-1 receptor; GABA-R: Gamma-aminobutyric acid receptor.

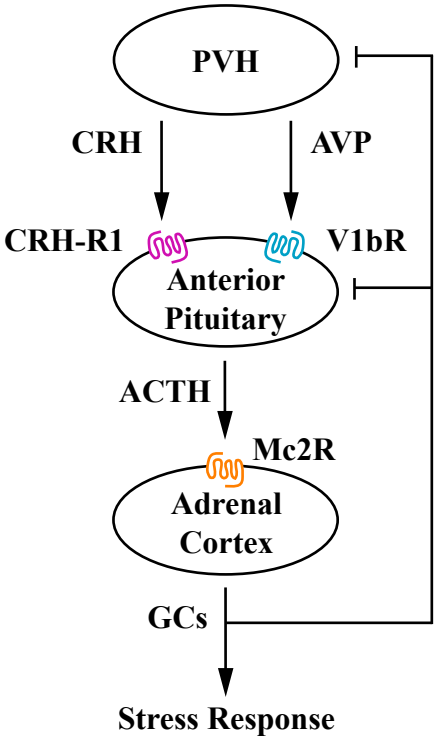

Figure 1.3: Diagram of the hypothalamic-pituitary-adrenal stress axis. PVH: Paraventricular nucleus of the hypothalamus; CRH: Corticotropin-releasing hormone; AVP: Arginine vasopressin; CRH-R1: CRH-Receptor 1; V1bR: Vasopressin receptor 1b; ACTH: Adrenocorticotropic hormone; Mc2R: Melanocortin-2 receptor: GCs: Glucocorticoids.

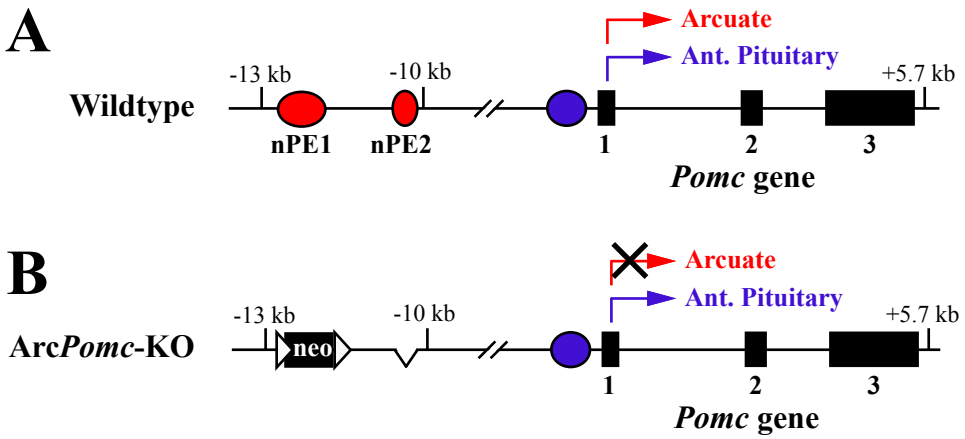

Figure 1.4: Schematic of WT and Arc*Pomc*-KO alleles. A, Two upstream enhancers (nPE: neural *Pomc* enhancer) drive expression of *Pomc* in the arcuate but are not necessary for expression of *Pomc* in the anterior pituitary. **B**, Insertion of a neomycin resistance cassette into nPE1 and deletion of nPE2 completely abolishes arcuate expression of *Pomc* but does not affect expression in the anterior pituitary. Blue circle: *Pomc* promoter; White triangles: LoxP sites.

Chapter 2: Arcuate Proopiomelanocortin Influences Voluntary Locomotor Activity Levels Independently of its Role in Food Intake[†]

Obesity in humans and rodents is associated with decreased physical activity levels. Inactivity may be caused by obesity or by environmental and/or genetic mechanisms and in turn contribute to obesity. Proopiomelanocortin (*Pomc*)-expressing neurons in the arcuate nucleus of the hypothalamus (Arc) are critical for body weight regulation, controlling both food intake and energy expenditure. Arc*Pomc*-knockout (KO) mice are morbidly obese, complicating studies to characterize a possible role for Arc*Pomc* in locomotor activity. In this study, we measured both spontaneous home cage as well as voluntary running wheel activity levels in obese Arc*Pomc*-KO mice and knockouts weight-matched to wildtype controls by caloric restriction. We found that obese Arc*Pomc*-KO mice exhibit decreased home cage locomotor activity which was normalized by weight-matching. In contrast, Arc*Pomc*-KO mice exhibited less voluntary running wheel activity than controls, regardless of their body weight. Thus we have dissociated these two types of locomotor activity and determined that decreased home cage activity in Arc*Pomc*-KO mice is secondary to hyperphagic obesity, but Arc*Pomc* plays a primary role in regulation of voluntary running wheel behavior.

[†] Data from Figures 2.4 and 2.5 and Table 2.2 were collected in collaboration with Dr. Miho Yamashita. Data from Figure 2.6 and Table 2.3 were collected in collaboration with Samantha Spierling. All of the work presented in Figure 2.8 was performed by Samantha Spierling under my direct instruction and supervision. Mouse colony maintenance and genotyping were performed by Jared Goldberg, Courtney Attard, and Eva Yokosawa.

Introduction

Obesity is a major worldwide health problem that is strongly associated with a number of comorbid conditions, including type 2 diabetes mellitus and cardiovascular disease. Obesity results from a positive energy balance created by increased food intake and/or decreased total energy expenditure (TEE). Basal metabolic rate, the thermic effect of food, and physical activity all contribute to TEE. Intrinsic physical activity levels are highly variable across individuals and are at least partially determined by genetic factors. The recent rise in obesity rates in humans has been accompanied by a decrease in physical activity levels, but the directionality of this relationship is unclear (78,79). Decreased physical activity and the resulting decrease in TEE could contribute to the development of obesity, but obesity in itself, regardless of its etiology, could also negatively affect physical activity levels (81).

Mice are a genetically tractable model well-suited to studying the roles of specific genes in the relationship between decreased activity levels and obesity, which are also highly correlated in mice (81). Many researchers have reported decreased locomotor activity levels in various genetically obese mouse models, but the direction of causation is often not investigated. Additionally, few groups have considered that laboratory mice are usually housed in an unnatural, small environment with little opportunity to engage in physical activity. Indeed, total physical activity can be divided into two categories: spontaneous, non-exercise activity or voluntary exercise (78,80). Mice in a typical home cage environment can only engage in spontaneous activity such as locomotion around the cage and grooming, whereas activity on a running wheel introduced into the home cage is believed to be representative of voluntary exercise (80). Levels of spontaneous home cage activity and voluntary running wheel activity usually correlate positively across mouse strain and sex, but access to a running wheel amplifies

activity levels and engages reward pathways (82). Very little is known about the neural and endocrine mechanisms regulating either type of activity, but there is evidence that they overlap extensively not only with each other, but also with pathways that regulate feeding behavior (78-80).

Proopiomelanocortin (POMC) is a propeptide expressed primarily in the pituitary and the arcuate nucleus of the hypothalamus (Arc), where its role in feeding behavior has been extensively studied. POMC is cleaved in a site-specific manner into the melanocortins α-melanocyte stimulating hormone (MSH), γ-MSH, and adrenocorticotrophic hormone (ACTH), as well as the opioid peptide β-endorphin. Mice lacking POMC specifically in the Arc (Arc*Pomc*-KO) develop morbid obesity associated with both increased food intake and decreased spontaneous home cage locomotor and voluntary running wheel activity (86,106). When the *Pomc* gene was reactivated in obese Arc*Pomc*-KO mice, food intake decreased and body weight returned toward that of wild-type (WT). In conjunction, spontaneous locomotor activity was normalized (86). However, whether this change was caused by the rescued *Pomc* gene activity independently of obesity or was a secondary effect of the return to normal body weight was not determined.

In the brain, melanocortins activate the melanocortin receptors Mc3r and Mc4r, which are antagonized by agouti-related peptide (AGRP), produced in neighboring neurons in the Arc. Central injection of melanocortin agonists increased, whereas antagonists decreased, spontaneous home cage locomotion in rats (83,84). *Mc3r*-KO mice, which have normal body weight but an increased fat to lean mass body composition ratio, showed decreased spontaneous and voluntary locomotor activity levels (26,27,89), although there have also been reports to the contrary (87,88). On the other hand, young, pre-obese *Mc4r*-KO mice showed normal levels of

spontaneous locomotor activity, whereas obese *Mc4r*-KO mice were hypolocomotive (28,91). Interestingly, providing *Mc4r*-KO mice access to a running wheel significantly improved their body weight and metabolic outcome (108,109).

Therefore, we hypothesized that melanocortin signaling influences physical activity levels directly as well as indirectly via its effects on body weight. To test this hypothesis, we measured spontaneous home cage locomotor activity and running wheel activity of obese Arc*Pomc*-KO mice and WT controls as well as Arc*Pomc*-KO mice weight-matched to the controls. Many studies mentioned above reported data only from males, whereas we performed these experiments in both sexes. We determined that Arc*Pomc* is not necessary for the expression of spontaneous home cage locomotion, because weight-matched Arc*Pomc*-KO mice showed the same activity levels as their WT controls. On the other hand, Arc*Pomc* regulates voluntary running wheel activity independently of obesity, particularly in females. We also describe a modulatory role for Arc*Pomc* in determining the amplitude of food anticipatory activity specifically in males.

Materials and Methods

Animals. Mice were housed in ventilated cages under controlled temperature (72 ± 2°F) and lighting conditions (12 hour light:dark cycle with lights on 6:00 a.m. to 6:00 p.m.). Arc*Pomc*-KO mice, also called fneoΔ1Δ2 (86,186), and β-endorphin-KO mice (184) were generated as described previously. In both cases, heterozygote pairs were bred to produce KO mice and their control wild-type (WT) littermates, and each sex was studied separately. A*d libitum*-fed mice had free access to water and standard laboratory chow (LabDiet 5L0D). Food-

restricted mice had free access to water but were administered a pre-weighed pellet of chow daily as described below. All animal studies were approved by the University Committee for Use and Care of Animals at the University of Michigan and followed the Public Health Service guidelines.

Home cage activity. WT and Arc*Pomc*-KO mice (n = 8 per sex and genotype) that had previously been group-housed were singly-housed for one week starting at age 18-19 weeks. At age 20 weeks, each home cage, with a water bottle and a surplus of food on the cage floor, was placed into the center of a 41 x 41 cm open field chamber and horizontal distance traveled per minute was recorded by infrared beam breaks using Activity Monitor software (Med Associates) for 23 hours each day for 3 days. During the 24th hour, the software was reset and the mice weighed to monitor health. Data from the 1st day was considered acclimation and data from the second two days was averaged and reported. Following ~10 weeks of food restriction (see below), this test was repeated with the modification that the daily food was given by gently removing the lid and placing the chow on the cage floor during data acquisition. For food restriction, WT mice were maintained at 85% of their starting body weight for 10 weeks by giving each mouse 2-3 g of chow per day whereas Arc*Pomc*-KO mice were brought down to the starting weight of the WT littermate controls over the course of 10 weeks by giving each mouse 1.5-2.5 g of chow per day. Food was provided daily at 10:00 am.

The presence of the home cage occasionally triggered a glitch in the monitoring software whereby the mouse appeared to "teleport" across the cage. To correct for this, a Matlab program was created to omit data in any 1-minute bin in which the velocity of the mouse was calculated by the software to be zero but a distance was nevertheless reported. Additionally, any 1-minute

bin in which the mouse was reported to be continuously active for more than 40 s was excluded. This time was based empirically on the amount a mouse was deemed likely to run continuously upon sensitization to morphine (see below).

Running wheels. Following weaning at 3 weeks of age, a separate cohort of mice was group housed for one week and then singly-housed on aspen bedding starting at age 4 weeks in a standard home cage either with or without a low-profile wireless running wheel (Med Associates). β-endorphin-KO and WT control mice were fed *ad libitum* and assigned either a running wheel or no wheel. Arc*Pomc*-KO mice were assigned to *ad libitum* feeding with a wheel or no wheel or to restricted feeding with a wheel (n = 5-7 per genotype, sex and condition). Each radiotelemetric wheel transmitted the number of revolutions per minute to a computer in the adjacent room, where data were collected for 3 nights and 2 days, then averaged, each week from age 5 to 11 weeks. Mice continued to have access to the wheel after 11 weeks but the data were not analyzed because running activity was affected by further tests performed on the mice (see below). Mice with *ad libitum* access to food were weighed once per week and provided a preweighed quantity of chow. Uneaten chow was weighed twice per week and the average daily intake calculated. Food-restricted, weight-matched (WM) Arc*Pomc*-KO mice were weighed once per day at approximately 4:00 p.m., and sufficient food was administered to maintain the Arc*Pomc*-KO mice at the same weight as the WT controls.

Metabolic Phenotyping. At age 12-14 weeks, body composition of the mice in the running wheel study was analyzed by the University of Michigan Animal Phenotyping Core by

nuclear magnetic resonance (NMR) using a Minispec LF90II (Bruker). Fat, fluid and lean mass for each animal were expressed both in absolute mass and as percentages of total body weight.

At age 13-15 weeks, mice underwent an intraperitoneal glucose tolerance test (ipGTT). After an 18-hour fast, tails were nicked at 9:00 a.m. and approximately 10 μL whole blood was collected. Fasting blood glucose was measured with a glucometer (AlphaTrak, Abbott) and then plasma was separated by centrifugation and stored at -20°C for insulin measurement. Meanwhile, 2 mg/kg glucose was administered i.p. and blood glucose was monitored at regular intervals for 4 hours. Area under the curve (AUC) was calculated using Prism 6 (GraphPad) assigning each mouse its own baseline (blood glucose at time 0). Plasma insulin was measured by an ultra-sensitive ELISA (Crystal Chem, Inc.).

At age 14-16 weeks, mice were fasted from 9:00 a.m. to 3:00 p.m. and then euthanized by decapitation. Trunk blood was collected into tubes with 10 μL of 75 ng/mL EDTA, and plasma was separated by centrifugation and stored at -20°C until analysis for total cholesterol by the Chemistry Core of the Michigan Diabetes Research Center.

Semi-quantitative real-time PCR. Following euthanasia, the hypothalamus of the running wheel mice was dissected, snap frozen on dry ice, and stored at -80°C. A separate cohort of adult group-housed female mice (6-8 month old, N = 8 per genotype) was euthanized by decapitation, the brain dissected and two blocks of the brain were microdissected, one containing the ventral tegmental area (VTA) and substantia nigra (SN) and another containing the nucleus accumbens (NAcc), and stored at -80°C. The VTA/SN and NAcc blocks were separated bilaterally and one half was used for analysis. After pretreatment with Qiazol Lysis Reagent (Qiagen), RNA was extracted from all tissues using RNeasy spin columns (Qiagen) and any contaminating DNA was

removed via Turbo DNase treatment (Life Technologies). Total RNA was quantified and quality-checked via NanoDrop (ThermoScientific). Reverse transcription was performed to produce cDNA from 400 ng total RNA using random hexamer primers (Goscript RT System, Promega). Real-time PCR was performed on all samples in duplicate using the StepOne Real Time PCR System (Applied Biosystems) and SYBR Green Master Mix (Life Technologies). Primers as listed in Table 2.1 were designed using Primer3 (187) to span at least one intron, when possible, and were used at a final concentration of 300 nM. The relative quantity of mRNA in the samples was calculated from a standard curve spanning 1000-fold change, normalized to reference gene *Gapdh* (hypothalamus, VTA/SN) or *Ppia* (NAcc) and then normalized to WT controls with no running wheel access. Occasional outliers were identified using Grubbs' outlier test and removed.

Morphine sensitization. An additional cohort of 5-9 month old group-housed mice were used to test locomotor sensitization to morphine (n=6 per sex, genotype and drug treatment; subsequently, data from males and females were collapsed for statistical analysis). The sensitization test was conducted over 11 consecutive days. On each day, each mouse was placed into a 41 x 41 cm open field chamber and its locomotor activity recorded by Activity Monitor software (Med Associates) for one hour. The first day served to acclimate the mice to the open field. The second day, each mouse was injected i.p. with 0.9% saline (WT: 10 µL/g body weight; Arc*Pomc*-KO: 5 µL/g body weight) immediately prior to being placed in the open field. Following the saline day, mice of each genotype were randomly assigned to either the saline control group or the morphine group. On days 1-4, the saline control group was injected with saline as above, whereas the morphine group was administered 10 mg/kg morphine (National

Institute on Drug Abuse). Following a three day break, each mouse was administered 10 mg/kg morphine. On the last day, to test for sensitization to the environment, all mice were injected with saline.

Immunohistochemistry. At age 6 months, a separate group of female mice (n=6 per genotype) were deeply anesthetized with 2% tribromoethanol i.p. and perfused transcardially with 10% sucrose followed by 4% paraformaldehyde (PFA) in phosphate-buffered saline (PBS) on a pressurized rig (Perfusion One; Leica). The brain was dissected and postfixed overnight in 4% PFA at 4°C then incubated in successive gradients of sucrose (10%, 20%, 30%) in KPBS at 4°C. Brains were sectioned coronally at 30 μm using a freezing microtome stage (SM 2010R, Leica) and stored in cryoprotectant solution (25 mM PBS with 30% ethylene glycol and 20% glycerol) at -20°C until use. Free-floating sections were washed three times in KPBS for 15 minutes per wash and then incubated overnight at 4°C in KPBS with 0.3% Triton X-100 (KPBS-T), 2% normal donkey serum and monoclonal mouse anti-tyrosine hydroxylase (TH) (1:500, Immunostar). Following three more washes, sections were incubated for two hours in donkey anti-mouse-AlexaFluor 488 (1:500, Invitrogen) in KPBS-T at room temperature. After three more washes, the sections were mounted on gelatin coated glass slides and cover slipped using polyvinyl alcohol mounting medium (Sigma Aldrich).

Imaging and Analysis. Sections were imaged using a Nikon 90i upright microscope equipped with an X-Cite 120Q fluorescent light source and CoolSNAP HQ2 CD camera (Photometrics) and a 4X objective. TH-labeled sections were imaged using a 488 excitation/525 emission filter cube and 900 ms exposure time. Each CNS nucleus was imaged utilizing rostral-

caudal coordinates obtained from the Mouse Brain Atlas (188). Coordinates for our nuclei of interest were Bregma -2.70 to -3.88 (substantia nigra pars compacta) and Bregma -2.80 to -3.16 (ventral tegmental area). All post-image analyses were performed in NIS-Elements AR (Nikon), and each nucleus was defined by a manually outlined region of interest (ROI). Images were set to the same pixel intensity to create a detectable signal in control animals. To quantify fluorescence of TH signal, presented in arbitrary units (AU), the mean pixel intensity from each ROI was multiplied by the ROI's binary area.

Statistical analysis. All data are presented as mean ± SEM. Males and females were analyzed separately, except in the morphine sensitization study where the sexes were combined. Home cage locomotion distances were analyzed by repeated measures ANOVA (RMANOVA) with genotype and nutritional status as the independent variables. Running wheel activity and body weight were also analyzed by RMANOVA with group and age as the independent variables. A significant interaction was followed by Sidak's multiple comparisons post hoc tests. Food intake, body composition, fasting blood glucose, glucose tolerance AUC, fasting plasma insulin, total cholesterol, and qPCR results (except those in Figure 2-8) were analyzed by one-way ANOVA followed by Dunnett's multiple comparisons tests to compare all groups to WT without a wheel and/or to Arc*Pomc*-KO without a wheel. Distance traveled in the morphine sensitization study was analyzed using two-way ANOVA followed by Tukey's multiple comparisons post hoc tests. qPCR and IHC data presented in Figure 2-8 were analyzed by unpaired Student's t-test between genotypes. All analyses were performed in Prism 6 (GraphPad).

Results

Arc*Pomc*-KO mice exhibit decreased spontaneous home cage locomotion secondary to obesity.

At age 20 weeks, *ad libitum*-fed Arc*Pomc*-KO mice of both sexes were morbidly obese, as described previously (86) (Figure 2.1A). Total spontaneous home cage locomotor activity of obese Arc*Pomc*-KO mice over 24 hours was markedly decreased from WT (Figure 2.1B). Following 10 weeks of caloric restriction, Arc*Pomc*-KO mice weighed the same as the starting weight of WT controls, whereas the WT controls weighed 85% of their starting weight (Figure 2.1A). Weight-matching Arc*Pomc*-KO mice increased their spontaneous 24-hour home cage activity to an equal level as the *ad libitum*-fed WT controls (Figure 2.1B). In females, food restricted WT and Arc*Pomc*-KO mice exhibited identical activity levels. In males, WT mice increased their activity levels after caloric restriction and therefore still had higher levels than Arc*Pomc*-KO mice.

Laboratory mice are nocturnal, and most spontaneous home cage activity occurs in the dark hours. Indeed, this is what we found in *ad libitum*-fed WT mice of both sexes (Figure 2.2). The deficit in spontaneous activity levels of obese Arc*Pomc*-KO mice described in Figure 2.1B was completely due to decreased activity at night, as there were no differences between genotypes during the day. In WT mice of both sexes, nocturnal activity decreased with food restriction. In contrast, the nocturnal activity of Arc*Pomc*-KO mice increased with food restriction such that, in food restricted mice, there was no difference in nocturnal activity levels between genotypes (Figure 2.2A). In both genotypes, day-time activity increased with food restriction. In females, this increase was of the same magnitude in both genotypes whereas it was somewhat blunted in Arc*Pomc*-KO male mice (Figure 2.2B).

Arc*Pomc*-KO male mice have impaired food anticipatory activity independent of obesity.

Restricting food access to a certain period only in the daytime is known to disrupt circadian locomotor activity patterns. Specifically, there is a burst in locomotor activity in the 2-3 hours immediately prior to food presentation which has been termed food anticipatory activity. Hourly analysis of spontaneous home cage activity revealed that *ad libitum*-fed WT mice showed two typical nocturnal bursts of activity, one at the beginning and one at the end of the dark cycle, and very little activity in the day time (Figure 2.3A). Obese Arc*Pomc*-KO mice also showed the same pattern although the activity levels were severely blunted, especially in females. Upon food restriction, WT mice of both sexes maintained the burst of activity at onset of night but additionally showed a much larger spike anticipating the time of food presentation (Figure 2.3B). Weight-matched Arc*Pomc*-KO mice also showed this second, food-entrained spike in activity levels, but the amplitude was blunted selectively in males.

Running wheel access slightly improves body weight and body composition in obese Arc*Pomc*-KO mice

Reasoning that low activity levels appeared to be secondary to obesity in Arc*Pomc*-KO mice, we postulated that giving these mice an opportunity to increase activity levels by providing a running wheel in the home cage from weaning onward might delay, improve, or prevent obesity. Indeed, Arc*Pomc*-KO mice given access to a running wheel had mildly improved body weight, but the effect was not as large as anticipated, especially in females (Figure 2.4A). The body weight of WT mice with a wheel was not different from WT without a wheel.

We also performed metabolic phenotyping of these mice at the end of the study. In WT mice of both sexes, access to a running wheel did not change body composition, fasting blood glucose or glucose tolerance, or fasting plasma insulin or cholesterol levels (Table 2.2). Obese Arc*Pomc*-KO male mice with access to a running wheel had improved body composition, as percentage of lean body mass was increased and percentage of fat body mass was decreased from obese Arc*Pomc*-KO mice without a wheel, although body composition was still different from WT controls. Additionally, obese Arc*Pomc*-KO male mice with a wheel had normalized levels of total plasma cholesterol (Table 2.2A). In females, obese Arc*Pomc*-KO mice with access to a wheel did not have an improved metabolic phenotype over Arc*Pomc*-KO mice without a wheel (Table 2.2B).

On the other hand, weight-matching Arc*Pomc*-KO mice of both sexes to WT controls normalized fasting blood glucose, glucose tolerance, fasting plasma insulin and total cholesterol levels. Weight-matching Arc*Pomc*-KO also improved body composition and absolute lean mass, expressed in grams, was not different from WT. However, weight-matched Arc*Pomc*-KO mice still had more fat mass than WT and therefore a decreased percentage of lean mass and increased percentage of fat mass (Table 2.2).

Arc*Pomc*-KO mice show low levels of voluntary running activity independent of obesity.

In WT mice of both sexes, wheel running activity at the beginning of the study was relatively low and increased over a period of 2-3 weeks until it plateaued (Figure 2.4B). In *ad libitum*-fed Arc*Pomc*-KO mice, the running wheel activity at age 5 weeks was the same as WT but rather than increasing and plateauing, activity levels gradually decreased with age and became less than WT by age 8 weeks in males and 7 weeks in females (Bonferroni's multiple

comparisons test, $P < 0.05$). Arc*Pomc*-KO mice weight-matched to WT from weaning increased running wheel activity similarly to WT in the beginning of the study but activity levels dropped off and were less than WT by age 8 weeks in females and age 11 weeks in males (Figure 2.4B) (Bonferroni's multiple comparisons test, $P < 0.05$).

At age 5 weeks, the total amount of running wheel activity was not different between the groups, and all mice ran on the wheels almost exclusively at night (Figure 2.5A). By the end of the study, both obese and weight-matched Arc*Pomc*-KO mice of both sexes showed significantly less running wheel activity at night than WT controls (Figure 2.5B). On the other hand, weight-matched Arc*Pomc*-KO mice ran more on the wheels during the day time. In this study, mice were fed at approximately 4:00 pm, so this shift in running rhythm is likely correlated with food anticipatory activity.

To test for a role of β-endorphin, one of the cleavage products of the POMC peptide, in regulation of running wheel activity, we repeated this experiment in β-endorphin-KO mice. Throughout the duration of the study, β-endorphin-KO mice of both sexes showed the same level of 24-hr voluntary wheel running activity as their WT littermate controls (Figure 2.6A). Additionally, there were no differences between WT and β-endorphin-KO mice in the diurnal pattern of running activity at the end of the study (Figure 2.6B).

Repeated morphine administration to obese Arc*Pomc*-KO mice increases locomotor activity to the same level as WT.

To confirm the physical ability of obese Arc*Pomc*-KO mice to run and to ascertain if brain reward circuitry was intact, we next performed a morphine sensitization study. When injected with saline immediately before being placed in an open field to which they had been

acclimated the previous day, Arc*Pomc*-KO mice had markedly decreased locomotor activity compared to WT (Figure 2.7A,B). However, when injected with morphine, both WT and Arc*Pomc*-KO mice increased the distance traveled in the open field to the same level (Figure 2.7A). The locomotor sensitization effect of morphine was measured by comparing the distance traveled on the first and last day of repeated morphine injection, and both genotypes showed sensitization (WT: $t(11) = 2.8$, $P < 0.05$; Arc*Pomc*-KO: $t(11) = 5.1$, $P < 0.001$; paired Student's t-test). Because baseline activity levels were different between genotypes, we normalized the distance traveled to the average for each group on the saline day. According to this metric, Arc*Pomc*-KO mice showed a more exaggerated sensitization than did WT mice (Figure 2.7C).

Arc*Pomc*-KO mice have altered brain expression of melanocortin system but not dopamine system genes.

mRNA levels of a panel of hypothalamic genes previously shown to be involved in food intake, metabolism, and voluntary running wheel activity were measured in the mice from the running wheel experiment (Table 2.3). As expected, *Pomc* mRNA was very low in all Arc*Pomc*-KO mice with no difference between groups. In obese Arc*Pomc*-KO mice of both sexes, mRNA levels of the anorexigenic peptide CART (cocaine and amphetamine-related transcript, *Cartpt*) were increased compared to WT. Likewise, mRNA levels of the orexigenic peptides neuropeptide Y (*Npy*) and agouti-related protein (*Agrp*) were decreased in obese Arc*Pomc*-KO compared to WT. None of these genes was affected by access to a running wheel in either genotype. Weight-matched Arc*Pomc*-KO mice had normalized levels of *Cartpt* but weight-matching did not affect levels of *Npy* and *Agrp*. Hypocretin (*Hcrt*, also known as orexin) and brain-derived neurotrophic factor (*Bdnf*) levels have previously been shown to be affected by

voluntary exercise (109), but no differences were found between groups in this study. Similarly, there were no differences in *Mc3r* expression (Table 2.3).

The dopaminergic system has been highly implicated in spontaneous and voluntary locomotor activity as well as motivation and reward. We measured expression levels of genes involved in the dopaminergic system in a separate cohort of female mice. mRNA levels of tyrosine hydroxylase (*Th*), the rate-limiting enzyme in production of dopamine, dopamine receptors *Drd1* and *Drd2* as well as the dopamine transporter *Slc6a3* were not different between genotypes in either the ventral tegmental area (VTA)/substantia nigra (SN) or the nucleus accumbens (NAcc) (Figure 2.8A). Because gene expression does not necessarily correlate with protein levels, immunohistochemistry was used to quantify immunoreactivity of TH protein in the VTA and SN pars compacta (SNc) (Figure 2.8B). In both structures, there was no difference in TH immunoreactivity between the genotypes (Figure 2.8C).

Discussion

This study was designed to disentangle a primary role for Arc*Pomc* in the regulation of spontaneous and voluntary locomotion from its effects on body weight via food intake. We found that obese Arc*Pomc*-KO mice exhibited decreased spontaneous home cage activity levels which were normalized by weight-matching, suggesting that Arc*Pomc* does not play a direct role in regulation of spontaneous locomotion. Rather, these data support the idea that obesity can lead secondarily to decreased spontaneous locomotion, although obese Arc*Pomc*-KO mice are physically capable of high levels of activity, as evidenced from the morphine sensitization assay. On the other hand, both obese and weight-matched Arc*Pomc*-KO mice showed less voluntary

running wheel activity than controls, suggesting that Arc*Pomc* is directly involved in this motivated behavior. We also found that male Arc*Pomc*-KO mice exhibited decreased food anticipatory activity (FAA).

ArcPOMC neurons receive and integrate peripheral signals related to energy status and could regulate locomotor activity in response to these signals. Specifically, catabolic POMC-derived melanocortin peptides may be expected to upregulate activity levels in response to positive energy balance in order to expend more energy. Indeed, similar studies have uncovered a critical role for leptin, an adipocyte-derived hormone well-studied for its role in feeding behavior, in control of physical activity. Leptin-deficient *ob/ob* mice are obese and hyperphagic, and they exhibit markedly decreased spontaneous home cage locomotion (94,95). Acute leptin administration increased spontaneous locomotor activity in *ob/ob* mice before any noticeable change in body weight occurred (94,95), suggesting that the obesity and hypolocomotion seen in *ob/ob* mice are dissociable and that leptin can directly modulate spontaneous activity levels independently of its role in regulation of body weight.

Reactivation of leptin receptor (LepR) in only the Arc of mice otherwise lacking LepR dramatically improved the decreased spontaneous home cage locomotion of LepR-null mice, while only mildly reducing body weight, leading to the hypothesis that leptin regulates spontaneous locomotor activity via neurons in the Arc (96). Both POMC and AGRP neurons in the Arc are leptin-responsive. Mice that were engineered to lack *LepR* expression only in *Agrp*-expressing neurons were mildly obese and showed less spontaneous locomotor activity than controls, whereas mice lacking *Lepr* only in *Pomc* neurons were also mildly obese but had normal locomotor activity levels (189). Additionally, mice with constitutively active Stat3, a transcription factor downstream of LepR, in *Agrp* neurons were lean and hyperlocomotive (99),

whereas constitutive activation of Stat3 in *Pomc* neurons led to mild obesity and insulin resistance but no change in activity levels (99,190). However, *Agrp*-KO mice exhibit normal levels of spontaneous home cage locomotion (29). Together these results suggest that leptin's effect on spontaneous locomotion is mediated via Arc AGRP neurons rather than POMC neurons and may not be dependent on melanocortin signaling, and our data are in agreement with this conclusion.

Ob/ob mice also have decreased voluntary running wheel activity, which increases acutely after leptin administration (94,95,191). The mechanism by which leptin regulates voluntary running wheel activity has been less well-studied than its effects on spontaneous locomotor activity. Since both leptin and Arc*Pomc* can modulate running wheel activity independently of obesity and Arc*Pomc* is known to be activated by leptin, it is certainly possible that Arc*Pomc* is downstream of leptin in one pathway controlling voluntary running wheel activity levels. ArcPOMC neurons also respond to other peripheral and central signals and could regulate voluntary activity independently of leptin. These questions deserve further investigation.

POMC is also cleaved into β-endorphin, which has been shown to be released into the bloodstream in humans (192,193) and into the cerebrospinal fluid in rats (194) during running, and some believe it may be involved in the cognitive and mood enhancements that are associated with exercise, although the mechanism is unknown. To test if the decreased voluntary running wheel activity that we observed in Arc*Pomc*-KO mice was due specifically to lack of β-endorphin, we repeated these experiments in a cohort of β-endorphin-KO mice, which have intact neural melanocortin signaling but are missing β-endorphin throughout the body (184). We hypothesized that if exercise activates reward circuitry via β-endorphin, mice lacking β-endorphin would not exhibit the same level of voluntary running wheel activity as WT controls.

However, we found that β-endorphin-KO mice ran the same distance as WT mice throughout the course of the experiment, which is in agreement with another report using running wheels in the same strain of mice (195). These data, together with the findings that mice selectively bred for high voluntary running levels display equal analgesia to WT mice and respond the same as WT mice when administered opioid antagonists (196), and that mice injected daily with naloxone do not change their running behavior (197), suggests that the endogenous opioid system, or at least β-endorphin, does not play a role in determining levels of voluntary locomotion. Thus we postulate that the lack of running wheel activity in Arc*Pomc*-KO mice described in this report is a direct result of lack of melanocortin signaling.

The dopaminergic system has been heavily implicated in control of locomotion and voluntary physical activity (for review, see (80,103)) in addition to motivation for other rewards. Dopaminergic neurons in the VTA receive both direct and indirect input from POMC neurons. However, using qPCR we found no difference between WT mice and obese Arc*Pomc*-KO mice in the mRNA levels of *Th* or any dopamine receptor or its plasma membrane transporter in the midbrain as well as no difference in TH protein levels by semi-quantitative immunofluorescence. Additionally, mRNA levels of several dopamine receptors and the transporter were not different between genotypes in the NAcc, a key target nucleus for VTA dopaminergic nerve terminals that has been implicated in motivation and reward in addition to locomotor activity. These results do not preclude the possibility of the dopaminergic system being involved in the downstream effects of Arc*Pomc* on locomotor activity, but indicate that chronic changes in gene transcription are not part of the mechanism. Rather, genotypic differences in the pattern or amount of dopamine release or receptor sensitivity could underlie the defect in voluntary locomotion observed in Arc*Pomc*-KO mice.

Both WT and Arc*Pomc*-KO mice exhibited profound sex differences in spontaneous home cage and voluntary running wheel behavior. Our results agree with previous studies that found female WT mice exhibited higher activity levels than male WT mice. Weight-matching Arc*Pomc*-KO mice rescued total daily spontaneous home cage activity, but not food anticipatory activity, to the same degree in mice of both sexes, whereas voluntary running wheel activity was more dramatically decreased in female than male Arc*Pomc*-KO mice. Mechanisms underlying sex differences in activity levels is an understudied field, and most reports have not differentiated between spontaneous home cage locomotor activity and running wheel activity. Gonadectomy of either sex reduces locomotor activity levels, and replacement with either estrogen or testosterone rescues that effect, suggesting that both of these hormones can increase locomotion (198). One study implicated estrogen receptor (ER)-α as a mediator of the sex differences in running wheel behavior (199), and approximately 25-30% of ArcPOMC neurons express ER-α (40). Therefore, estrogen signaling in ArcPOMC neurons could be one mechanism by which gonadal hormones influence voluntary activity levels. Another possibility is that estrogen regulates voluntary wheel running behavior via actions at another site and that estrogen levels are decreased by Arc*Pomc* ablation. Circulating levels of sex hormones in Arc*Pomc*-KO mice have not been measured, but the uterine mass of the females is approximately half that of WT, suggesting an estrogen deficiency (unpublished observation).

Mice are known to exhibit food anticipatory activity (FAA) when food access is restricted to a certain time each day. There is extensive evidence that FAA does not rely on any known circadian clock but rather on some as-yet unidentified food entrainable oscillator (112). Whereas I have hypothesized above that spontaneous and voluntary activity may be upregulated when energy balance becomes positive, FAA is believed to reflect foraging behavior and occurs

when rodents are in a negative energy balance. Thus the mechanisms regulating spontaneous/voluntary activity and FAA are unlikely to be the same. Indeed, leptin is not necessary for FAA, as *ob/ob* mice actually exhibited increased FAA over WT mice (95). We have now shown that ArcPOMC is also not necessary for FAA, since it is intact in Arc*Pomc*-KO mice. However, the amplitude of FAA is decreased specifically in male Arc*Pomc*-KO mice. Another group studying male *Mc3r*-KO mice has observed a similar phenotype in those mice (87,88). Therefore, ArcPOMC acting via Mc3r may play a modulatory role in FAA specifically in males, but the physiological significance of this pathway is unclear. Interestingly, FAA comprises a greater percentage of total activity levels in male mice compared to female mice, an effect which is dependent on sex hormones (200). Hypothalamic *Pomc* expression in rats is positively regulated by testosterone (201). Based on these previous studies, the relatively lower level of FAA exhibited by male Arc*Pomc*-KO in comparison to male WT mice could reflect an absence of this "boosting" effect of testosterone on FAA.

Ad libitum-fed Arc*Pomc*-KO mice given access to a running wheel did not have a markedly improved metabolic phenotype. In females, none of the metabolic parameters measured were improved by access to a running wheel, whereas in males, fat mass and cholesterol were somewhat lowered. The study was designed to dissociate positive effects of exercise from those of normalized body weight, but the results are difficult to interpret because obese Arc*Pomc*-KO mice did not exhibit high levels of voluntary running wheel activity. Weight matching Arc*Pomc*-KO mice to WT mice by food restriction did restore plasma glucose, insulin and cholesterol levels to normal even without increasing activity levels, suggesting that reduction in body weight, and in particular fat mass, is the more important factor for promoting metabolic health.

In order to identify potential downstream mediators of Arc*Pomc*'s regulation of locomotion and metabolism, we used qPCR to measure hypothalamic mRNA levels of a panel of candidate genes in the mice from the running wheel study. The anorexigenic peptide *Cartpt* was upregulated in obese Arc*Pomc*-KO mice but normalized after weight-matching, suggesting its upregulation to be a compensatory effect secondary to obesity. The orexigenic peptides *Agrp* and *Npy* were downregulated in obese Arc*Pomc*-KO mice but, with the exception of *Agrp* in males, were not normalized by weight-matching. This suggests that ArcPOMC may directly stimulate expression of *Agrp* and/or *Npy* in the hypothalamus independent of body weight. Another explanation is that, although weight-matched Arc*Pomc*-KO mice weighed the same as WT mice, they still had elevated fat mass and were hyperleptinemic (data not shown), and enhanced leptin signaling to AGRP/NPY neurons could inhibit transcription of those genes. Previously identified putative mediators of physical activity levels include *Bdnf* and *Hcrt* (94), but we found no change in the mRNA levels of these genes in any group studied.

In summary, Arc*Pomc* affects locomotor activity in two distinct ways. Arc*Pomc*-KO mice developed hyperphagic obesity, and as a consequence exhibited decreased levels of spontaneous home cage locomotor activity levels. Thus obesity in Arc*Pomc*-deficiency, while primarily caused by altered food intake, could be exacerbated by decreased spontaneous activity. Arc*Pomc* is not necessary for spontaneous locomotion, as locomotor activity levels of Arc*Pomc*-KO mice were normalized by weight-matching. However, Arc*Pomc* plays a modulatory role in the degree of voluntary running wheel independently of body weight, and Arc*Pomc*-deficiency could additionally contribute to obesity via decreased motivated exercise behavior.

Table 2.1: Primers used for semi-quantitative RT-PCR in the hypothalamus, midbrain and ventral striatum.

Gene Symbol	Gene Name	Forward Primer, 5'-3'	Reverse Primer, 5'-3'
Agrp	Agouti-related neuropeptide	TGTGTTCTGCTG TTGGCACT	GCTCGGTCTGCA GTTGTCTT
Bdnf	Brain-derived neurotrophic factor	TTGTTTTGTGCC GTTTACCA	TGTGATGGGGAT CCTTTTGT
Cartpt	Cocaine and amphetamine-regulated transcript prepropeptide	CGAGAAGAAGT ACGGCCAAG	GTCGTCCCTTCA CAAGCACT
Drd1	Dopamine receptor D1	GAGCGTGGTCTC CCAGAT	GTCCCTAGATTC CCCAAGGA
Drd2	Dopamine receptor D2	AAGCGCCGAGTT ACTGTCAT	GGCACGTAGAAC GAGACGAT
Gapdh	Glyceraldehyde-3-phosphate dehydrogenase	GGTGCTGAGTAT GTCGTGGA	GTGGTTCACACC CATCACAA
Hcrt	Hypocretin (Orexin)	CTCCAGGCACCA TGAACTTT	AGTTCGTAGAGA CGGCAGGA
Mc3r	Melanocortin 3 receptor	AGGAAAGCCCTC ACCTTGAT	GCGAAGAGGAA CATGTGGAT
Npy	Neuropeptide Y	GTGTGTTTGGGC ATTCTGG	TGTCTCAGGGCT GGATCTCT
Pomc	Proopiomelanocortin	GAGCTGGTGCCT GGAGAG	TTTTCAGTCAGG GGCTGTTC
Ppia	Peptidylprolyl isomerase A (Cyclophilin A)	CACCGTGTTCTT CGACATCA	CAGTGCTCAGAG CTCGAAAGT
Slc6a3	Solute carrier family 6, member 3 (Dopamine transporter)	AACCTGTACTGG CGGCTATG	ATGGAGGATGTG GCAATGAT
Th	Tyrosine hydroxylase	TGAAGCCAAAAT CCACCACT	TGACACTTTCCT TGGGAACC

Table 2.2: Metabolic parameters after running wheel access in obese and weight-matched Arc*Pomc*-KO mice.

	Without Wheel		With Wheel			One-way ANOVA
A. Male	**WT**	**Arc*Pomc*-KO**	**WT**	**Arc*Pomc*-KO**	**WM Arc*Pomc*-KO**	F(4,20) =
Body Weight, g	22.1 ± 0.9	43.8 ± 0.9 ***	22.9 ± 0.5	36.8 ± 2.2 ***, †††	22.1 ± 0.3 †††	83.2 *P* < 0.001
Food Intake, g	4.0 ± 0.2	5.9 ± 0.2 ***	3.9 ± 0.1	5.4 ± 0.2 ***	3.7 ± 0.1 †††	25.6 *P* < 0.001
Lean Mass, g	17.4 ± 0.8	23.0 ± 0.5 ***	17.8 ± 0.4	21.1 ± 0.7 ***	15.8 ± 0.3 †††	24.7 *P* < 0.001
Lean Mass, %	76.3 ± 0.7	49.3 ± 0.3 ***	76.6 ± 0.9	52.7 ± 0.8 ***, †	65.9 ± 1.1 ***, †††	253.1 *P* < 0.001
Fat Mass, g	1.5 ± 0.1	17.5 ± 0.3 ***	1.3 ± 0.1	13.5 ± 0.9 ***, †††	4.6 ± 0.4 ***, †††	238.5 *P* < 0.001
Fat Mass, %	6.5 ± 0.5	37.6 ± 0.5 ***	5.7 ± 0.5	33.6 ± 1.0 ***, ††	19.2 ± 1.3 ***, †††	322.1 *P* < 0.001
Fasting blood glucose, mg/dL	89.4 ± 10.9	133.0 ± 9.2 **	89.8 ± 9.5	122.6 ± 11.5	80.8 ± 3.3 ††	6.4 *P* < 0.01
GTT AUC, mg*hr/dL	25584 ± 1898	44393 ± 6781	31223 ± 6166	42559 ± 7238	31161 ± 2224	2.2 n.s.
Fasting plasma insulin, ng/mL	0.44 ± 0.10	3.63 ± 0.31 **	0.52 ± 0.10	3.03 ± 1.00 *	1.46 ± 0.71 †	7.2 *P* < 0.001
Cholesterol, mg/dL	61.8 ± 5.2	91.0 ± 4.0 ***	61.0 ± 2.1	73.2 ± 7.1 †	56.0 ± 2.2 †††	10.5 *P* < 0.001
B. Female						
Body Weight, g	19.0 ± 0.3	39.4 ± 0.4 ***	19.4 ± 0.4	35.3 ± 2.3 ***	20.3 ± 0.4 †††	80.9 *P* < 0.001
Food Intake, g	4.4 ± 0.3	5.9 ± 0.2 ***	4.1 ± 0.2	5.2 ± 0.2	3.2 ± 0.1 **, †††	26.0 *P* < 0.001
Lean Mass, g	14.8 ± 0.4	20.7 ± 0.5 ***	14.9 ± 0.4	18.2 ± 0.9 **, †	13.1 ± 0.2 †††	30.3 *P* < 0.001
Lean Mass, %	76.1 ± 1.1	48.8 ± 0.5 ***	75.5 ± 0.5	47.1 ± 0.7 ***	60.5 ± 0.9 ***, †††	300.1 *P* < 0.001
Fat Mass, g	1.4 ± 0.2	16.7 ± 0.7 ***	1.4 ± 0.1	15.6 ± 1.1 ***	5.3 ± 0.3 ***, †††	154.4 *P* < 0.001
Fat Mass, %	7.4 ± 1.2	39.3 ± 0.7 ***	7.2 ± 0.4	40.3 ± 0.6 ***	24.6 ± 0.9 ***, †††	395.7 *P* < 0.001
Fasting blood glucose, mg/dL	86.4 ± 6.0	109.0 ± 11.3	80.4 ± 3.6	123.4 ± 7.4 **	77.4 ± 4.3 ††	8.7 *P* < 0.001
GTT AUC, mg*hr/dL	24,882 ± 4,714	55,413 ± 9,747 **	24,927 ± 2,933	41,604 ± 5,377	30,845 ± 1,233 ††	6.0 *P* < 0.01
Fasting plasma insulin, ng/mL	0.51 ± 0.24	2.08 ± 0.50	0.60 ± 0.11	3.57 ± 0.87 ***	0.69 ± 0.17	8.8 *P* < 0.001
Cholesterol, mg/dL	46.6 ± 3.9	88.4 ± 3.3 ***	48.4 ± 1.7	83.8 ± 3.3 ***	43.3 ± 2.8 †††	49.7 *P* < 0.001

Measurements in 12-15 week old male (**A**) and female (**B**) WT and obese Arc*Pomc*-KO mice with or without a wheel and weight-matched Arc*Pomc*-KO with a wheel are shown. Data are mean ± SEM and were analyzed by one-way ANOVA between groups (n.s.: not significant). N = 5 per sex and group. * $P < 0.05$, ** $P < 0.01$, *** $P < 0.001$ compared to WT without a wheel; † $P < 0.05$, †† $P < 0.01$, ††† $P < 0.001$ compared to obese Arc*Pomc*-KO without a wheel by Dunnett's post hoc multiple comparison tests.

Table 2.3: Hypothalamic gene expression levels after access to a running wheel in obese and weight-matched Arc*Pomc*-KO mice.

	Without Wheel		With Wheel			One-way ANOVA
A. Male	**WT**	**Arc*Pomc*-KO**	**WT**	**Arc*Pomc*-KO**	**WM Arc*Pomc*-KO**	F(4,20) =
Pomc	100 ± 14	8 ± 2 ***	99 ± 8	7 ± 1 ***	6 ± 1 ***	50.1 $P < 0.001$
Cart	100 ± 4	164 ± 9 ***	98 ± 5	136 ± 12 *	101 ± 12 †††	11.0 $P < 0.001$
Npy	100 ± 12	49 ± 1 ***	87 ± 11	50 ± 1 ***	59 ± 3 **	12.2 $P < 0.001$
Agrp	100 ± 15	50 ± 3 ***	81 ± 7	59 ± 4 **	77 ± 8	6.0 $P < 0.01$
Mc3r	100 ± 1	93 ± 4	84 ± 3	92 ± 6	94 ± 5	1.7 n.s.
Hcrt	100 ± 6	86 ± 3	90 ± 6	84 ± 6	93 ± 10	1.0 n.s.
Bdnf	100 ± 4	104 ± 3	105 ± 5	95 ± 7	94 ± 2	1.2 n.s.
B. Female						
Pomc	100 ± 11	3 ± 0 ***	120 ± 23	4 ± 1 ***	2 ± 0 ***	31.9 $P < 0.001$
Cart	100 ± 12	133 ± 8	84 ± 5	136 ± 7	80 ± 13 ††	6.7 $P < 0.01$
Npy	100 ± 13	43 ± 3 **	77 ± 8	43 ± 3 **	47 ± 10 **	7.7 $P < 0.001$
Agrp	100 ± 9	36 ± 2 ***	106 ± 14	39 ± 6 ***	37 ± 10 ***	14.6 $P < 0.001$
Mc3r	100 ± 10	110 ± 8	86 ± 11	102 ± 10	95 ± 20	0.4 n.s.
Hcrt	100 ± 8	75 ± 9	97 ± 11	74 ± 3	69 ± 12	2.1 n.s.
Bdnf	100 ± 10	86 ± 6	95 ± 15	89 ± 6	105 ± 29	0.2 n.s.

Hypothalamic mRNA levels of genes associated with energy homeostasis and locomotor activity were assayed by semi-quantitative real-time PCR, normalized to *Gapdh*, and expressed as a percentage of WT without a wheel. Data from male (**A**) and female (**B**) WT and obese Arc*Pomc*-KO mice with or without a wheel and weight-matched Arc*Pomc*-KO with a wheel are shown. Data are mean ± SEM and were analyzed by one-way ANOVA between groups (n.s.: not significant). N = 5 per sex and group. * $P < 0.05$, ** $P < 0.01$, *** $P < 0.001$ compared to WT without a wheel; †† $P < 0.01$, ††† $P < 0.001$ compared to obese Arc*Pomc*-KO without a wheel by Dunnett's post hoc multiple comparison tests.

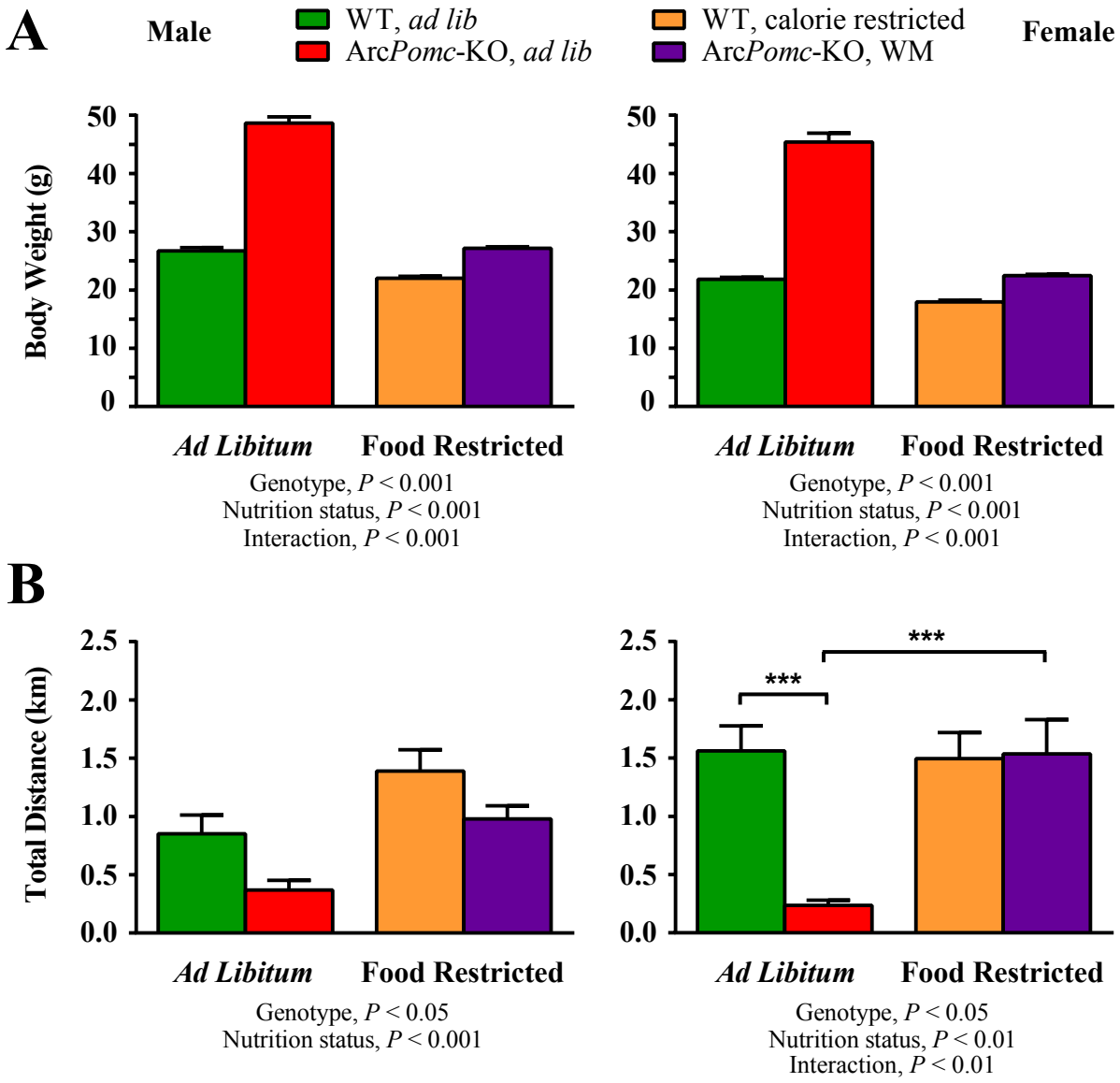

Figure 2.1: Spontaneous home cage locomotor activity levels in obese and weight-matched Arc*Pomc*-KO mice. In both panels, male (left) and female (right) data are shown. **A**, Body weight of 20-week old WT and Arc*Pomc*-KO mice fed *ad libitum* and following 10 weeks of food restriction. RMANOVA showed a significant effect of genotype (Male, $F(1,14) = 403.1$; Female, $F(1,14) = 264.5$), nutrition status (Male, $F(1,14) = 504.1$; Female, $F(1,14) = 361.5$), and an interaction (Male, $F(1,14) = 208.2$; Female, $F(1,14) = 183.6$). **B**, 24-hour spontaneous home cage horizontal locomotion distance of *ad libitum*-fed and food restricted WT and Arc*Pomc*-KO mice. RMANOVA in males showed a significant effect of genotype ($F(1,14) = 7.1$) and nutrition status ($F(1,14) = 29.8$) but no interaction, whereas in females there was a significant effect of genotype ($F(1,14) = 8.1$), nutrition status ($F(1,14) = 9.3$), and an interaction ($F(1,14) = 11.4$). N = 8 per sex and genotype. *** $P < 0.001$ by Sidak's post-hoc multiple comparisons tests. Post hoc test results are not shown in panel A for clarity but each comparison was significant, $P < 0.001$, except between *ad lib* WT and WM Arc*Pomc*-KO, which were not different from each other in either sex.

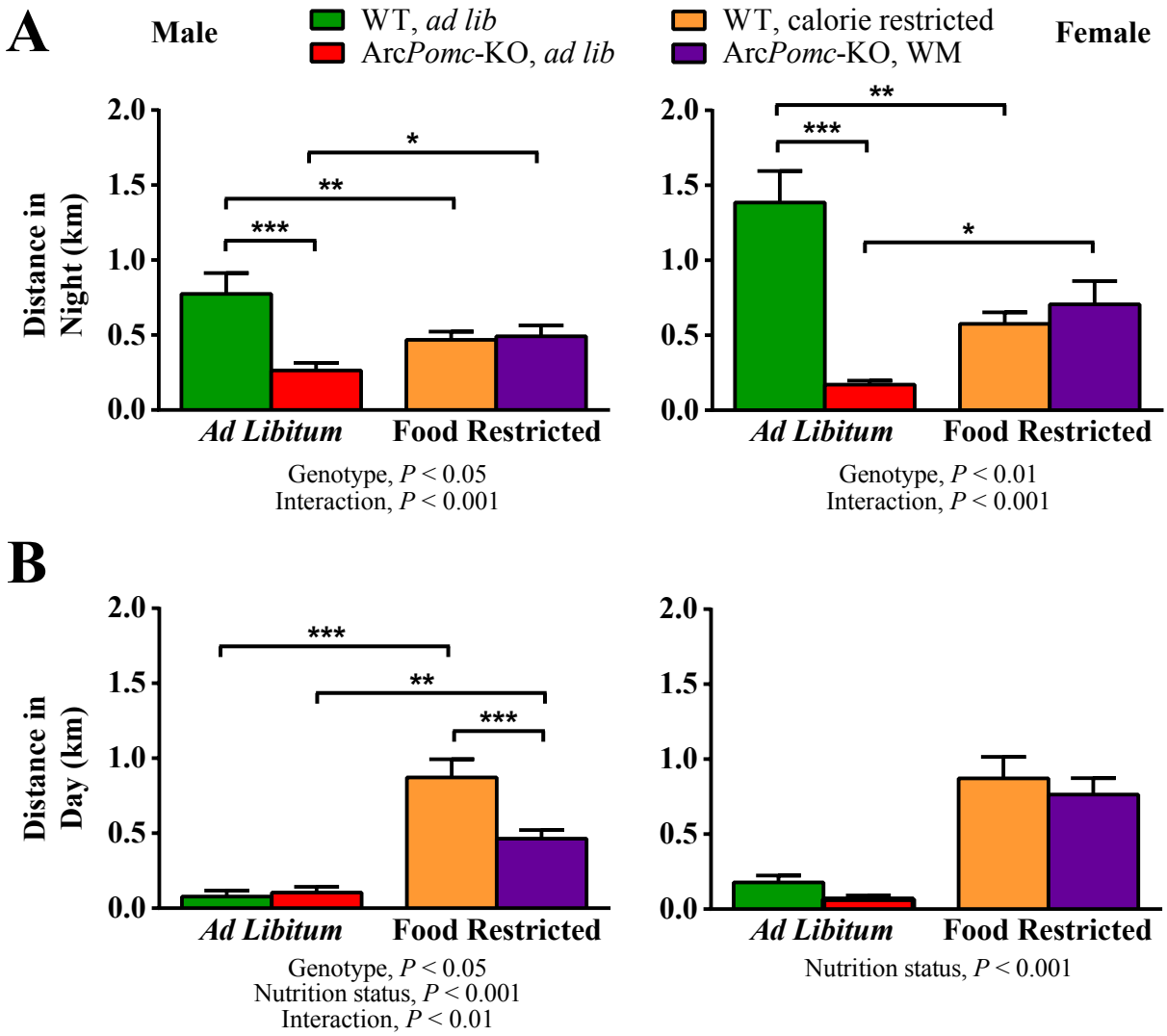

Figure 2.2: Diurnal distribution of spontaneous home cage locomotor activity in obese and weight-matched Arc*Pomc*-KO mice. In both panels, male (left) and female (right) data are shown. **A**, Night-time spontaneous home cage horizontal locomotion distance of *ad libitum*-fed and food restricted WT and Arc*Pomc*-KO mice. In both sexes, RMANOVA showed a significant effect of genotype (Males, $F(1,14) = 5.2$; Females, $F(1,14) = 15.5$) and an interaction between genotype and nutrition status (Males, $F(1,14) = 18.7$; Females, $F(1,14) = 24.1$). **B**, Day-time spontaneous home cage horizontal locomotion distance of *ad libitum*-fed and food restricted WT and Arc*Pomc*-KO mice. In males, RMANOVA revealed a significant effect of genotype ($F(1,14) = 6.6$), nutrition status ($F(1,14) = 65.6$), and an interaction ($F(1,14) = 9.4$), whereas in females there was only a significant effect of nutrition status ($F(1,14) = 66.4$). N = 8 per sex and genotype. * $P < 0.05$, ** $P < 0.01$, *** $P < 0.001$ by Sidak's post-hoc multiple comparisons test.

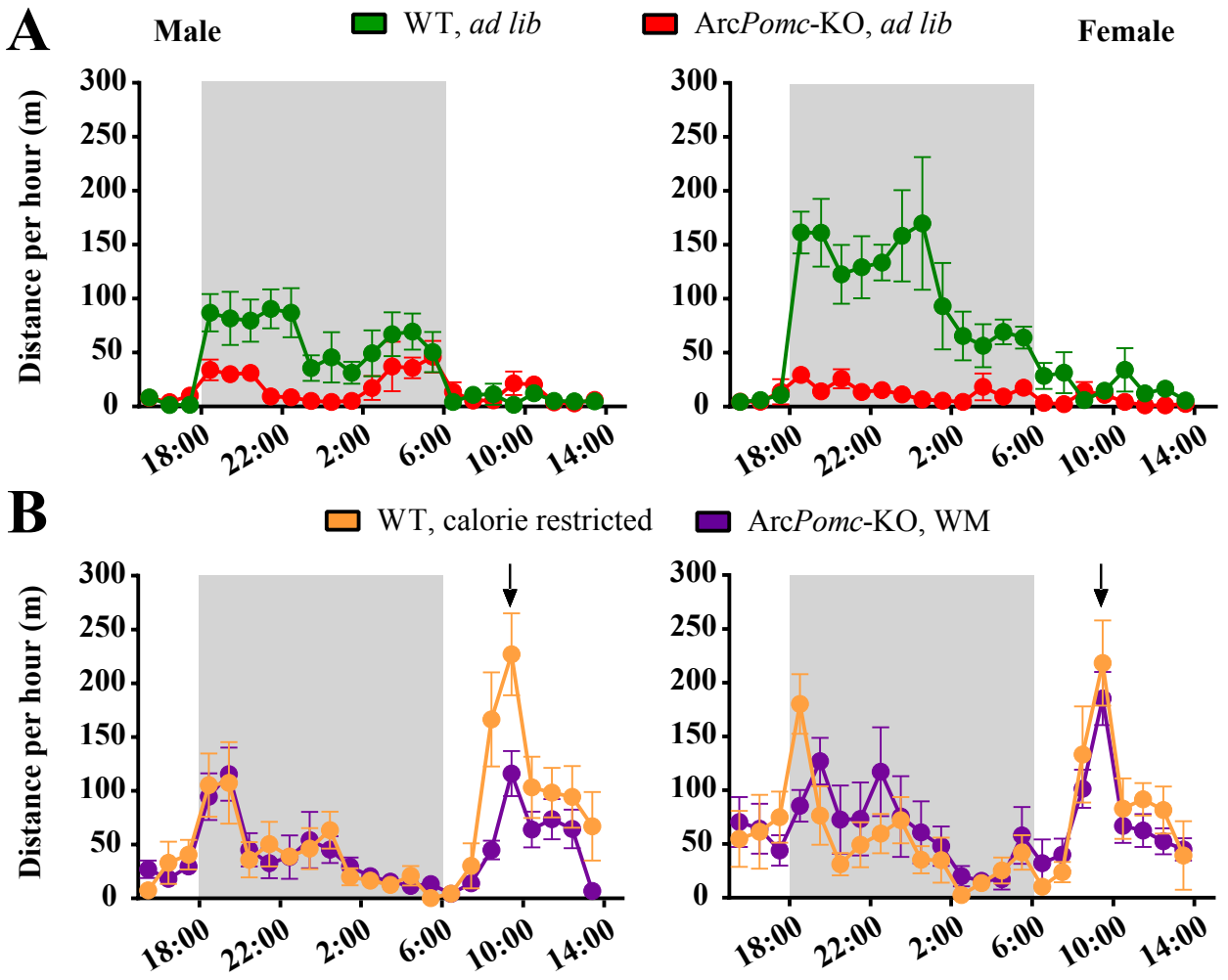

Figure 2.3: Hourly bins of spontaneous home cage locomotor activity in obese and weight-matched Arc*Pomc*-KO mice. In both panels, male (left) and female (right) data are shown and the gray box represents the dark cycle. **A**, Spontaneous home cage horizontal lcoomotor activity of *ad-libitum* fed WT and obese Arc*Pomc*-KO mice in 1-hour bins over 23 hours. **B**, Spontaneous home cage horizontal locomotor activity of food-restricted WT and weight-matched Arc*Pomc*-KO mice in 1-hour bins over 23 hours. Arrows mark the time when the daily food allotment was administered. N = 8 per sex and genotype.

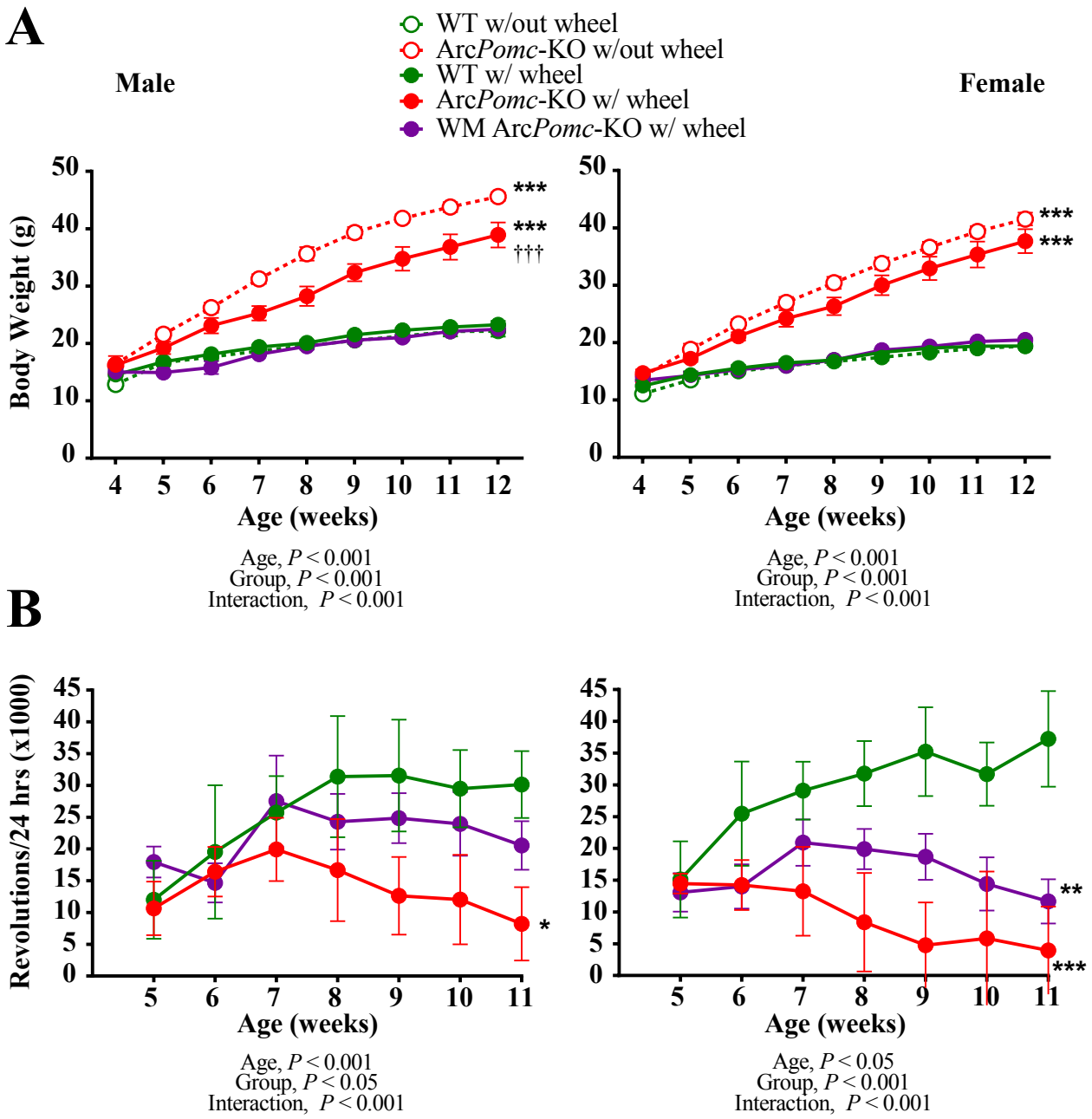

Figure 2.4: Body weight and voluntary running wheel activity in obese and weight-matched Arc*Pomc*-KO mice. In both panels, male (left) and female (right) data are shown. **A**, Body weight measured weekly from age 4-12 weeks in WT and Arc*Pomc*-KO mice with or without a wheel as well as weight-matched (WM) Arc*Pomc*-KO with a wheel. In both sexes, RMANOVA showed a significant effect of time (Males, $F(8,168) = 617.0$; Females, $F(8,176) = 594.4$), group (Males, $F(4,21) = 64.7$; Females, $F(4,22) = 66.8$), and an interaction (Males, $F(32,168) = 55.7$; Females, $F(32,176) = 55.0$). **B**, 24-hour running wheel activity in WT, obese and WM Arc*Pomc*-KO measured weekly from age 5-11 weeks. In both sexes, RMANOVA showed a significant effect of time (Males, $F(6,72) = 10.4$; Females, $F(6,84) = 2.8$), group (Males, $F(2,12) = 4.1$; Females, $F(2,14) = 14.2$), and an interaction (Males, $F(12,72) = 4.4$;

Females, F(12,84) = 6.4). N = 5-7 per sex and group. * $P < 0.05$, ** $P < 0.01$, *** $P < 0.001$ compared to WT without a wheel (Panel A) or WT with a wheel (Panel B); ††† $P < 0.001$ compared to obese Arc*Pomc*-KO without a wheel. Symbols indicate a main difference between groups by Dunnett's post hoc multiple comparisons tests.

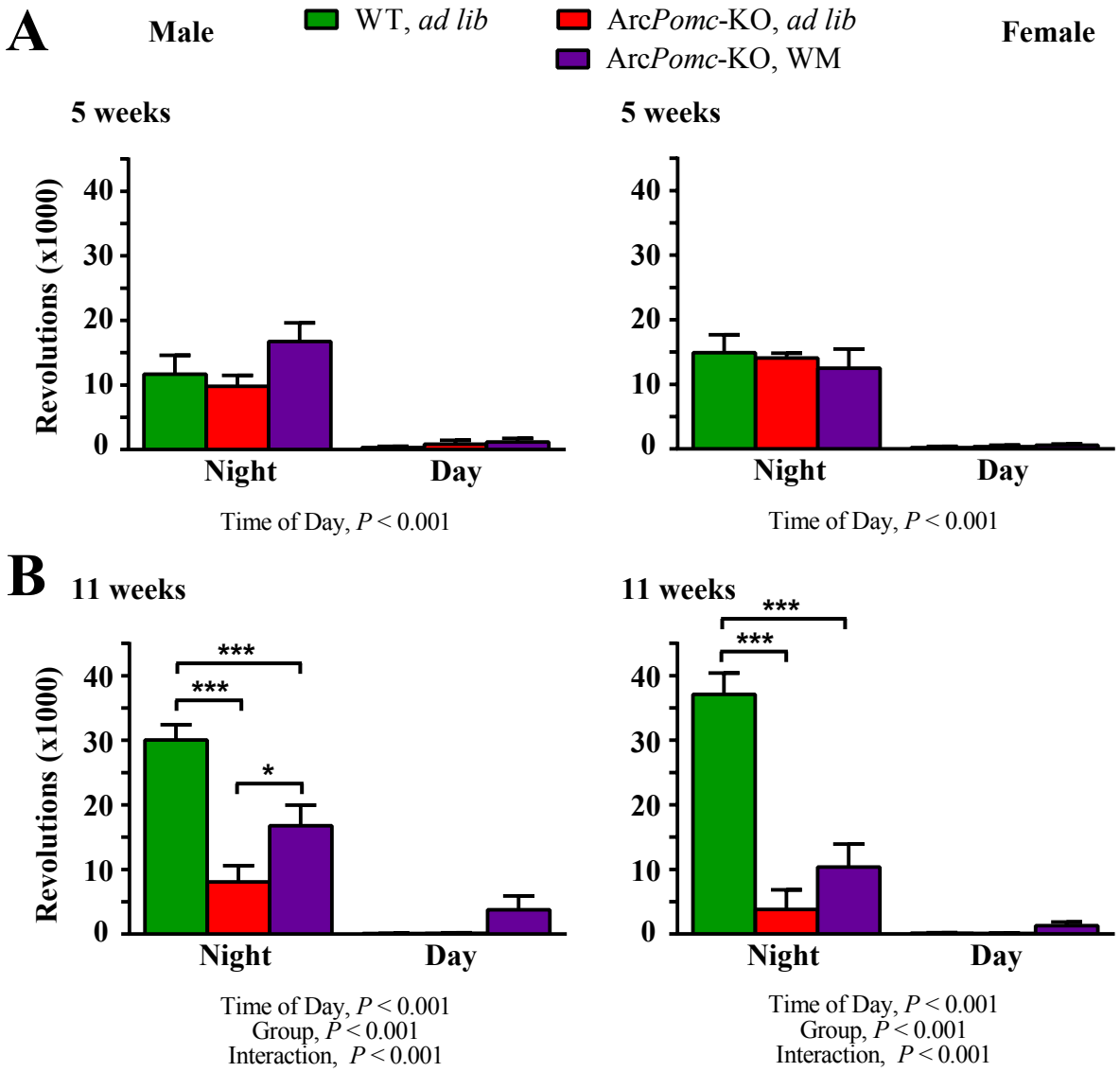

Figure 2.5: Diurnal distribution of voluntary running wheel activity in obese and weight-matched Arc*Pomc*-KO mice. In both panels, male (left) and female (right) data are shown. **A**, Running wheel activity of WT, obese and WM Arc*Pomc*-KO mice at 5 weeks old divided into the 12-hr dark and 12-hr light periods. RMANOVA in both sexes showed a significant effect only of time of day (Male: $F(1,12) = 55.2$; Female: $F(1,14) = 77.2$). **B**, Running wheel activity of WT, obese and WM Arc*Pomc*-KO mice at 11 weeks old divided into the 12-hr dark and 12-hr light periods. RMANOVA in both sexes showed a significant effect of time of day (Male: $F(1,12) = 97.3$; Female: $F(1,14) = 65.4$), group (Male: $F(2,12) = 13.5$; Female: $F(2,14) = 23.3$), and an interaction (Male: $F(2,12) = 15.0$; Female: $F(2,14) = 23.5$). N = 5-7 per sex and group. * $P < 0.05$, *** $P < 0.001$ by Sidak's post hoc multiple comparisons tests.

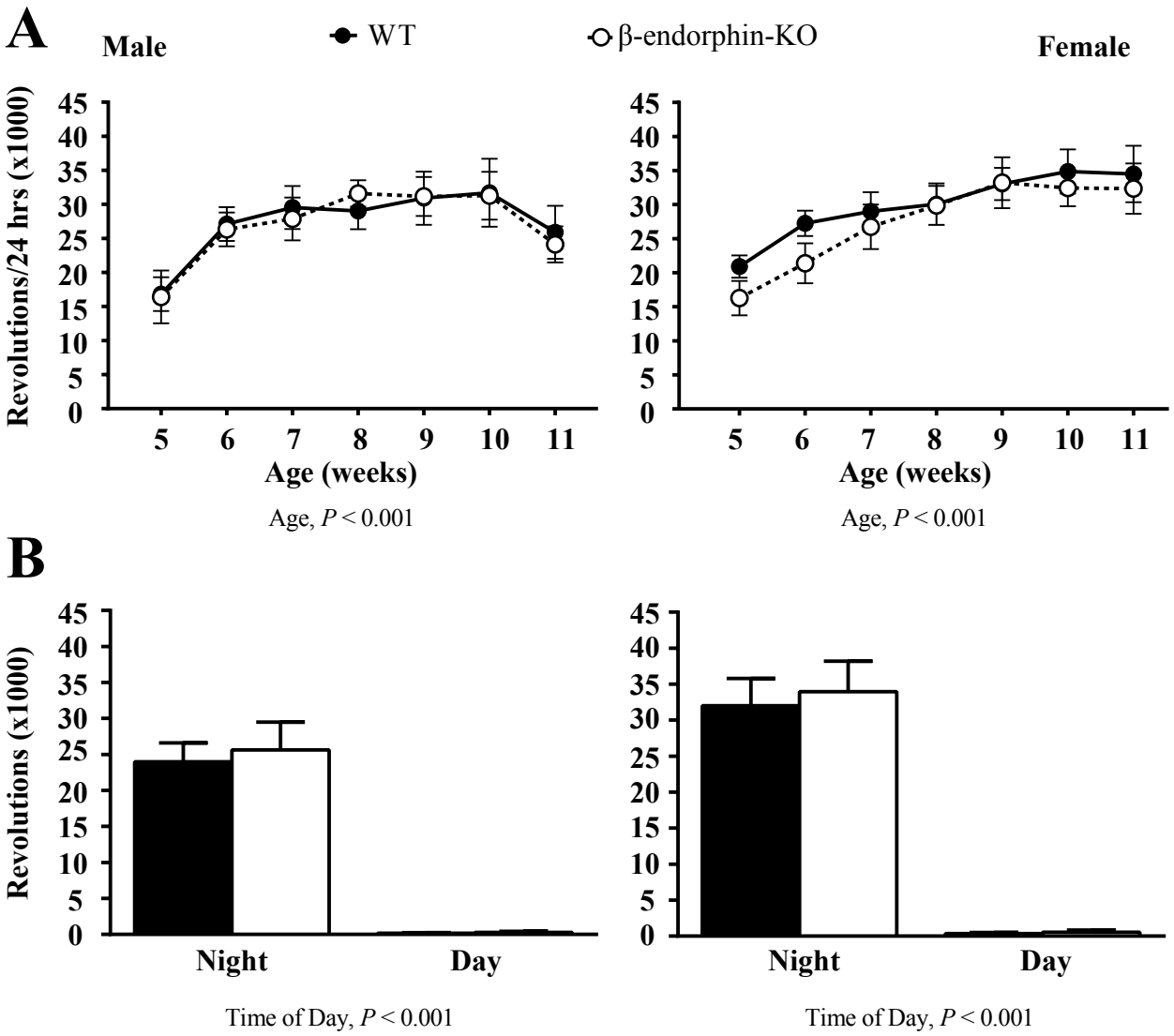

Figure 2.6: Voluntary wheel running activity levels of β-endorphin-KO mice. Male (left) and female (right) data are shown. **A**, 24-hour running wheel activity in WT and β-endorphin-KO mice mouse weekly from age 5-11 weeks. In both sexes, RMANOVA showed a significant effect of time (Males, $F(6,77) = 5.0$; Females, $F(6,72) = 11.8$) but not genotype. **B**, Running wheel activity of WT and β-endorphin-KO mice at 11 weeks old divided into the 12-hr dark and 12-hr light periods. RMANOVA in both sexes showed a significant effect of time of day (Males, $F(1,22) = 102.8$; Females, $F(1,24) = 130.2$) but not genotype. N = 6-7 per sex and genotype.

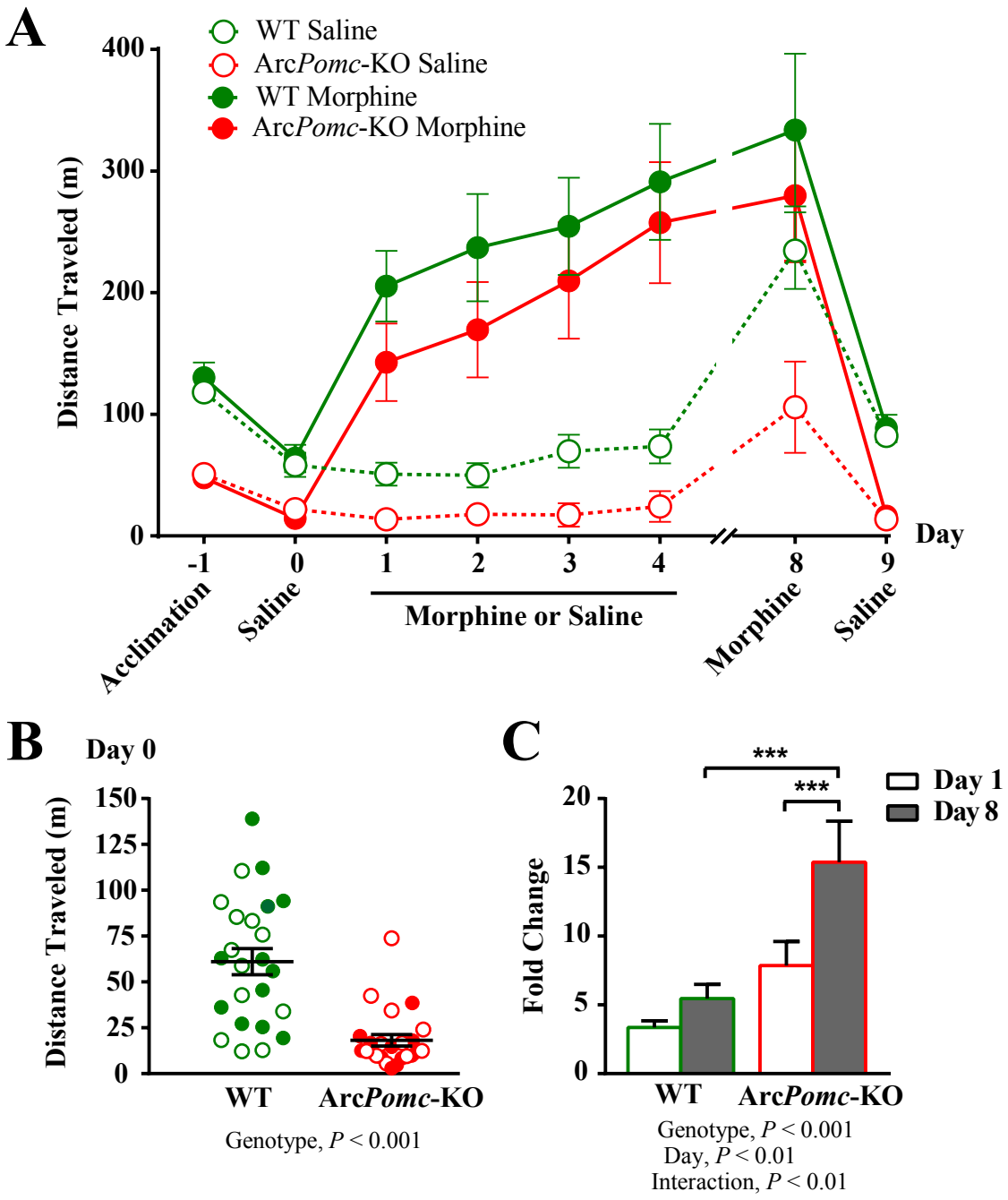

Figure 2.7: Locomotor sensitization to morphine in obese Arc*Pomc*-KO mice. For this study, the sexes were combined. **A**, Distance traveled in one hour by WT and Arc*Pomc*-KO mice in both the saline control and experimental morphine groups on each day of the study. **B**, Distance traveled by each mouse on Day 0 for one hour immediately following i.p. injection of saline. The open versus closed circles indicate the group each mouse was assigned to for the following day of the test. Two-way ANOVA showed no effect of future drug group (saline or morphine) but a significant effect of genotype ($F(1,44) = 29.3$). **C**, Distance traveled by the morphine-administered groups on Day 1 and Day 8 (Panel A) were normalized to the genotype average from Day 0 (Panel B) and expressed as fold change to represent the sensitization

effect. RMANOVA showed a significant effect of genotype ($F(1,22) = 33.5$), day ($F(1,22) = 8.8$), and an interaction ($F(1,22) = 10.6$). N = 12 per genotype and treatment. *** $P < 0.001$ by Sidak's post hoc multiple comparisons tests.

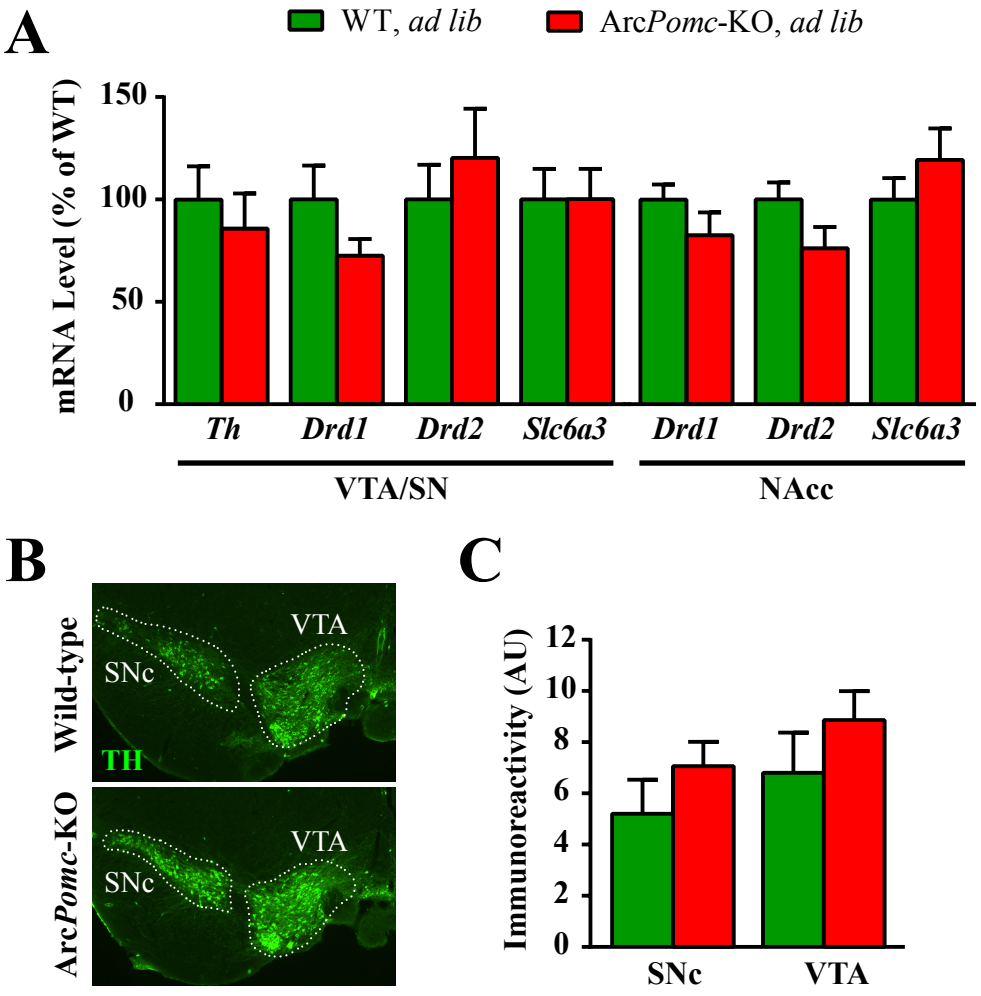

Figure 2.8: mRNA and protein levels of the dopaminergic system in female Arc*Pomc*-KO mice. A, mRNA levels of genes in the dopaminergic system were assayed by semi-quantitative real-time PCR, normalized to *Gapdh* (VTA/SN) or *Ppia* (NAcc) and expressed as a percentage of WT. **B**, Representative images from Bregma -3.08 mm of TH immunoreactivity in the VTA and SNc of each genotype are shown. **C**, Intensity of TH immunostaining in coronal sections 120 μm apart throughout the length of the VTA and SNc was measured and summed in each mouse, and group averages are shown. N = 8 per genotype (Panel A) or 6 per genotype (Panel C). Data were analyzed with unpaired Student's t-test between genotypes but no significant differences were found.

Chapter 3: Arcuate-Specific *Proopiomelanocortin*-Deficiency Activates the Hypothalamic-Pituitary-Adrenal Axis Independently of Vasopressin 1B Receptor[†]

Proopiomelanocortin (POMC) and its bioactive peptides are produced in anterior pituitary corticotroph cells, and peripheral release of these peptides plays a major role in the hypothalamic-pituitary-adrenal (HPA) stress axis. In the absence of pituitary-derived POMC peptides, the HPA axis does not develop at all. The other primary group of POMC-peptide producing cells is a subset of neurons in the arcuate nucleus of the hypothalamus (Arc), which may also play a role in regulating the HPA axis. In this study, we have made use of a recently-developed genetic mouse model that does not express *Pomc* specifically in the hypothalamus but expresses *Pomc* at normal levels in the pituitary (Arc*Pomc*-KO mouse). We have found that Arc*Pomc*-KO mice have a hyperactive HPA axis, as indicated by adrenocortical hypertrophy and elevated circulating plasma stress hormones, in association with increased expression of critical HPA genes in the hypothalamus and pituitary. We identified hypothalamic arginine vasopressin (AVP) acting via AVP receptor 1b (V1bR) in the pituitary as a likely modulator of the HPA axis downstream of Arc*Pomc*. Surprisingly, crossing Arc*Pomc*-KO with *Avpr1b*-KO mice did not rescue the dysregulated HPA axis of Arc*Pomc*-KO mice. Based on these results, we conclude that ArcPOMC tonically inhibits the HPA axis, opposite to the stimulatory actions of pituitary POMC. Consequently, reduced *Pomc* expression in the hypothalamus mediates the central dysregulation of the HPA axis independently of V1br-mediated AVP signaling.

[†] Courtney Attard prepared, processed and analyzed the data presented in Figure 3.5C,D. Mouse colony maintenance and genotyping were performed by Jared Goldberg, Courtney Attard, and Eva Yokosawa. *Avpr1b*-KO mouse line kindly provided by Drs. Kazuaki Nakamura and Akito Tanoue.

Introduction

Proopiomelanocortin (POMC) is a propeptide produced mainly in the arcuate nucleus of the hypothalamus (Arc) and the anterior lobe of the pituitary. POMC peptides released from ~3000 neurons in the Arc play a critical role in the control of food intake and energy expenditure, whereas POMC peptides produced by corticotrophs in the anterior pituitary are mainly involved in activation of the hypothalamic-pituitary-adrenal (HPA) stress axis (7,13,202). Two strains of mice with a global deficiency in the POMC propeptide due to genetic mutation in the *Pomc* gene (*Pomc*-knockout (KO)) have been generated by separate laboratories (23,24). Both strains are hyperphagic and obese due to loss of anorexigenic and catabolic peptide signaling in the central nervous system (CNS). Furthermore, the adrenal glands do not develop properly postnatally secondarily to the absence of circulating adrenocorticotrophic hormone (ACTH). Therefore, *Pomc*-KO mice have no measurable circulating glucocorticoids (GCs) either basally or upon stimulation by a stressor (4,179).

The predominant GC in rodents is corticosterone, which is a critical regulator of the body's response to stress. Corticosterone is the final effector molecule in the HPA stress axis, and GC dysregulation can profoundly impact the immune, cardiovascular, reproductive and metabolic systems. In an effort to separate the primary metabolic role of *Pomc* in the CNS from secondary effects caused by lack of corticosterone, we previously crossed *Pomc*-KO mice with a mouse engineered to carry a transgene directing *Pomc* expression only to pituitary cells but not to neurons, effectively creating a neuron-specific *Pomc*-KO (181). We found that genetic restoration of corticosterone to *Pomc*-KO mice exacerbated their metabolic phenotype, mostly through increased fat accretion, in agreement with another group that restored corticosterone to

Pomc-KO mice via the drinking water (145,181). We predicted that expression of the pituitary-specific *Pomc*-expressing transgene would completely normalize corticosterone in *Pomc*-KO mice, and indeed we found that the diurnal rhythm of corticosterone as well as the rise in corticosterone in response to a stressor were preserved. Surprisingly, specifically in male neuron-specific *Pomc*-KO mice, plasma corticosterone levels were significantly elevated over WT controls (181,182), suggesting a direct role for hypothalamic *Pomc* in inhibition of the HPA axis. However, presence of the *Pomc*-null allele, but not the transgene, was associated with development of late-onset pituitary adenomas, predoimenantly arising from intermediate lobe melanotrophs, complicating our interpretations of these results (182).

The production and release of ACTH in corticotrophs is controlled by corticotropin-releasing hormone (CRH) and arginine vasopressin (AVP), both of which are released into the median eminence by cells in the paraventricular nucleus of the hypothalamus (PVH). The PVH receives and integrates synaptic and peptidergic inputs from across the CNS, including the brainstem, amygdala, hippocampus and other hypothalamic nuclei, but many of these connections have not been fully characterized. ArcPOMC neurons project directly to the PVH and to several candidate relay nuclei such as the amygdala, but a consensus on the role of Arc POMC neurons in regulation of the HPA axis has not been reached.

Opioids are known to have an inhibitory role on the HPA axis, and β-endorphin is one of the cleavage products of the POMC propeptide (183). However, the HPA axis of β-endorphin-KO mice was completely normal (184), suggesting that the specific lack of neuronal β-endorphin did not cause the observed increase in the HPA axis of neuron-specific *Pomc*-KO mice. The other major cleavage products of POMC in the Arc, including α-melanocyte stimulating hormone (MSH) and γ-MSH, are known as the melanocortins. Pharmacological manipulations in

rats have suggested an acute stimulatory rather than inhibitory role for central melanocortins on the HPA axis. Injection of α-MSH or the synthetic melanocortin receptor agonist melanotan II into either the cerebral ventricles or the PVH increased circulating corticosterone for up to thirty minutes (168,170,171,174). Physiologically, *Pomc* is expressed at a relatively constant, high level and is believed to be involved in setting a tonic signal in the brain. Implantation of an ACTH-containing pellet into the median eminence of rats for one week decreased corticosterone (161), suggesting that the melanocortins may affect the HPA axis differently on different time scales. Moreover, there may be a species difference in the actions of the melanocortins on the HPA axis, and similar experiments have not been reported in mice.

In this study, we have found that a newly-developed Arc*Pomc*-KO mouse model, which does not develop pituitary tumors, exhibits the same HPA phenotype as we reported previously in the neuron-specific *Pomc*-KO mouse model, confirming a role for neuronal *Pomc* in the regulation of the HPA axis. We then extensively characterized the HPA axis of Arc*Pomc*-KO mice and identified hypothalamic arginine vasopressin (AVP) as a possible downstream effector for arcuate POMC. To test the role of AVP in the dysregulated HPA axis of Arc*Pomc*-KO mice, we crossed these mice with mice lacking vasopressin receptor 1b (V1bR), the receptor expressed in the anterior pituitary by which AVP regulates release of ACTH, and characterized the HPA axis of the double-knockout (DKO) mice. Unexpectedly, the DKO did not rescue the HPA phenotype of the Arc*Pomc*-KO mice, indicating that arcuate POMC inhibits the HPA axis independently of AVP signaling via V1bR.

Materials and Methods

Animals. All mouse strains were backcrossed onto the C57Bl/6J background for at least ten generations. Arc*Pomc*-KO mice, also called fneoΔ1Δ2, have been described previously and are phenotypically indistinguishable from a similar reactivatable Arc*Pomc*-KO mouse in the absence of rescue (86,186). KO and wildtype (WT) littermates were generated by breeding Arc*Pomc* heterozygotes. *Avpr1b*-KO mice were kindly provided by Dr. Akito Tanoue (203). Heterozygotes were crossed with Arc*Pomc*-heterozygotes to create the experimental Arc*Pomc*:*Avpr1b*-DKO group as well as three control groups: Arc*Pomc*-KO, *Avpr1b*-KO and WT. *Ad libitum* fed mice (standard chow) were housed in groups of 2-5 of mixed genotypes in ventilated cages at 72 ± 2°F with lights on 6:00 am to 6:00 pm and free access to water. For calorie restriction, 20-week old mice were singly-housed and given enough food daily at 10:00 am to obtain and maintain the desired body weight. WT mice were restricted to 85% of their starting body weight and Arc*Pomc*-KO mice were restricted to the average of the starting weight of the WT group for each sex. Animal studies were approved by the University Committee for Use and Care of Animals at the University of Michigan and followed the Public Health Service guidelines.

Stress-free plasma collection. Whole blood for unstressed corticosterone analysis was collected from pair-housed mice via tail nick within 2 minutes of cage disturbance from one mouse per cage per day. Samples were collected at ages 4, 6 and 8 weeks at 9:00 am and at 5:00 pm at least two days apart. Morning and evening samples from the same age were always from the same mouse whereas some mice were also used at multiple ages (n=9-10 per sex, genotype

and age). For analysis of plasma at age 2 weeks, all pups in a litter were decapitated at 5:00 pm, trunk blood collected into heparinized capillary tubes, and a tail sample taken to determine genotype (n=10 per sex and genotype). For the longitudinal study in Figure 3.9, samples were collected at 5:00 pm from the same mice (n=6-8 per sex and genotype) at each age. Blood samples were centrifuged for 10 min at 2,000 rpm and plasma was stored at -20°C prior to hormone analysis.

Restraint stress. All restraint stress experiments were performed for 20 minutes on pair-housed mice between 9:00 am and 10:00 am. For Arc*Pomc*-KO mice and controls at age 8 weeks (n=6-8 per sex and genotype) and Arc*Pomc*:*Avpr1b*-DKO mice and controls at age 16 weeks (n = 6-8 per sex and genotype), a basal blood sample was obtained from both mice in each cage for analysis of basal corticosterone within 2 minutes of cage disturbance. Lean mice were coaxed into a 50-mL conical tube modified with breathing holes whereas obese mice were coaxed into a modified rat restraint device (BrainTree Scientific). For restraint stress of Arc*Pomc*-KO mice and controls at age 4-6 months (n = 5-6 per sex and genotype), a baseline morning plasma sample was collected from one mouse per cage per day. One week later, mice were subjected to restraint as described. For all experiments, mice in the restraint devices were placed back into the home cages for 20 minutes, then immediately removed and euthanized by decapitation. To measure basal ACTH in Arc*Pomc*-KO mice, a separate cohort of pair-housed 8-week old mice (n=7-8 per sex and genotype) and of group-housed 16-week old mice (n = 3-9 per sex and genotype) were euthanized by decapitation at 9:00 am. Trunk blood was collected into a microcentrifuge tube containing 10 µL of 75 mg/ml EDTA, centrifuged at 3,500 rpm, and aliquots of plasma were stored at either -20°C (corticosterone) or -80°C (ACTH) prior to assay.

Hormone analysis. Plasma samples were analyzed for corticosterone by enzyme immunoassay (EIA, Arbor Assays) or for ACTH by enzyme-linked immunosorbent assay (ELISA, MD Bioproducts) or immunoradiometric assay (IRMA, DiaSorin). For the corticosterone assay, plasma was diluted 1:100 in assay buffer, assayed in singlet, and concentration was determined based on the optical density of the standard curve using a four-parameter logistic fit in Prism 6.0 (GraphPad). Sample values below the lowest value on the standard curve (7.8 ng/mL) were assigned that value. For both ACTH assays, 200 µL plasma was required. Individual samples containing less than 200 µL plasma were diluted up to 1:4 in assay buffer, assayed in singlet, and concentration was determined as above, although the readout from the IRMA was cpm as determined by gamma counter. All plasma samples from 8-week old mice were analyzed by ELISA and all samples from 4-6 month old mice were analyzed by IRMA. Sample values below the lowest value on the standard curve (6.2 pg/mL, EIA; 9.9 pg/mL, IRMA) were assigned that value.

Behavioral tests. Two cohorts of mice were administered a battery of 3-4 consecutive tests separated by approximately one week. For young, pre-obese mice, the first test was performed at age 4 weeks and the last at age 8 weeks (n = 6-9 per sex and genotype). The older, obese mice were tested between 12 and 15 weeks of age (n = 5-9 per sex and genotype). For all tests, mice were housed in the adjoining room from the testing room and were brought into the testing room to acclimate for at least 30 minutes, and tests were performed between 9:00 am and 12:00 pm. The open field test was performed first. For three consecutive days, mice were gently placed into a 41 x 41 cm box and their movement was tracked using infrared beams. On the third

day, the total distance moved and the percentage of time each mouse spent in the center of the field was calculated using Activity Monitor software (MedPC). For the elevated plus maze test, each mouse was placed into the center of the maze facing a closed arm. Each arm of the maze measured 30 x 5 cm with a 5 x 5 cm center block between the arms. Movement was recorded by video camera for 5 minutes. The videos were later analyzed for time spent in the closed arms, open arms, or center of the maze. For the forced swim, mice were gently placed into a beaker with diameter 15 cm of room temperature water and their behavior recorded for 6 minutes by video camera. The last 4 minutes of each video was scored for swimming/struggling/climbing or floating behavior. For the novelty-suppressed feeding test, mice were fasted overnight and then placed into a large open field (different from the one mentioned above, but also 41 x 41 cm) with a small piece of regular rodent chow at the center and video recorded for 10 minutes. The videos were analyzed for time to approach food and time to eat food. Following the test, each mouse was returned to the home cage and its behavior monitored for 5 minutes.

Semi-quantitative real-time PCR. Singly-housed 5-6 month old males (n=8 per genotype) were euthanized at 5:00 pm by decapitation and both adrenal glands were collected and stored at -80°C. At age 8 or 16 weeks, pair-housed mice (n = 7-8 per age, sex and genotype) were euthanized by decapitation at 9:00 am, and the hypothalamus and anterior pituitary were dissected and stored at -80°C. Total nucleic acid from each tissue was extracted using RNeasy spin columns (Qiagen) and DNA was removed via Turbo DNase treatment (Life Technologies). Total RNA was quantified and quality-checked via NanoDrop (ThermoScientific). Reverse transcription was performed to produce cDNA from 180 (anterior pituitary) or 500 (hypothalamus, adrenal) ng total RNA using random hexamer primers (Goscript RT System,

Promega). Real-time PCR was performed on all samples in duplicate using the StepOne Real Time PCR System (Applied Biosystems) and SYBR Green Master Mix (Life Technologies). Primers listed in Table 3.1 were designed using Primer3 (187) to span at least one intron, when possible, and were used at a final concentration of 300 nM. The relative quantity of mRNA in the samples was calculated from a standard curve spanning 1000-fold change, normalized to reference gene *Hprt* and then normalized to WT controls. Occasional outliers were identified using Grubbs' outlier test and removed.

Adrenal gland histology and analysis. Histology was performed on the adrenal glands of the WT and Arc*Pomc*-KO control groups from the Arc*Pomc*:*Avpr1b*-DKO study. Glands were stored in 10% buffered formalin at 4°C, and one gland from each mouse was paraffin-embedded in the same orientation by the Morphology and Imaging Module of the University of Michigan Vision Core Center. Each gland was cut on a microtome into the center and 6 μm sections collected onto glass slides. After drying overnight, slides were deparaffinized, stained with Gill's hematoxylin and eosin (H&E), then dehydrated and coverslipped. An image was taken of a representative section from each adrenal under 4X objective using a Nikon 90i upright microscope and DS-Fi1 color camera. In each cross-section, two regions of interest, the entire adrenal gland and only the medulla, were easily visible from the H&E staining and were outlined and the area computed using Elements software (Nikon). From these data the area of the cortex was calculated (total adrenal – medulla).

Immunohistochemistry. For all immunohistochemistry, mice were deeply anesthetized with 2% tribromoethanol and perfused transcardially with 10% sucrose followed by 4%

paraformaldehyde (PFA) in phosphate-buffered saline (PBS) on a pressurized rig (Perfusion One; Leica). Whole pituitaries from 8-10 week old mice (n=5 per sex and genotype) were collected, post-fixed in 4% PFA for 4 hours then saturated in increasing concentrations of sucrose (10%, 20%, 30%) in KPBS for 8-12 hours each at 4°C. Each pituitary was then embedded in OCT (Tissue-Tek) in the same orientation and sectioned at 10 μm on a cryostat (Leica) at -20°C. Sections from the approximate middle of the gland, containing visible sections of all three lobes, were collected directly onto gelatinized slides, dried and frozen at -80°C until use. Brains collected from both 8-week old mice (n=5-6 per sex and genotype) and 20-week old mice (n=6 per sex and genotype) were postfixed overnight in 4% PFA then saturated in increasing concentrations of sucrose (10%, 20%, 30%) in KPBS for 24 hours each at 4°C. Brains were sectioned coronally at 30 μm using a freezing microtome stage (Leica) and free-floating sections were stored in cryoprotectant solution (25 mM PBS with 30% ethylene glycol and 20% glycerol) at -20°C until use.

Immunostaining was performed on slide-mounted pituitary sections that were thawed for one hour and blocked off with a PAP pen (Vector Labs) and on free-floating coronal brain sections approximately 120 μm apart according to the same protocol. Tissue was washed three times for 15 minutes in KPBS and then incubated overnight at 4°C in KPBS with 0.3% Triton X-100 (KPBS-T), 2% normal donkey or goat serum and the primary antibody. Primary antibodies used were rabbit anti-ACTH (1:5,000, The National Hormone and Peptide Program) and guinea pig anti-arginine vasopressin (AVP) (1:1,000, Peninsula Laboratories). Three washes were performed and tissue was incubated in the secondary antibody at room temperature for two hours (donkey anti-rabbit-FITC or goat-anti-guinea pig-FITC, 1:500, Invitrogen). Following additional

washes, free-floating brain sections were then mounted on gelatin coated glass slides and all slides were coverslipped using ProLong Antifade Gold (Invitrogen).

Imaging and Analysis. Sections were imaged using a Nikon 90i upright microscope equipped with an X-Cite 120Q fluorescent light source and CoolSNAP HQ2 CD camera (Photometrics) and a 4X (pituitary) or 10X (brain) objective. Fluorescent signals were detected using a 488 excitation/525 emission filter cube and images were recorded from all sections using a constant exposure time (1.5 s for ACTH, 900 ms for AVP). All post-image analyses were performed in ImageJ (204). In the pituitary, one representative section from each animal was chosen, each lobe outlined manually and the mean intensity and size calculated. To calculate ACTH signal intensity of the anterior lobe, the mean intensity of the posterior lobe (considered background) was subtracted from the mean intensity of the anterior lobe and multiplied by its size. In the brain, four consecutive sections of PVH were imaged utilizing rostral-caudal coordinates obtained from the Mouse Brain Atlas (205) of Bregma -0.70 to -1.06. Each section of PVH was manually outlined along with a background square lateral to the PVH where no signal was visible. The mean background pixel intensity was subtracted from the mean intensity of the PVH and the signal intensities from each of the four sections per animal were added.

In situ hybridization. [^{35}S]-cRNA antisense riboprobes to mouse *Crh* (206) and rat *Avp* (207) were prepared from previously described plasmids. The plasmids were linearized with HindII (*Crh*) or EcoRI (*Avp*) and 1 μg of each linearized plasmid was used for *in vitro* transcription with Sp6 RNA polymerase (Promega) in the presence of [^{35}S]-labeled UTP (Perkin Elmer) to generate the probe. The reactions were allowed to occur for 1.5 hrs at 40°C, remaining

template DNA was digested with RNAse-free DNase for 20 minutes at 37°C and the probes were purified through Sephadex G-50 Illustra NICK columns (GE Healthcare) as described by the manufacturer. Probe radioactivity was counted in a liquid scintillation counter (Perkin Elmer), diluted in hybridization buffer (65% formamide, 13% dextran sulfate, 1.3x Denhardt's solution, 1.3 mM EDTA, 0.26 M NaCl, 13 mM Tris pH 8) (208) at a concentration of 5 x 10^6 cpm/mL and stored at -20°C in 1 mL aliquots.

Pair-housed 8-week old mice were euthanized by decapitation within one minute of cage disruption at either 9:00 am or 5:00 pm (subsequently time points were collapsed, n= 7-9 per sex and genotype). Brains were dissected, flash frozen in isopentane chilled on dry ice, and stored at -80°C. Coronal sections containing the PVH were cut at 16 μm on a cryostat (Leica), collected in three series on gelatinized slides and stored at -80°C. Hybridization was performed as previously described (208). Briefly, sections were fixed for 1 hour in 10% buffered formalin, rinsed in KPBS and acetylated in 0.1 M triethanolamine pH 8 containing 0.25% acetic anhydride. Sections were then rinsed in 2X saline sodium citrate buffer (SSC) and dehydrated through ascending alcohol concentrations. Probe was applied and hybridization was carried out at 60°C for 20 hours. Sections were then washed in 4X SSC and digested with DNase-free RNase A (10 μg/mL) for 25 minutes at 37°C. Finally, sections were desalted in washes of increasing stringency (from 4X SSC to 0.1X SSC) containing 1 mM dithiothreitol, dehydrated through ascending ethanol concentrations and exposed to a storage phosphor screen (Molecular Dynamics) for 3 days (*Crh*) or 1 day (*Avp*). The screen for *Crh* was scanned on a Typhoon 9400 Variable Mode Imager (GE Healthcare) and optical density for PVH of each section quantified using ImageQuant software. For *Avp*, the screen was scanned on a Molecular Imager (BioRad) and optical density for PVH of each section quantified using Personal Imager FX. Representative

images for data presentation in Figure 3.8 were exposed to BioMax MR film (Kodak), developed and scanned into the computer.

Statistics. All data are presented as mean ± SEM. Diurnal corticosterone and qPCR data were analyzed with unpaired Student's t-test between genotypes, and males and females were analyzed separately. The hormonal response to stress was analyzed with either repeated measures ANOVA (RMANOVA) (corticosterone) or a standard two-way ANOVA (ACTH) using genotype and stress as the independent variables. Two-way ANOVA using sex and genotype as the independent variables was performed on adrenal weight, adrenal area, and signal intensity in the ISH and IHC studies. In the DKO experiment, two-way ANOVA was performed with each gene (Arc*Pomc* and *Avpr1b*) as an independent variable. A significant interaction in an RMANOVA was followed by Sidak's multiple comparison post hoc tests whereas a significant interaction in a standard two-way ANOVA was followed by Tukey's multiple comparison post hoc tests. All analyses were performed in Prism 6 (GraphPad).

Results

The HPA axis of Arc*Pomc*-KO mice is dysregulated in a sex- and age-specific manner.

In an effort to separate a primary effect of Arc*Pomc* on the HPA axis from a secondary effect that could be due to obesity or metabolic complications, we measured plasma corticosterone concentrations at the diurnal peak (~5:00 pm) and nadir (~9:00 am) both before and during the initial onset of obesity. Arc*Pomc*-KO mice started to weigh statistically more than WT littermates at age 5-6 weeks, as described previously (86). At 2 weeks of age all mice had

relatively low corticosterone levels at the diurnal peak (Figure 3.1A). This likely reflects that the mice were still in the stress hyporesponsive period, which is characterized by low levels of circulating corticosterone and is believed to end between postnatal days 9 and 18 in mice (209,210). Starting at age 4 weeks, before the onset of obesity in Arc*Pomc*-KO mice, male Arc*Pomc*-KO mice had elevated corticosterone specifically at the diurnal peak whereas female Arc*Pomc*-KO mice were identical to controls (Figure 3.1A). At the diurnal nadir, female Arc*Pomc*-KO mice had elevated corticosterone at age 4 weeks, which normalized by age 6 weeks, whereas male Arc*Pomc*-KO had a trend toward elevated corticosterone levels across all ages (Figure 3.1B).

We next subjected a naïve cohort of 8-week old mice to restraint stress (Figure 3.2). Mice of both sexes and genotypes responded to the stressor with a rise in corticosterone. In males, although basal corticosterone levels were not different, Arc*Pomc*-KO mice showed an exaggerated elevation of corticosterone after stress. On the other hand, there was no effect of genotype in females (Figure 3.2A). ACTH levels were increased in all groups by exposure to a stressor but there was no effect of genotype in either sex (Figure 3.2B).

To assess how this HPA phenotype was affected by age and/or obesity, we repeated the restraint stress experiment in a separate cohort of 4-6 month, obese Arc*Pomc*-KO mice and WT controls. Basal evening corticosterone levels showed the same pattern as in younger mice. Female Arc*Pomc*-KO mice had the same levels as controls (WT, 118 ± 19 ng/mL; Arc*Pomc*-KO, 114 ± 16 ng/mL) and male Arc*Pomc*-KO mice exhibited elevated corticosterone (WT, 46 ± 5 ng/mL; Arc*Pomc*-KO, 138 ± 21 ng/mL; $t(9) = 2.6$, $P < 0.05$). In all groups, restraint stress in the morning caused a significant increase in corticosterone. In males, Arc*Pomc*-KO mice had higher corticosterone than WT both before and after stress, whereas female Arc*Pomc*-KO mice had

increased basal corticosterone but a normal response to stress (Figure 3.3A). Restraint stress also caused a significant increase in plasma ACTH in all groups. Interestingly, in both sexes, Arc*Pomc*-KO mice showed a blunted ACTH response to stress compared to WT although basal ACTH levels were not different (Figure 3.3B).

Arc*Pomc*-KO mice exhibit an anxiety-like behavioral phenotype

The best-characterized anxiety tests require approximately equal levels of locomotion in the study groups, but Arc*Pomc*-KO mice were hypolocomotive as they become obese, as discussed in Chapter 2. We therefore performed anxiety tests on a group of young, pre-obese mice as well as a group of older, obese mice. In the open field, all of the young mice ran approximately the same total distance (Male WT: 46.9 ± 8.4 m; Male Arc*Pomc*-KO: 34.4 ± 5.0 m; Female WT: 36.7 ± 8.2 m; Female Arc*Pomc*-KO: 34.9 ± 3.2 m) but Arc*Pomc*-KO mice of both sexes spent less time in the center of the field, suggesting an anxious phenotype (Figure 3.4A). The same effect held true in older, obese Arc*Pomc*-KO mice, but their total distance traveled in the open field was less than controls (Male WT: 38.2 ± 4.2 m; Male Arc*Pomc*-KO:17.5 ± 1.6 m ; Female WT: 42.8 ± 2.1 m ; Female Arc*Pomc*-KO: 24.6 ± 5.3 m; Effect of genotype in 2-way ANOVA: $F(1,24) = 26.0$, $P < 0.001$).

We next tested anxiety using the elevated plus maze. In young, pre-obese mice, there was no genotype difference in the amount of time spent in the open arms of the maze (Figure 3.4B). However, in the older cohort, Arc*Pomc*-KO mice spent significantly less time in the open arms, indicating an anxious phenotype. Whether this result represents true anxiety or is an artifact of the hypolocomotion in the obese mice is difficult to determine. To test for a depressive phenotype, we also performed the forced swim test. In both the young and older cohorts, there

were no group differences in the amount of time that each mouse spent floating versus struggling or swimming, indicating that Arc*Pomc*-KO mice do not have a depressive phenotype (data not shown).

Lastly, we performed the novelty-suppressed feeding test, reasoning that the presumably higher drive for food in the obese mice may overcome their general hypolocomotive phenotype. This test was performed in 8 week old mice, which are beginning to become obese but are not yet morbidly so. Surprisingly, we found that, although all the mice approached the food during the 10-minute test session (data not shown), only one of the 15 Arc*Pomc*-KO mice started to eat the food. This is in stark contrast to WT controls, which ate the food in an average of about 5 minutes (Figure 3.4C). All mice ate food within 5 minutes of returning to the home cage. These results support the findings of the open field and suggest that Arc*Pomc*-KO mice exhibit an anxious phenotype even at a young age.

Arc*Pomc*-KO mice have an enlarged adrenal cortex

Because basal plasma corticosterone was elevated and corticosterone rose disproportionately to ACTH after restraint stress in Arc*Pomc*-KO male mice, we next examined the adrenal glands. Females had heavier adrenals than males regardless of genotype, and Arc*Pomc*-KO mice of both sexes had heavier adrenals than WT controls (Figure 3.5A). To confirm that adrenal enlargement was not simply due to body weight increase, we also measured adrenal weight in a separate group of Arc*Pomc*-KO mice matched to body weight of WT by caloric restriction. Because food restriction is a stressor itself, we restricted WT mice to 85% of their body weight as a control. Even under these conditions, Arc*Pomc*-KO mice of both sexes had heavier adrenals than WT (Figure 3.5B). H&E staining of representative adrenal cross-

sections from 16-week old obese mice are shown (Figure 3.5C). There was no difference between groups in the area of the medulla. In WT mice, cortical area was larger in female than male mice, and Arc*Pomc*-KO mice of both sexes had significantly larger adrenocortical area than WT controls, but there was no sex difference (Figure 3.5D). Semi-quantitative RT-PCR of whole adrenal gland in obese males revealed up-regulation of several cortex-specific genes involved in ACTH signaling and glucocorticoid biosynthesis in the Arc*Pomc*-KO mice, including the ACTH receptor (*Mc2r*), melanocortin receptor accessory protein (*Mrap*), steroidogenic factor-1 (*Nr5a1*), and 11-β-hydroxylase (*Cyp11b1*), as well as down-regulation of two medulla-specific genes involved in catecholamine synthesis, tyrosine hydroxylase (*Th*) and phenylethanolamine-N-methyltransferase (*Pnmt*) (Figure 3.5E).

Increased expression of ACTH secretagogue receptors in the anterior pituitary of Arc*Pomc*-KO mice

Enlarged adrenocortical area is most often caused by chronic over-stimulation of the adrenal by circulating ACTH. Immunostaining for ACTH in whole pituitary glands (Figure 3.6A) showed no differences between groups in anterior lobe size or number of corticotrophs (data not shown) nor in the intensity of staining in the anterior lobe (Figure 3.6B). Semi-quantitative RT-PCR was used to compare mRNA levels in the anterior lobe from mice at two ages. mRNA levels of corticotropin releasing hormone receptor 1 (*Crhr1*) and vasopressin receptor 1b (*Avpr1b*) were increased at both ages 8 weeks and 16 weeks in male Arc*Pomc*-KO mice, whereas female Arc*Pomc*-KO mice only showed elevated *Crhr1* levels at 16 weeks (Figure 3.6C,D). *Pomc* mRNA levels were not different between genotypes at either age. In females, CRH binding protein (*Crhbp*) levels were decreased in Arc*Pomc*-KO mice at both ages.

Hypothalamic arginine vasopressin is increased in Arc*Pomc*-KO mice

Semi-quantitative RT-PCR was also used to assay hypothalamic gene expression at age 8 weeks and 16 weeks. At age 8 weeks, hypothalamic mRNA levels of *Crh*, *Avp*, glucocorticoid receptor (*Nr3c1*), and *Crhbp* were not different between genotypes, but neuropeptide Y (*Npy*) was significantly lower in Arc*Pomc*-KO mice of both sexes than in WT controls (Figure 3.7A). At age 16 weeks, *Npy* was still decreased in Arc*Pomc*-KO mice. In addition, *Avp* was significantly increased in Arc*Pomc*-KO mice of both sexes, whereas *Crh* was increased only in males (Figure 3.7B).

To confirm the gene expression changes identified in the hypothalamus and to increase our spatial resolution, we performed *in situ* hybridization (ISH) for *Crh* and *Avp* in unstressed 8-week old mice. In the PVH, no differences between genotypes were found in the intensity of *Crh* signal, whereas *Avp* signal intensity was elevated in the PVH of Arc*Pomc*-KO mice (Figure 3.8A,B). Using immunohistochemistry (IHC) to semi-quantitatively compare protein levels, we found that the PVH in Arc*Pomc*-KO of both sexes had more intense staining for AVP than WT, and female Arc*Pomc*-KO mice had even higher staining intensity than male Arc*Pomc*-KO mice, although no sex difference was apparent in WT animals (Figure 3.8C,D). The numbers of cells positive for AVP per PVH was not different between groups (data not shown).

V1bR signaling does not mediate the dysregulated HPA axis of Arc*Pomc*-KO male mice

To test the role of elevated AVP in the dysregulated HPA axis of Arc*Pomc*-KO mice, we generated a double knockout also lacking the vasopressin 1B receptor (Arc*Pomc*:*Avpr1b*-DKO). At age 16 weeks, in both sexes, mice possessing the Arc*Pomc*-KO allele had heavier adrenals

than WT regardless of *Avpr1b* genotype. In females, *Avpr1b*-KO was associated with a slight but significant decrease in adrenal weight consistent with the original report of these mice (203), but there was no interaction with the Arc*Pomc* allele (Figure 3.9A).

Non-stressed plasma samples were taken for corticosterone analysis at the circadian peak at multiple ages between 6 and 16 weeks (Figure 3.9B). Male mice lacking the Arc*Pomc* gene had higher corticosterone at each time point measured regardless of *Avpr1b* genotype, whereas there were no differences in females. Lack of V1br was associated with increased corticosterone in males at age 8 weeks but a decrease in females at age 16 weeks.

Finally, we studied the hormonal response of the DKO mice to restraint stress (Figure 3.9C). In males, in agreement with Figure 3.3A, baseline morning plasma corticosterone levels were elevated in mice possessing the Arc*Pomc*-KO allele, whereas there was no difference in females and no effect of the *Avpr1b* allele. Following 20 minutes of restraint stress, corticosterone levels were significantly elevated from baseline in all four groups. In males, mice lacking the Arc*Pomc* allele had higher corticosterone stress response than those with the WT allele. Additionally, there was a decrease in the corticosterone response to stress specifically in *Avpr1b*-KO mice as related to WT, whereas the *Avpr1b* allele did not affect corticosterone in mice lacking Arc*Pomc.* In females, surprisingly, both the Arc*Pomc*-KO and *Avpr1b*-KO allele were associated with a slightly decreased corticosterone stress response.

Discussion

Using genetic mouse models coupled with an array of molecular biological techniques, we have identified Arc*Pomc* as an important regulator of the HPA axis. Furthermore, we have

proven that this regulation, although associated with changes in hypothalamic vasopressin levels, does not depend on signaling via V1br. These data support and significantly expand upon previous data from our laboratory that used a similar genetic model for Arc*Pomc*-deficiency. Our results suggest that ArcPOMC may have two distinct roles in the regulation of the HPA axis. First, it appears to be necessary to masculinize the HPA axis in development. Second, ArcPOMC may be involved in the control of the HPA axis by metabolic signals such as insulin and leptin.

Sexual dimorphism of the HPA axis, wherein adult females have higher corticosterone levels than males both basally throughout the circadian cycle and in response to a stressor, has been well characterized in rats and mice (for review, see (211)). The ontogeny of these sex differences is poorly understood, although it is generally accepted that the HPA axis is intrinsically feminine and can be masculinized by a perinatal testosterone surge (212). Testosterone can signal via the androgen receptor (AR) or it can be converted to estradiol, by aromatase, and signal via the estrogen receptors (ER-α, ER-β). Indeed, studies in rats have implicated an organizational role for both testosterone and estrogen signaling in the masculinization of the HPA axis (213), but the neural mechanism is completely unknown.

The sexual dimorphism of basal corticosterone has been reported as early as age 5 weeks in mice (214). Many studies measure basal corticosterone in the morning, close to the diurnal nadir, but sex differences are more easily apparent closer to the diurnal peak (215). By analyzing corticosterone at both time points, we have extended these previous results by reporting a sex difference in plasma corticosterone in WT mice at 4 weeks of age. Starting at this age, the plasma corticosterone level of male Arc*Pomc*-KO mice was significantly elevated from WT male but indistinguishable from female mice. This suggests that ArcPOMC is necessary for the masculinization of the HPA axis in development.

A possible role for ArcPOMC in the sexual differentiation of the brain has not been previously explored. In adult mice there are only approximately 3,000 POMC neurons in the Arc (5), but *Pomc* is expressed transiently during mid-gestation in Arc progenitor cells that go on to become AGRP or kisspeptin-positive and POMC-negative (51,53). Almost all ArcPOMC neurons in development, starting at embryonic day 15.5 (e15.5), express ER-α, which can bind to the upstream neuronal enhancer region of the *Pomc* gene *in vitro* (40). Additionally, many Arc neurons express AR by e15.5 (216). In adult rats, *Pomc* expression is positively regulated by testosterone following its conversion to estradiol (201,217), but similar experiments have not been reported in neonatal mice. Thus ArcPOMC neurons in development, regardless of whether they express *Pomc* in adulthood, could be directly stimulated by the perinatal testosterone surge and play an important role in the masculinization of the HPA axis.

Neuropsychiatric disorders such as depression and anxiety are more prevalent in females than males and can be associated with an elevated HPA axis as well as obesity. To determine whether Arc*Pomc*-KO mice had a depressed or anxious phenotype, we performed a battery of behavioral tests. Using the forced swim as a measure of depression, we found that the Arc*Pomc*-KO mice did not exhibit a depressive phenotype. To control for the hypolocomotion apparent in obese Arc*Pomc*-KO mice, we performed anxiety tests in both young, pre-obese mice as well as older, obese mice. The results from the open field and, particularly, the novelty-suppressed feeding tests suggest that Arc*Pomc*-KO mice exhibit an anxious phenotype even from a young age. The fact that young Arc*Pomc*-KO mice of both sexes show the same phenotype suggests that the anxiety may not be due to a dysregulated HPA axis or obesity. Rather, melanocortin signaling in the brain may directly act as an anxiolytic, although there are some studies suggesting the opposite (218).

As early as 2 months of age, both male and female Arc*Pomc*-KO exhibited adrenocortical hypertrophy and by 4-6 months they showed a relative flattening of the diurnal HPA rhythm due to increased nadir corticosterone levels as well as a decreased ACTH, but normal or exaggerated corticosterone, response to stress. Rodent models of type I and type II diabetes mellitus (DM) which lack insulin and leptin, respectively, show a similar array of HPA abnormalities. Peripheral injection of streptozotocin (STZ) selectively kills the pancreatic β-cells, results in hypoinsulinemia and hyperglycemia, and is used as a model for type I DM (219). STZ-treated diabetic rats exhibited elevated ACTH and corticosterone particularly at the diurnal nadir and a blunted rise in ACTH and corticosterone upon stimulation by a stressor, all of which was normalized by administration of exogenous insulin (220-224). Leptin-deficient *ob/ob* mice, which are morbidly obese and are used as a model of type II DM (134), showed increased adrenocortical volume (225-227) and elevated corticosterone both basally throughout the diurnal cycle and in response to stress (135-137,228). Treatment of *ob/ob* mice with exogenous leptin decreased but did not normalize basal and stressed corticosterone levels (229,230), and leptin decreased the corticosterone response to fasting and restraint stress in WT mice (231,232).

Arc*Pomc*-KO mice are not considered a model of DM because, although they are hyperleptinemic, hyperinsulinemic and insulin resistant, fasting blood sugar is relatively normal (86). Indeed, although there is a tight relationship between hyperglycemia and HPA overactivation, causing many groups to assume causality, at least one study has reported that hyperglycemia is not necessary for HPA axis dysregulation in type I DM (233). Rather, HPA dysregulation in DM could be due to altered signaling by leptin and/or insulin and independent of blood glucose levels. Approximately 70% of ArcPOMC neurons express leptin receptor (LepR) and are activated by leptin (5,34). Arc*Pomc* neurons also express insulin receptor (InsR)

and insulin stimulates *Pomc* expression (38). Thus it is possible that leptin and/or insulin could directly activate ArcPOMC neurons and thereby inhibit the HPA axis. However, mice lacking either the LepR or the InsR or both specifically on cells expressing *Pomc* have been reported to have normal basal and stressed corticosterone levels, so it is also possible that leptin and/or insulin could activate ArcPOMC neurons indirectly (47,234,235). Supporting this idea, mice lacking InsR in the whole hypothalamus showed elevated basal and stressed corticosterone, a phenotype that was somewhat recapitulated when InsR was ablated only from AGRP neurons (236). Thus our current study suggests that ArcPOMC neurons may integrate leptin and insulin signaling onto the HPA axis and that leptin and/or insulin resistance at the level of the Arc could contribute to HPA dysregulation seen in DM.

Other studies have identified NPY, which is co-expressed in AGRP neurons in the Arc, as a neuropeptide that is inhibited by insulin and leptin and can activate the HPA axis (230,231,237-239). *Npy* is upregulated in the hypothalamus of both STZ-treated rats and *ob/ob* mice (240-242), suggesting that elevated NPY may play a role in the hyperactivation of the HPA axis in DM. In Arc*Pomc*-KO mice, hypothalamic *Npy* levels are markedly decreased below those of WT even at a young age. It seems likely that the decreased *Npy* levels are a direct result of hyperleptinemia, but this phenotype needs to be explored further. The fact that similar HPA phenotypes are observed in models that are associated with either marked increase or marked decrease in hypothalamic NPY suggests that there are parallel pathways by which insulin and/or leptin can affect the HPA axis at the level of the Arc. Alternatively, STZ-treated rats and *ob/ob* mice also showed markedly decreased hypothalamic *Pomc* (243,244), and the lack of inhibitory POMC could activate the HPA axis independently of NPY. *Npy*-KO mice have normal corticosterone (245,246). Interestingly, deletion of the NPY receptor 2 from *ob/ob* mice

increases arcuate *Pomc* mRNA and normalizes corticosterone levels, suggesting POMC could be downstream of the effects of NPY on the HPA axis (247).

The initial cause of the dysregulation of the HPA axis in DM is unclear, but constantly elevated corticosterone acts as a chronic stressor. AVP has been shown to play an important role in regulating ACTH release in several models of chronic stress (248,249). Both STZ-treated rats and *ob/ob* mice, along with the Arc*Pomc*-KO mice, had increased expression of *Avp* mRNA in the hypothalamus (250,251). To test the role of AVP signaling via pituitary V1bR in the dysregulated HPA axis of Arc*Pomc*-KO mice, we crossed these mice with *Avpr1b*-KO mice. In agreement with previously published results, we found that female, but not male, mice homozygous for the *Avpr1b*-KO allele had slightly decreased adrenal gland size, and homozygous mice of both sexes had a somewhat blunted corticosterone response to stress (203). However, these differences were not affected by Arc*Pomc* genotype and deletion of the *Avpr1b* gene did not rescue the increased adrenal size and elevated corticosterone levels of Arc*Pomc*-KO mice. Therefore we conclude that HPA dysregulation in Arc*Pomc*-KO mice occurs independently of AVP signaling via the V1bR despite upregulation of AVP in the hypothalamus and *Avpr1b* in the pituitary of these mice. In agreement with our results, Brattleboro rats, which do not produce AVP, showed the same increase in adrenal size and plasma corticosterone following STZ treatment as did normal rats (252).

Having eliminated AVP, it is likely that CRH is the downstream factor inducing dysregulation in the HPA axis of Arc*Pomc*-KO mice. *Crhr1* mRNA in the anterior pituitary was also increased in male Arc*Pomc*-KO mice at both ages studied and in older female Arc*Pomc*-KO mice. In the hypothalamus, elevated *Crh* was seen only in older male Arc*Pomc*-KO mice. Further experiments will be necessary to confirm and characterize a role for CRH in the

described HPA phenotype. Interestingly, specifically in females, *Crhbp* levels were markedly downregulated in the anterior pituitary of Arc*Pomc*-KO mice. This is likely secondary to disruption of the hypothalamic-pituitary-gonadal axis. Although we did not measure plasma estrogen directly, the uterine weight of Arc*Pomc*-KO mice is approximately half that as WT (unpublished observation), indicating decreased estrogen levels. CRH-BP has been shown to be positively regulated by estrogen (253,254).

Because the HPA phenotype of Arc*Pomc*-KO mice described herein does not occur in β-endorphin-KO mice (184), we posit that it is caused specifically by lack of melanocortin signaling in the brain, where melanocortins signal via two known receptors, the melanocortin 3 and 4 receptors (Mc3r, Mc4r). As mentioned above, acute central injection of Mc3r/Mc4r agonists activated the HPA axis in rats (168,170,171,174). This activation could be prevented by pretreatment with an Mc4r-specific antagonist (170), and Mc4r-KO rats showed a reduced HPA response to restraint stress (177). Together, these studies suggest that signaling via the Mc4r can activate the HPA axis, whereas our data shows that elimination of the endogenous agonist of the Mc4r activates the HPA axis. The discrepancy here could be explained by a species-specific difference in the role of POMC on the HPA axis. Knockout mice of each receptor have been generated, but the HPA axis of these knockouts has not been well characterized beyond reports of normal basal corticosterone at a single time point (25-27). Alternatively, the phenotype we have described in this study is likely due to a combined loss of signaling at both Mc3r and Mc4r and suggests that Mc3r may be more important in regulation of the HPA axis than previously acknowledged.

In conclusion, in addition to its well-characterized roles in feeding behavior and energy expenditure, Arc*Pomc* is involved in regulation of anxious behavior and the HPA axis. Mice

lacking Arc*Pomc* show an anxious phenotype and have a hyperactivated HPA axis as indicated by elevated basal and stress-induced corticosterone levels and adrenal hypertrophy. Although these mice also have elevated hypothalamic AVP as well as increased expression of *Avpr1b* in the anterior pituitary, signaling via this pathway is not necessary for the hyperactive HPA axis observed. Together these results suggest neural melanocortins as a novel target that tonically inhibits the HPA axis as well as prevents anxious behavior.

Table 3.1: Primers used for semi-quantitative RT-PCR analysis of the HPA axis.

Gene Symbol	Gene Name	Forward Primer, 5'-3'	Reverse Primer, 5'-3'
Avp	Arginine vasopressin	TCGCCAGGATGC TCAACAC	TTGGTCCGAAGC AGCGTC
Avpr1b	Arginine vasopressin receptor 1b	ATCCGAACCGTG AAGATGAC	CAGAAGCATCGA GATGGTGA
Crh	Corticotropin releasing hormone	CACCTACCAAGG GAGGAGAA	GCGGGACTTCTG TTGAGATT
Crhbp	Corticotropin releasing hormone binding protein	ATGATGCCCTTA GCAGACCTGTGT TAC	CAAATGTCACAC GGTTAATGTGTT TCC
Crhr1	Corticotropin releasing hormone receptor 1	CGCAAGTGGATG TTCGTCT	GGGGCCCTGGTA GATGTAGT
Cyp11b1	Cytochrome P450, family 11, subfamily b, polypeptide 1	CTCCATGTTCAA AACCACCA	CTGCCAGCTCTC GATACACA
Hprt	Hypoxanthine-guanine phosphoribosyltransferase	GATTAGCGATGA TGAACCAGGTT	CCTCCCATCTCC TTCATGACA
Mc2r	Melanocortin-2 receptor (ACTH receptor)	GTGACAAAGCCA AGGAGAGG	TGGTGTTTGCCG TTGACTTA
Mrap	Melanocortin 2 receptor accessory protein	CCGCTCACCAGC TATGAGTA	AGAAAGAGGAG CACCACGAA
Npy	Neuropeptide Y	GTGTGTTTGGGC ATTCTGG	TGTCTCAGGGCT GGATCTCT
Nr3c1	Glucocorticoid receptor	AGGCCGCTCAGT GTTTTCTA	ACACGTCAGCAC CCCATAAT
Nr5a1	Steroidogenic factor 1, Sf-1	ATCTACCGCCAG GTCCAGTA	GCATGCAACTGG AGCACTAA
Pnmt	Phenylethanolamine-N-methyltransferase	AGACCTGAGCAA CCCTGATG	TGGTGATGTCCT CAAAGTGG
Pomc	Proopiomelanocortin	GAGCTGGTGCCT GGAGAG	TTTTCAGTCAGG GGCTGTTC
Th	Tyrosine hydroxylase	TGAAGCCAAAAT CCACCACT	TGACACTTTCCT TGGGAACC

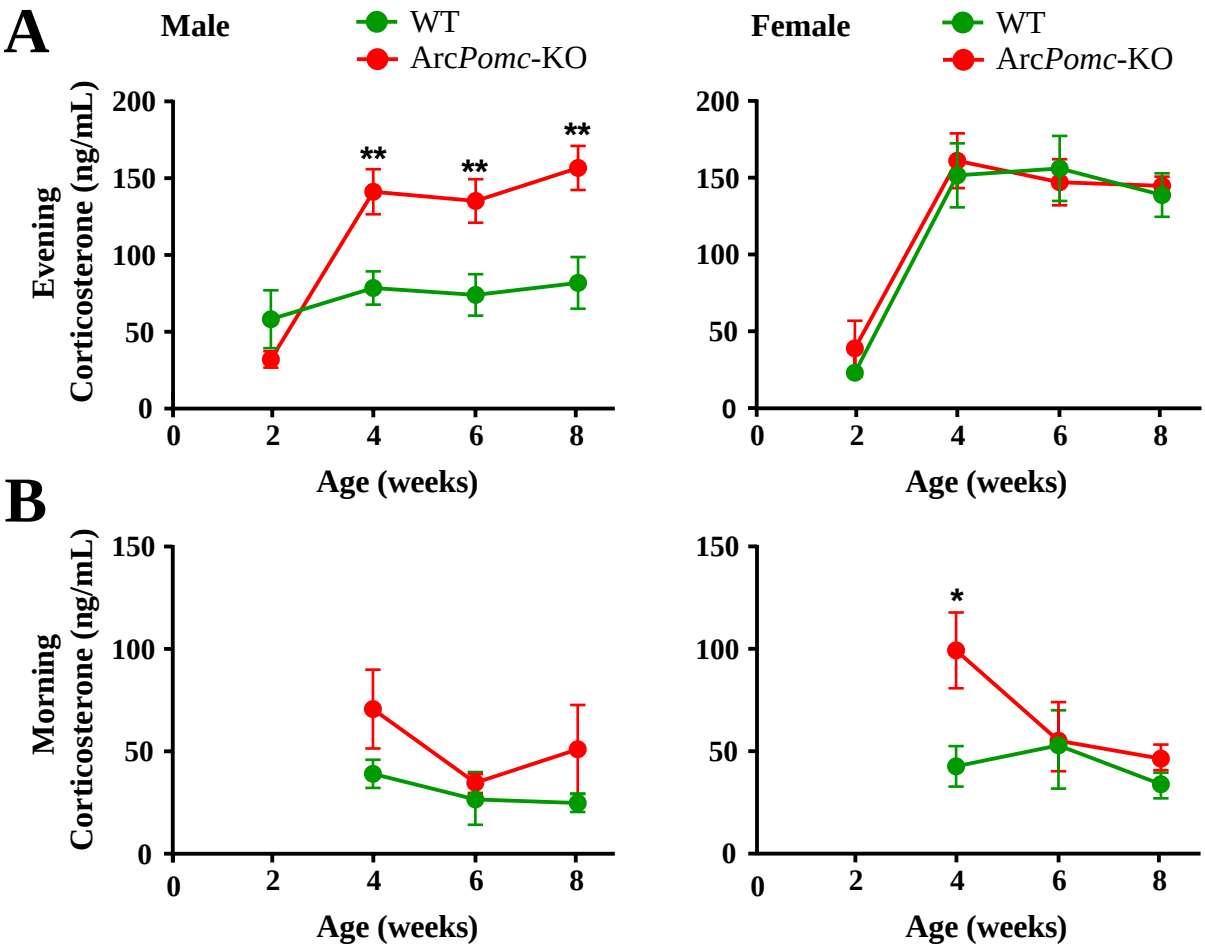

Figure 3.1: Diurnal rhythm of plasma corticosterone during development in Arc*Pomc*-KO mice. In both panels, male (left) and female (right) data are shown. **A**, Unstressed corticosterone levels at the diurnal peak (5:00 pm) from ages 2-8 weeks. Analysis of each time point by unpaired Student's t-test between genotypes showed that male Arc*Pomc*-KO mice had higher corticosterone than WT at ages 4-8 weeks (4 weeks, $t(18) = 3.4$; 6 weeks, $t(18) = 3.1$; 8 weeks, $t(18) = 3.4$). **B**, Unstressed corticosterone levels at the diurnal nadir (9:00 am) from age 4-8 weeks. Two-way ANOVA revealed a strong trend towards a genotype effect in males ($F(1,54) = 4.0$, $P = 0.051$). Analysis of each time point by unpaired Student's t-test between genotypes showed that female Arc*Pomc*-KO mice had higher corticosterone than WT at age 4 weeks ($t(19) = 2.6$). N = 9-10 per sex, genotype and age. * $P < 0.05$; ** $P < 0.01$ by unpaired Student's t-test between genotypes.

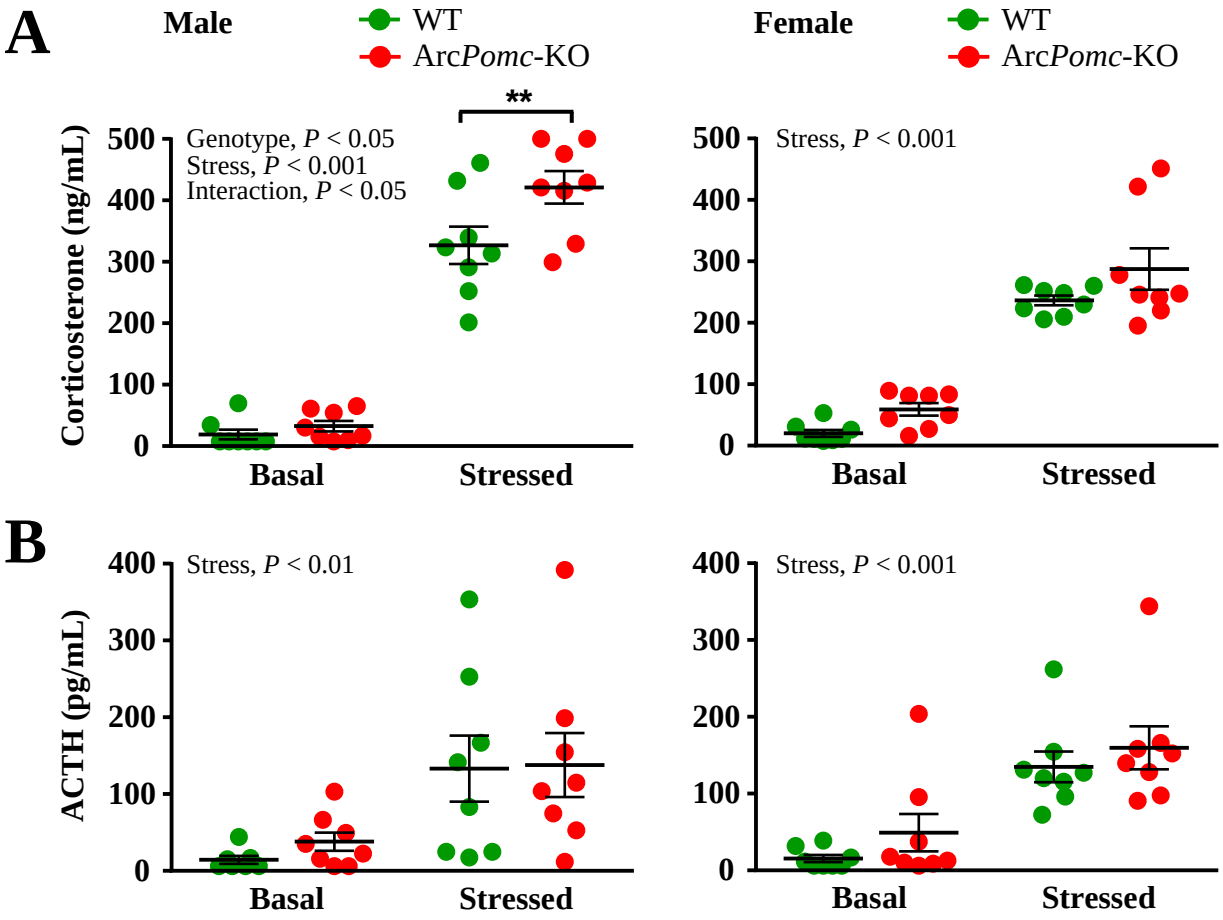

Figure 3.2: Hormonal stress response of young Arc*Pomc*-KO mice. In both panels, male (left) and female (right) data are shown. **A**, Corticosterone levels before (basal) and immediately following a 20-minute restraint stress. In males, RMANOVA revealed a significant main effect of genotype ($F(1,14) = 5.0$), stress ($F(1,14) = 421.3$), and an interaction ($F(1,14) = 5.7$), whereas in females there was only a main effect of stress ($F(1,14) = 127.2$). **B**, ACTH levels in unstressed and stressed mice. Two-way ANOVA revealed only a significant main effect of stress (Male: $F(1,27) = 11.9$; Female: $F(1,28) = 24.2$) but not genotype. N = 8 per sex, genotype and condition. ** $P < 0.01$ by Sidak's post-hoc comparison test.

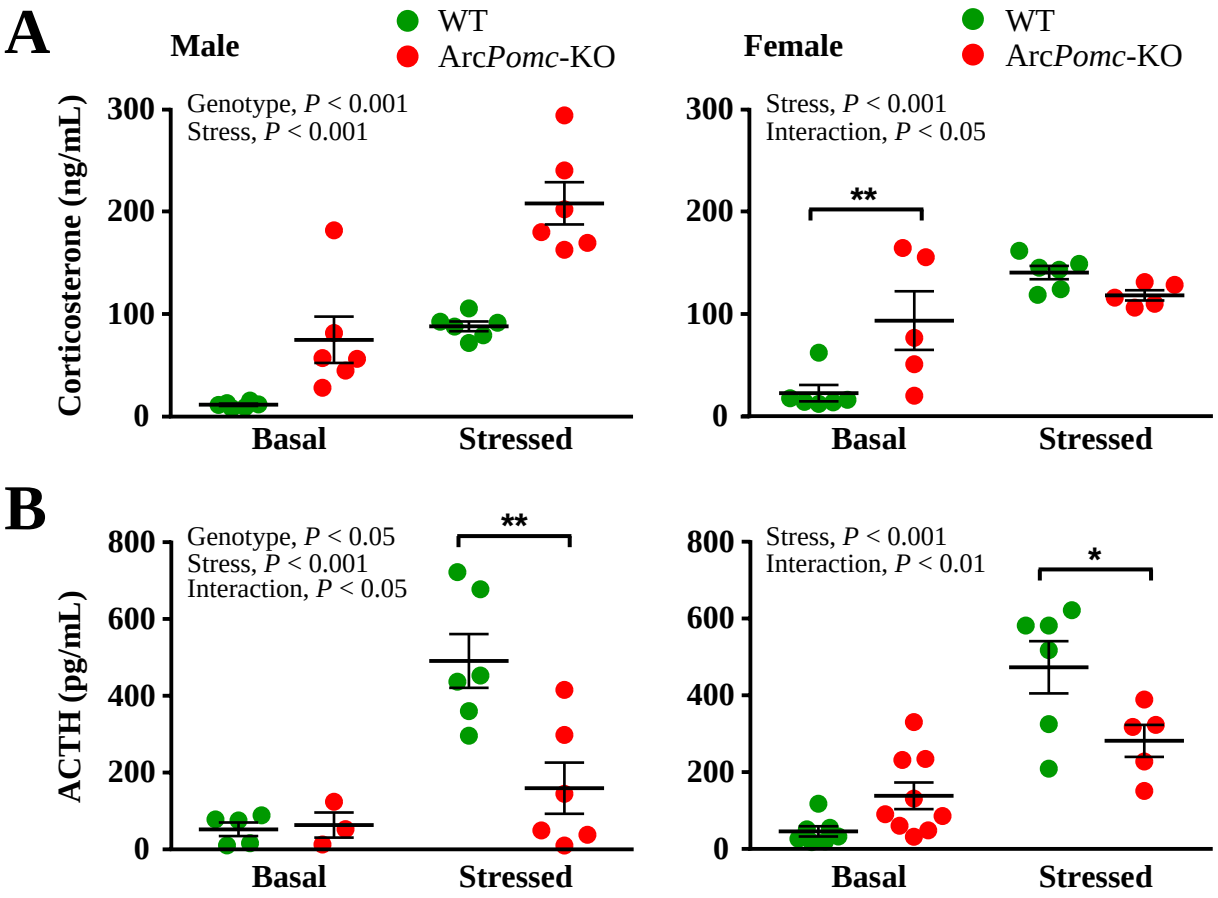

Figure 3.3: Hormonal stress response of older, obese Arc*Pomc*-KO mice. In both panels, male (left) and female (right) data are shown. **A**, Corticosterone levels before (basal) and immediately following a 20-minute restraint stress. In males, RMANOVA revealed a significant effect of genotype ($F(1,10) = 40.4$) and stress ($F(1,10) = 40.7$) but no interaction. In females, there was a significant effect of stress ($F(1,9) = 24.1$) and an interaction ($F(1,9) = 10.3$). **B**, ACTH levels in unstressed and stressed mice. Two-way ANOVA in males revealed a significant effect of genotype ($F(1,16) = 6.5$), stress ($F(1,16) = 17.9$) and an interaction ($F(1,16) = 7.4$). In females, there was a significant effect of stress ($F(1,23) = 45.2$) and an interaction ($F(1,23) = 11.2$). N = 5-6 per sex and genotype (Panel A) and 3-9 per sex, genotype and condition (Panel B). * $P < 0.05$; ** $P < 0.01$ by Sidak's (Panel A) or Tukey's (Panel B) post-hoc comparison test.

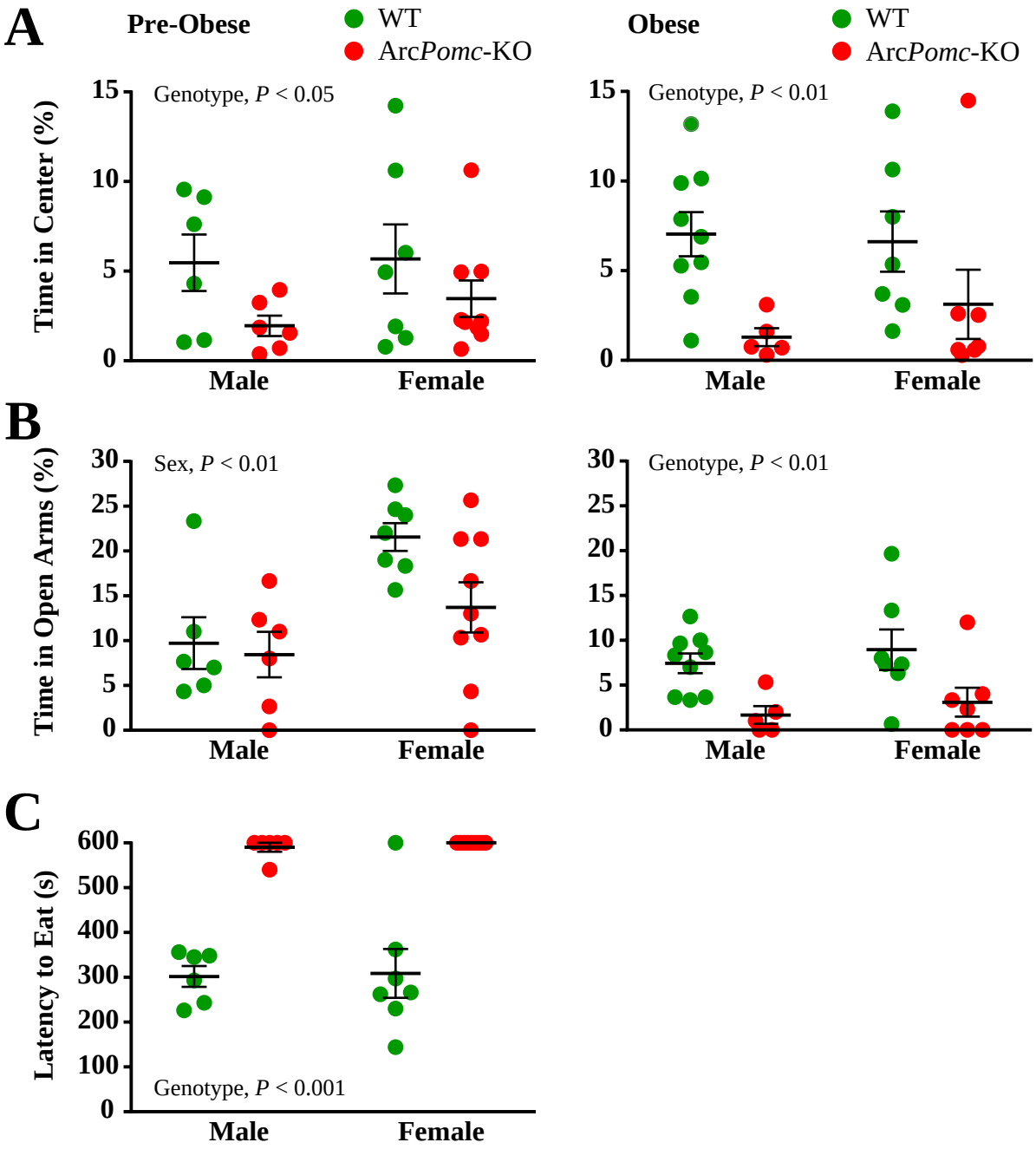

Figure 3.4: Behavioral anxiety tests in Arc*Pomc*-KO mice. In all panels, data from separate cohorts of young, pre-obese (left) and older, obese (right) mice are shown. **A**, Percentage of time spent in the center of an open field. In both groups, two-way ANOVA revealed only a significant effect of genotype (Pre-obese: $F(1,24) = 4.3$; Obese: $F(1,24) = 8.8$) but not of sex or an interaction. **B**, Percentage of time spent in the open arms of the elevated plus maze. Two-way ANOVA in the young, pre-obese mice showed only an effect of sex ($F(1,24) = 10.7$) whereas in the obese mice there was only a significant effect of genotype ($F(1,24) = 12.6$). **C**, Latency to eat in the novelty-suppressed feeding test. Mice that never ate in the 10 minute test were assigned a value of 600 s. Two-way ANOVA revealed a significant effect of genotype ($F(1,24) = 95.0$). N = 5-9 per sex, genotype and condition.

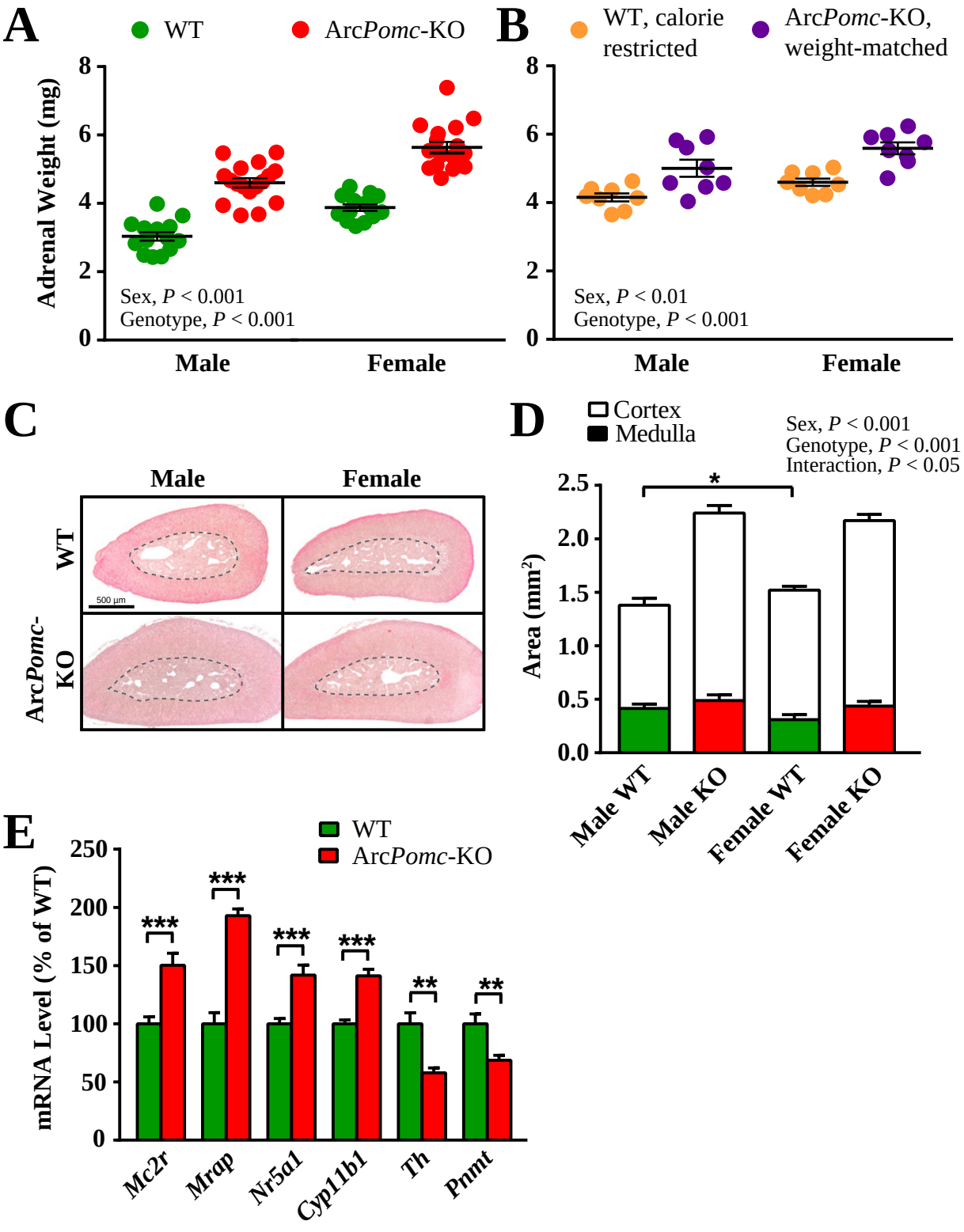

Figure 3.5: Characterization of adrenal glands of Arc*Pomc*-KO mice A, Weight of adrenal glands of 8-week old mice. Two-way ANOVA showed a significant effect of sex ($F(1,58) = 46.7$) and genotype ($F(1,58) = 147.2$) but no interaction. **B**, Weight of adrenal glands of 30-week old WT mice calorie restricted to 85% of body weight and Arc*Pomc*-KO mice matched

to starting body weight of WT. Two-way ANOVA found a significant effect of sex ($F(1,28) = 9.0$) and genotype ($F(1,28) = 29.1$) but no interaction. **C**, Representative H&E-stained cross-sections of adrenal glands from 16-week old mice, where the outline of the medulla is indicated by a dotted line. **D**, Quantification of the area of the medulla was not different between groups, whereas two-way ANOVA of cortical area revealed a significant effect of genotype ($F(1,20) = 124.6$) and an interaction ($F(1,20) = 5.1$). **E**, Semi-quantitative RT-PCR of adrenal glands from 5-6 month old male mice. Data were analyzed by unpaired Student's t-test between genotypes: *Mc2r*, $t(14) = 4.2$; *Mrap*, $t(14) = 8.4$; *Nr5a1*, $t(14) = 4.3$; *Cyp11b1*, $t(14) = 6.3$; *Th*, $t(14) = 4.1$; *Pnmt*, $t(14) = 3.3$. N = 16 per sex and genotype (Panel A), 8 per sex and genotype (Panel B), 6 per sex and genotype (Panel D) and 8 per genotype (Panel E). * $P < 0.05$; ** $P < 0.01$; *** $P < 0.001$ by Tukey's multiple comparisons post hoc test (**D**) or Student's unpaired t-test between genotypes (**E**) .

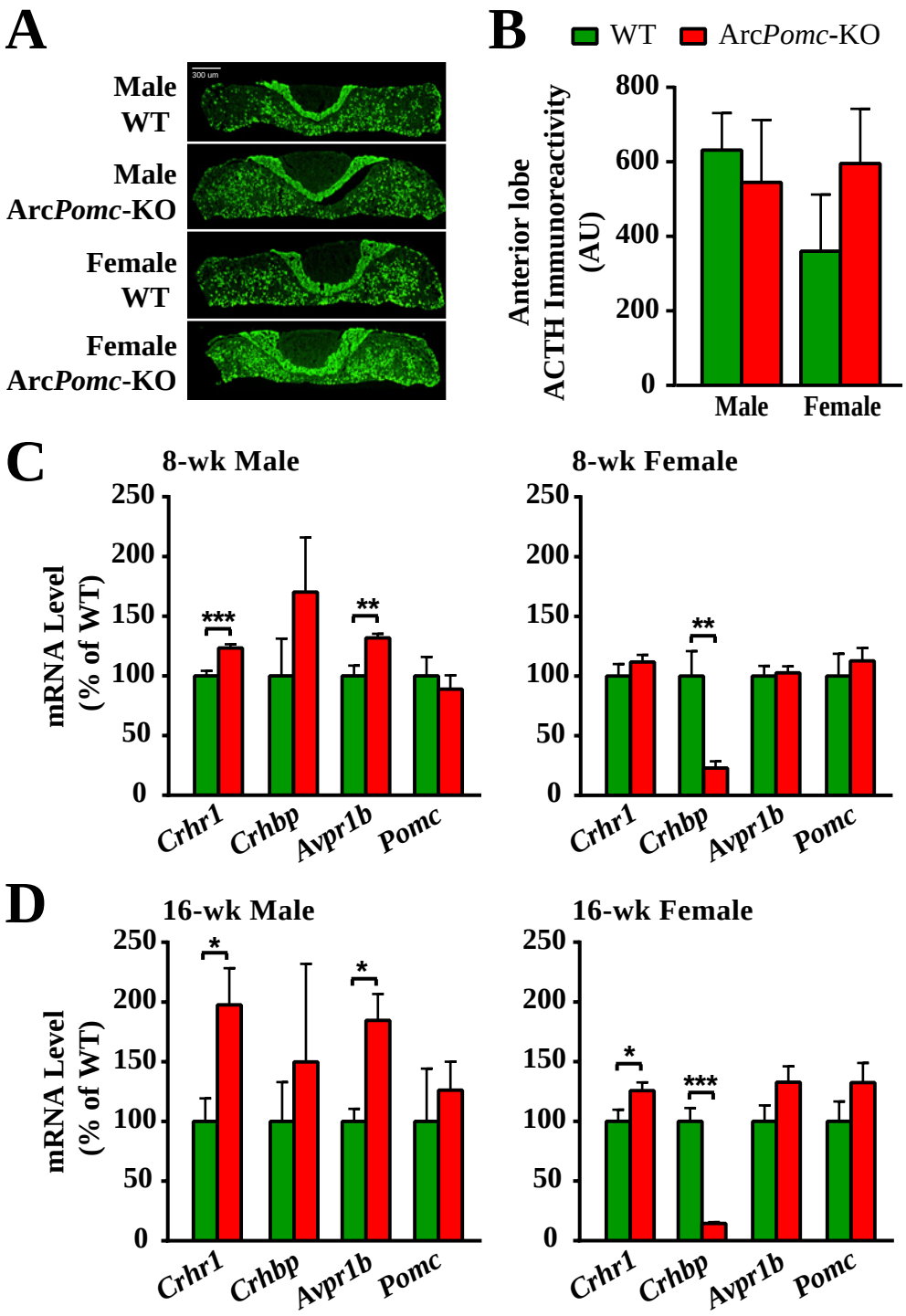

Figure 3.6: Characterization of pituitary glands of Arc*Pomc*-KO mice. In panels C and D, male (left) and female (right) are shown. **A,** Representative sections of whole pituitary showing immunohistochemistry for ACTH. **B**, Quantification of intensity of ACTH staining in the anterior lobe. Two-way ANOVA showed no differences between groups. **C**, mRNA levels in the anterior lobe of 8-week old mice. Data were analyzed by unpaired Student's t-test between genotypes (Male: *Crhr1*, t(14) = 4.6; *Avpr1b*, t(14) = 3.8; Female: *Crhbp*, t(14) = 3.6) **D**, mRNA levels in the anterior lobe of 16-week old mice. Data were analyzed by unpaired

Student's t-test between genotypes (Male: *Crhr1*, t(10) = 2.4; *Avpr1b*, t(10) = 3.0; Female: *Crhr1*, t(13) = 2.2; *Crhbp*, t(15) = 9.1). N = 5 per sex and genotype (Panel B) and 7-8 per sex, genotype and age (Panels C,D). * $P < 0.05$; ** $P < 0.01$; *** $P < 0.001$ by unpaired Student's t-test between genotypes.

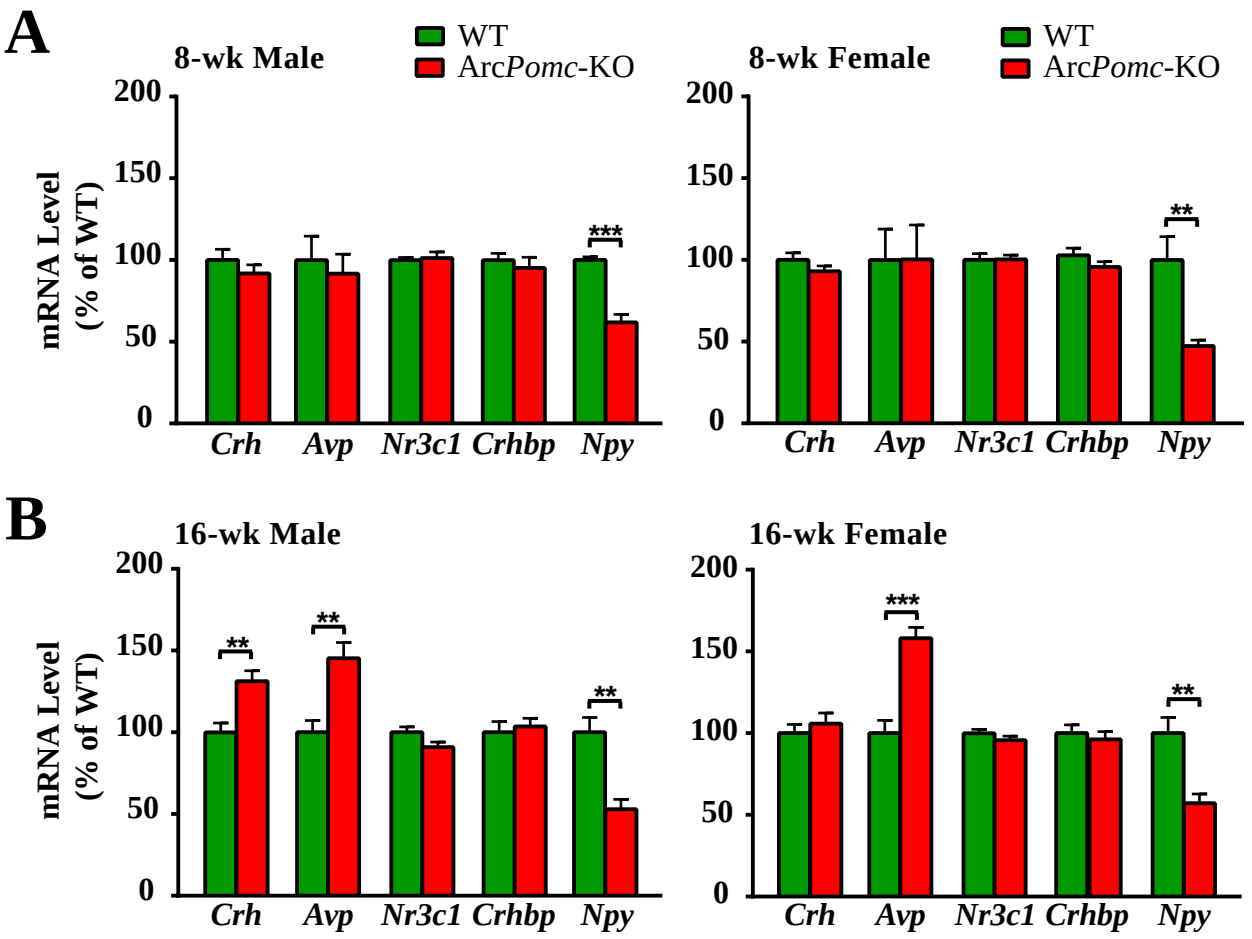

Figure 3.7: Characterization of the hypothalamus of Arc*Pomc*-KO mice. In both panels, male (left) and female (right) data are shown. **A**, mRNA levels in the whole hypothalamus of 8-week old mice. Data were analyzed by unpaired Student's t-test between genotypes (Male: *Npy*, t(12) = 6.6; Female: *Npy*, t(15) = 3.8). **B**, mRNA levels in the whole hypothalamus of 16-week old mice. Data were analyzed by unpaired Student's t-test between genotypes (Male: *Npy*, t(13) = 4.2, *Avp*, t(15) = 3.8, *Crh*, t(15) = 3.5; Female: *Npy*, t(15) = 4.0, *Avp*, t(16) = 5.6]. N = 7-8 per sex, genotype and age. ** $P < 0.01$; *** $P < 0.001$ by unpaired Student's t-test between genotypes.

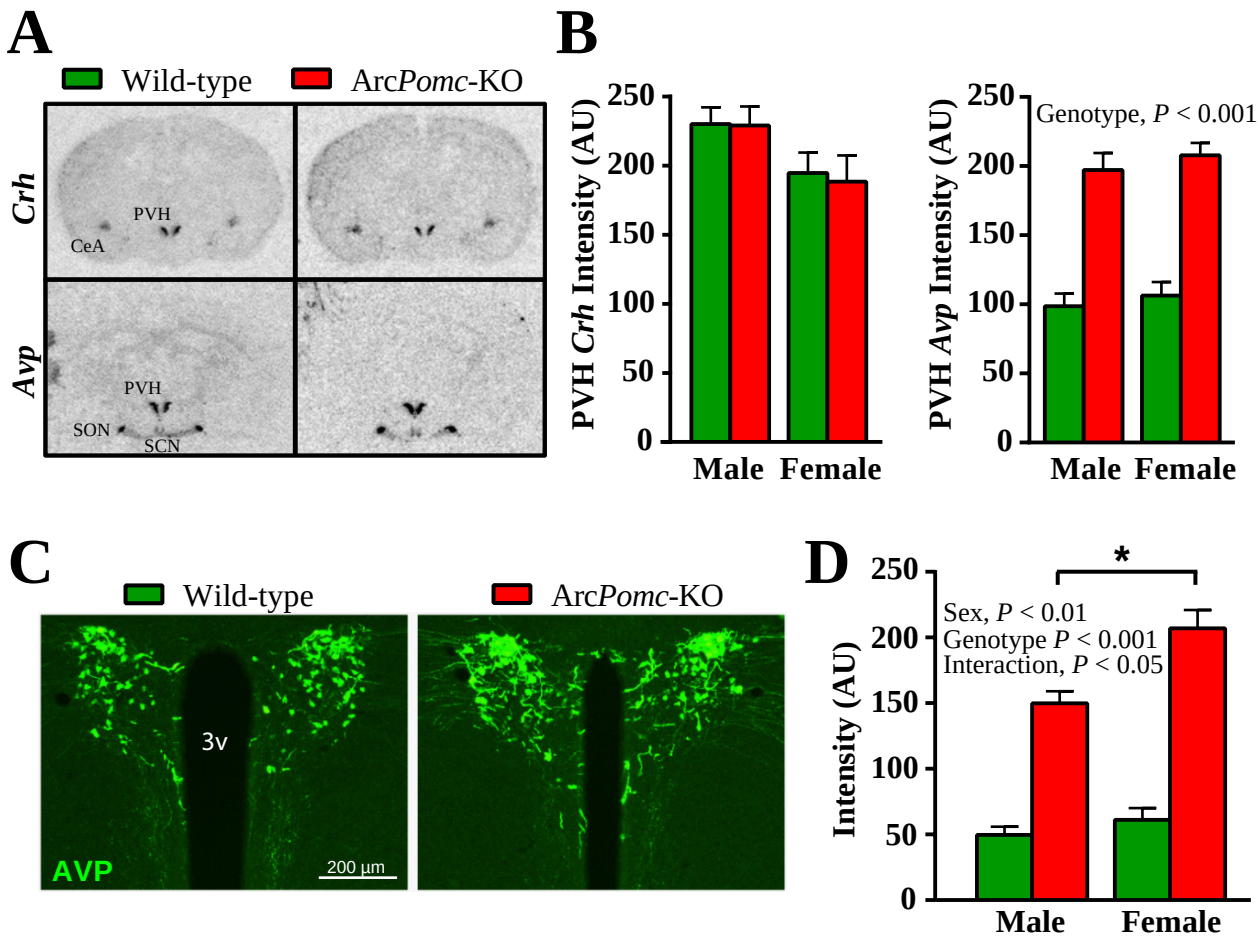

Figure 3.8: Paraventricular hypothalamus of Arc*Pomc*-KO mice. A, Representative images of *Crh* and *Avp* ISH in both genotypes. **B**, Quantification of *Crh* and *Avp* signal intensity only in the PVH in all four groups. Two-way ANOVA of *Crh* signal showed no differences between groups while two-way ANOVA of *Avp* signal revealed a significant main effect of genotype ($F(1,26) = 86.7$). **C**, Representative images of AVP IHC in the PVH of mice from both genotypes. **D**, Quantification of total PVH signal in all four groups. Two-way ANOVA revealed a significant main effect of sex ($F(1,20) = 11.7$), genotype ($F(1,20) = 152.4$), and an interaction ($F(1,20) = 5.3$). N = 5-9 per sex and genotype. * $P < 0.05$ by Tukey's multiple comparisons post hoc test. CeA, central amygdala; SON, supraoptic nucleus; SCN, suprachiasmatic nucleus; 3v, third ventricle.

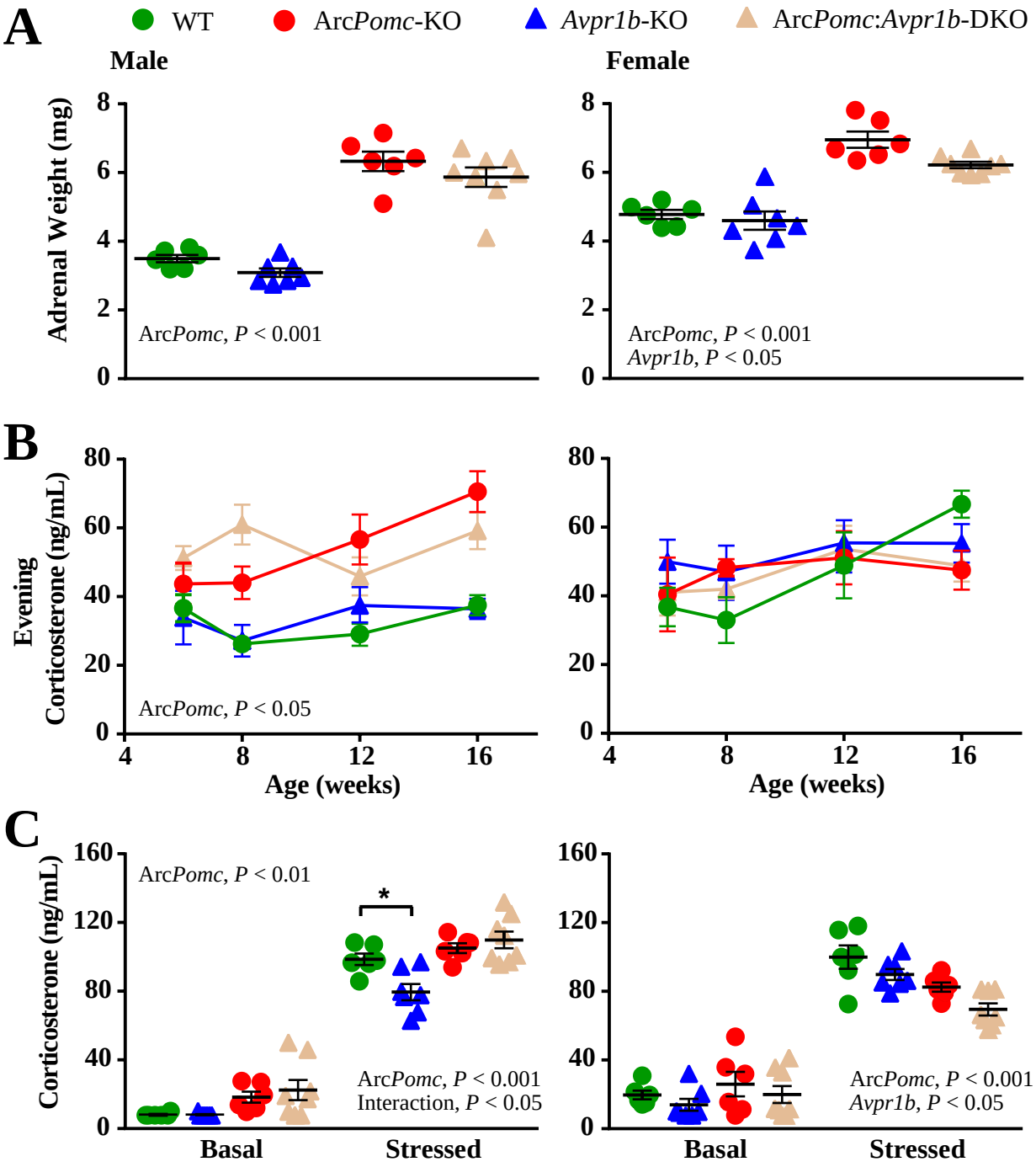

Figure 3.9: HPA axis of Arc*Pomc*:*Avpr1b*-DKO mice. Male (left) and female (right) data are shown. **A**, Adrenal weights of 16-week old mice. Two-way ANOVA using each gene as an independent variable revealed a significant effect of Arc*Pomc* in males ($F(1,23) = 52.3$) and of both genes in females (Arc*Pomc*, $F(1,23) = 96.9$; *Avpr1b*, $F(1,23) = 5.7$) but no interaction. **B**, Unstressed evening corticosterone levels from age 6 weeks to 16 weeks. Two-way ANOVA revealed a significant effect of Arc*Pomc* gene at each time point in males (6 weeks, $F(1,20) = 4.4$; 8 weeks, $F(1,23) = 29.7$; 12 weeks, $F(1,23) = 4.6$; 16 weeks, $F(1,23) = 35.9$). There was a significant effect of *Avpr1b* genotype in males at age 8 weeks ($F(1,23) = 4.4$, $P < 0.05$) and in females at age 16 weeks ($F(1,23) = 7.7$, $P < 0.05$) (not indicated on graph). **C**, Corticosterone

levels before (basal) and immediately following a 20-minute restraint stress in 16-week old mice. Two-way ANOVA on basal corticosterone revealed only a significant main effect of Arc*Pomc* gene in males ($F(1,23) = 10.5$) and no differences between groups in females. Two-way ANOVA on stressed corticosterone revealed a significant main effect of Arc*Pomc* ($F(1,23) = 18.2$) as well as a significant interaction ($F(1,23) = 7.7$) in males and in females there was a significant effect of both Arc*Pomc* ($F(1,23) = 20.3$) and *Avpr1b* ($F(1,23) = 7.5$, $P < 0.05$) but no interaction. N = 6-8 per sex, genotype and condition. * $P < 0.05$ by Tukey's post hoc comparison test.

Chapter 4: Summary, Conclusions and Future Directions

Hypothalamic POMC has been extensively studied over the last 30 years for its critical roles in feeding behavior and energy expenditure. Using a genetic knockout mouse model that does not express *Pomc* specifically in the Arc, I have provided here extensive evidence that hypothalamic POMC-derived peptides are also involved in regulation of locomotor activity levels and the HPA stress axis.

In Chapter 2, I showed that Arc*Pomc*-KO mice exhibited hyperphagic obesity and very low levels of spontaneous home cage locomotor activity. Reversing the obesity by caloric restriction over a period of several weeks normalized spontaneous home cage activity levels, suggesting that the originally observed decreased levels were secondary to obesity, leading me to conclude that ArcPOMC does not play a direct role in regulating spontaneous activity levels. Spontaneous and voluntary locomotor activity levels are correlated, and I therefore hypothesized that providing young, pre-obese Arc*Pomc*-KO mice with the opportunity to engage in voluntary running wheel activity may positively affect the obesity and metabolic outcome. However, male Arc*Pomc*-KO mice provided home cage running wheels for 8 weeks showed only negligible improvement in body weight and metabolic outcome over control Arc*Pomc*-KO mice without wheels, whereas there was no improvement in female Arc*Pomc*-KO mice with access to running wheels. This lack of improvement was associated with running wheel activity levels that were much lower than WT. Surprisingly, even Arc*Pomc*-KO mice that were prevented from becoming

obese by caloric restriction had markedly decreased running wheel activity levels. β-endorphin-KO mice, on the other hand, exhibited the same level of running wheel activity as controls. From these studies, I conclude that ArcPOMC-derived melanocortin peptides, but not β-endorphin, can act directly to increase voluntary, but not spontaneous, locomotor activity levels.

In Chapter 3, I showed that the HPA stress axis of Arc*Pomc*-KO mice was dysregulated in a sex-specific manner that worsened with age and/or obesity. Young, pre-obese (4 weeks old) male Arc*Pomc*-KO mice had elevated evening peak corticosterone levels that were not different from females of either genotype and may reflect a failure of the HPA axis to masculinize in these mice. Young adult (8 weeks old) male Arc*Pomc*-KO mice had a normal ACTH but exaggerated corticosterone response to restraint stress whereas female Arc*Pomc*-KO mice were not different from WT. Additionally, Arc*Pomc*-KO mice of both sexes had enlarged adrenal glands due to increased adrenocortical area. Adult (16 weeks old) Arc*Pomc*-KO mice of both sexes were obese and had elevated basal morning nadir corticosterone levels and a blunted rise of ACTH, but normal or exaggerated increase in corticosterone, in response to restraint stress. Arc*Pomc*-KO mice weight-matched to WT controls by caloric restriction and obese Arc*Pomc*-KO mice had larger adrenal glands than WT, suggesting that the dysregulation of the HPA axis in older Arc*Pomc*-KO mice is not due solely to development of obesity. Rather, the obesity phenotype and the dysregulated HPA phenotype caused by the primary genetic insult may both worsen in parallel, and thus I conclude that ArcPOMC directly inhibits the HPA stress axis.

A caveat of these studies is that they were performed exclusively in a single genetic knockout mouse model, which by its nature reveals only the phenotype that occurs in an animal in the complete absence of the gene. To fully understand the physiological functions of ArcPOMC neurons and the mechanisms by which they occur, these types of studies should be

combined with other methods. Site-specific administration of exogenous receptor agonists and antagonists has historically been a commonly used complementary approach. As thoroughly detailed in Chapter 1, exogenous administration of melanocortin agonists in general increased, whereas antagonists decreased, locomotor activity levels in normal rats. This is in agreement with my conclusions from the characterization of Arc*Pomc*-KO mice presented in Chapter 2.

Puzzlingly, although there are a handful of reports based on administration of melanocortin agonists that agree with our conclusion that ArcPOMC plays an inhibitory role in the HPA axis, the majority of published studies conclude the opposite. The most likely reasons for this discrepancy are differences in the time scale of intervention, e.g. acute injection versus life-long knockout, as well as dosages of agonists used by different groups. In order to more fully understand the complex relationship between the neural melanocortin system and the HPA axis, further experiments must be performed. For example, it would be prudent to undertake a series of experiments in which varying doses of melanocortin ligands are administered for various lengths of time and HPA outcome measured.

The lack of *Pomc* expression in the Arc in our model has been well-validated by *in situ* hybridization (data not shown), immunohistochemistry (86), and semi-quantitative real-time PCR, but there is always the possibility that the primary genetic manipulation caused unidentified off-target effects. Additionally, compensation for the lack of Arc*Pomc* may have occurred during development in the knockouts. To rule out these possibilities, the experiments conducted in Chapters 2 and 3 could be repeated in another genetic knockin mouse model with LoxP sites flanking the upstream neuronal *Pomc* enhancers (this mouse would first need to be generated). Site-specific injection of a Cre-expressing viral vector into the arcuate nucleus of adult mice would lead to excision of the neuronal enhancers and eliminate *Pomc* expression in

only those neurons. This method would circumvent possible off-target and developmental effects of the Arc*Pomc*-KO allele and comparison of the phenotypes of the two genetic models would allow confirmation or revision of my conclusions.

A useful mouse model that allows re-expression of Arc*Pomc* upon injection of tamoxifen into adult Arc*Pomc*-KO mice already exists (86). After rescue, approximately 70-80% of ArcPOMC neurons begin to express *Pomc*, but the degree of body weight normalization depends on the age and obesity of each mouse at the time of tamoxifen injection. Performing similar experiments as those described here in mice with restored Arc*Pomc* expression at different ages could help to further unravel the relationship between ArcPOMC, obesity, locomotion, and the HPA axis. Normalization of these parameters by the restoration of Arc*Pomc* expression in adult mice would strongly argue against the possibility of irreversible developmental consequences of *Pomc* deficiency.

The specific roles of ArcPOMC identified in this report should be confirmed by rescue of the Arc*Pomc*-KO. This could be accomplished by treating Arc*Pomc*-KO mice either acutely or chronically with melanocortin agonists or by activating downstream neurons using opto- or chemo-genetic approaches. Ideally, such an effort could also identify the key sites of downstream action. For example, if optogenetic activation of *Mc4r*-expressing cells in the PVH rescued the hyperactive HPA phenotype described in Arc*Pomc*-KO mice, I could conclude that the Arc to PVH circuit is critical for POMC regulation of the HPA axis.

However, efforts to identify possible downstream target sites of ArcPOMC in regulation of either the HPA axis or locomotor activity levels have thus far been unsuccessful. The neural circuitry controlling the HPA axis has been studied extensively but there is still a lot that is unknown. Diverse signals converge onto neurons in the paraventricular nucleus of the

hypothalamus (PVH) expressing CRH and/or AVP, which are activated by stress. Although mRNA levels of *Avp* in the hypothalamus and *Avpr1b* in the anterior pituitary were highly elevated in Arc*Pomc*-KO mice, suggesting that ArcPOMC may normally inhibit AVP production and/or release, genetic deletion of *Avpr1b* did not rescue the observed HPA dysregulation. By process of elimination, these results suggest that it is CRH which mediates the HPA effects of melanocortin signaling. There are direct projections from POMC neurons to the PVH, and some CRH neurons in the PVH express *Mc4r* (170). However, Mc4R is G_s-coupled and pharmacologic administration of melanocortin agonists activates rather than inhibits these target cells. It is within the realm of possibility that melanocortins activate a noncanonical pathway specifically in CRH-expressing PVH neurons. Alternatively, POMC neurons could inhibit CRH neurons indirectly via an unidentified relay of GABAergic interneurons or some other anti-stress signal. The bed nucleus of the stria terminalis would be a logical candidate to study first because of its known afferent input from ArcPOMC neurons, integration of stress signals from other limbic nuclei, and efferent projections to the PVH (255). Testing this hypothesis via pharmacological or opto- or chemo-genetic approaches would be an extensive undertaking.

Neural mechanisms regulating the initiation and duration of spontaneous and voluntary locomotion are much less well-characterized than those regulating the HPA axis. In rodents, running wheel activity is rewarding and activates the dopaminergic system, so I hypothesized that decreased running wheel activity in Arc*Pomc*-KO mice may be due to disrupted reward pathways. Classically, the melanocortin system is believed to be involved solely in homeostatically-regulated feeding, whereas other pathways were thought to regulate hedonic feeding, but recent evidence has showed extensive overlap of these two systems. In fact, impaired dopaminergic signaling has been characterized in other obese mouse models, including

ob/ob, which have decreased dopamine and TH levels (256). The reward deficiency hypothesis posits that decreased dopamine levels, reflecting an impaired reward system, may cause an animal to eat more in order to obtain the normal level of rewarding feeling (257). Conversely, others argue that excessive activation of reward pathways by increased dopamine could lead to overeating and obesity (258). A third possibility is that alterations in the dopaminergic pathway observed in obesity are secondary to and possibly compensatory for the hyperphagia and/or obesity.

Using semi-quantitative real-time PCR and immunohistochemistry, however, we could find no differences between genotypes in the dopaminergic system. These were only a first-pass effort, were one-time static measurements of mRNA and protein levels in specific regions, and it certainly remains possible that the dopamine system could be dysregulated in Arc*Pomc*-KO mice. In an attempt to determine a possible functional role of an altered reward system in the hyperphagia observed in Arc*Pomc*-KO mice, I subjected them to a progressive ratio test wherein the effort required to obtain each progressive food pellet increased exponentially. Arc*Pomc*-KO mice responded to this test with an equal breakpoint as WT for access to normal chow food (Figure 4.1), suggesting that the hyperphagia seen in this model is not due to enhanced rewarding value of food. Furthermore, it is clear that the dopaminergic reward pathways are grossly intact in Arc*Pomc*-KO mice, as both WT and Arc*Pomc*-KO mice developed conditioned place preference for morphine (Figure 4.2) and had identical locomotor sensitization to repeated morphine exposure.

In contrast, the associative learning process that encodes reward, which has also been shown to involve dopamine, may be impaired in Arc*Pomc*-KO mice, as they exhibited marked difficulty in initially learning to lever press for food in operant chambers (unpublished

observation). In this light, one could view the lack of increased running wheel activity with age (Figure 2.4) as an impairment in the association of running wheel activity with reward. Therefore, although we do not yet have direct evidence that Arc*Pomc*-KO mice have dysregulated dopaminergic signaling, several signs point in that direction, and I feel that this line of research is worth pursuing. A next step would be to measure dopamine release in the nucleus accumbens under baseline conditions and after presentation of a reward, such as a sucrose pellet, to wildtype and Arc*Pomc*-KO mice.

Although it is unknown whether dopamine is involved, it has recently been discovered that activation of AGRP neurons encodes a negative valence whereas activation of PVH Mc4r-expressing neurons in the hungry state encodes a positive valence (58,73). These findings lead me to postulate that activation of POMC neurons could encode a positive valence. To test this hypothesis, I could perform a conditioned place preference test wherein one side of the chamber is paired with optogenetic stimulation of ArcPOMC neurons. If place preference is observed, it would indicate that ArcPOMC neuron activation could encode a positive valence associated not only with eating but possibly with other stimuli and behaviors as well. To test that the valence signal is carried by POMC and not by other neuromodulators expressed in ArcPOMC neurons, these tests could be repeated in Arc*Pomc*-KO mice or in wildtype mice pretreated with a melanocortin receptor antagonist. Furthermore, the response of Arc*Pomc*-KO mice to more natural stimuli such as palatable food, sucrose water, or access to sex should be assessed, as it is becoming increasingly evident that all rewards may not activate reward pathways equally.

Another complementary angle to approach this question would be to measure the real-time activation of ArcPOMC neurons in awake animals presented with various rewarding stimuli using recently developed *in vivo* calcium imaging techniques. Using these methods, ArcPOMC

neurons have recently been shown to become rapidly activated by exposure to food, but not by a non-food object, and the degree of activation was associated with the palatability of the food (57). Discovering the response of ArcPOMC neurons to other rewarding stimuli such as sucrose, drugs of abuse, or even access to a running wheel could help to unravel a possible role for these neurons in encoding valence of stimuli.

Although up until this point, I have discussed locomotor activity levels and HPA axis regulation as two separate phenomena, it is also possible that they are related. Acute and forced treadmill exercise is known to activate the HPA axis, but the HPA response to voluntary wheel running exercise seems to be more complex. Access to a running wheel for only two weeks in rats and four weeks in mice resulted in increased corticosterone levels, both basally and in response to a stressor and to ACTH injection, due to increased adrenal sensitivity to ACTH (198,199). However, after 6 additional weeks of voluntary wheel running, adrenal sensitivity and corticosterone levels were normalized. Another study showed that rats given access to running wheels for 6 weeks had a decreased HPA response to mild stressors but normal response to high-intensity stressors (200). Interestingly, after 10 weeks of running wheel access, Zucker diabetic fatty rats had improved metabolic outcome associated with decreased corticosterone and adrenal sensitivity to ACTH (36).

Similar long-term studies have not been reported in mice, but it is possible that the hyperactivity of the HPA axis that we observed in Arc*Pomc*-KO mice could be secondary, at least in part, to sedentary behavior. On the other hand, corticosterone levels can also affect physical activity. Although this has most often been studied in the context of a novel environment or in response to administration of drugs of abuse (255), chronic corticosterone administration was also associated with decreased spontaneous home cage activity (259,260).

Therefore, it is possible that the decreased locomotor activity observed in Arc*Pomc*-KO mice could be partly due to the hyperactive HPA axis. These are merely speculations and further studies would need to be performed to confirm a mechanistic relationship between locomotor activity and HPA axis activation in Arc*Pomc*-KO mice.

Overall, I speculate that each physiologic role of hypothalamic POMC is performed in the service of defending body weight. Most obviously, melanocortin signaling decreases food intake. I have now shown by inference from the Arc*Pomc*-KO mouse model that melanocortin signaling also tonically inhibits the HPA axis, preventing chronically increased corticosterone levels that can lead to increased feeding and fat deposition as well as decreased locomotor activity. Additionally, melanocortin signaling increases levels of voluntary locomotion. Whether these two pathways influence each other is at this point unclear, and much more work is needed to fully elucidate all the ways in which hypothalamic POMC affects physiology.

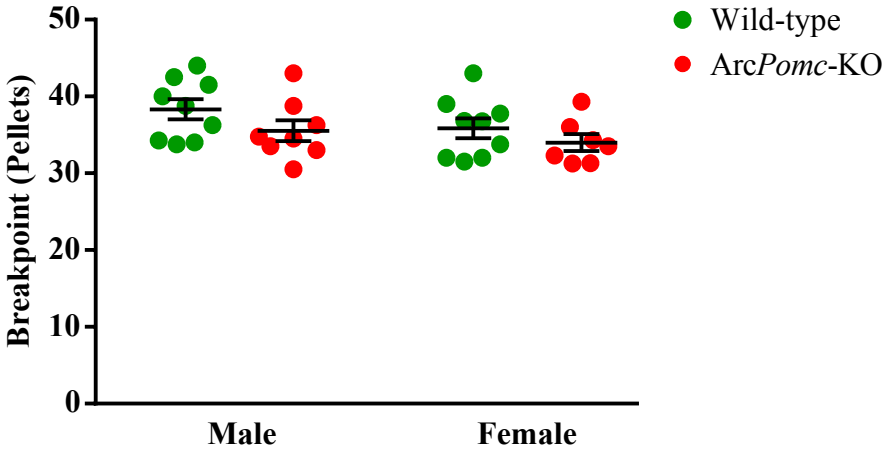

Figure 4.1: Performance for food reward of Arc*Pomc*-KO mice on a progressive ratio schedule of reinforcement. 4-6 month old mice were trained to lever press for access to a 20-mg standard laboratory food pellet (TestDiet 5TUM) at a fixed ratio of 30. Mice were then fasted during the day and the progressive ratio started at onset of dark. The required number of presses, Y, for each pellet, x, increased according to the equation $Y = 18e^{0.1x}$. Breakpoint was determined as the number of pellets acquired before a time-out period of 30 minutes passed with no pellet acquired. Each mouse was then administered enough food in the remaining dark period to maintain the mouse at 85% of starting body weight. The progressive ratio test was repeated for 10 nights in a row and the breakpoints on the last seven nights were averaged. Data were analyzed by two-way ANOVA using genotype and sex as the independent variables, but there were no differences between groups. N = 7-9 per sex and genotype.

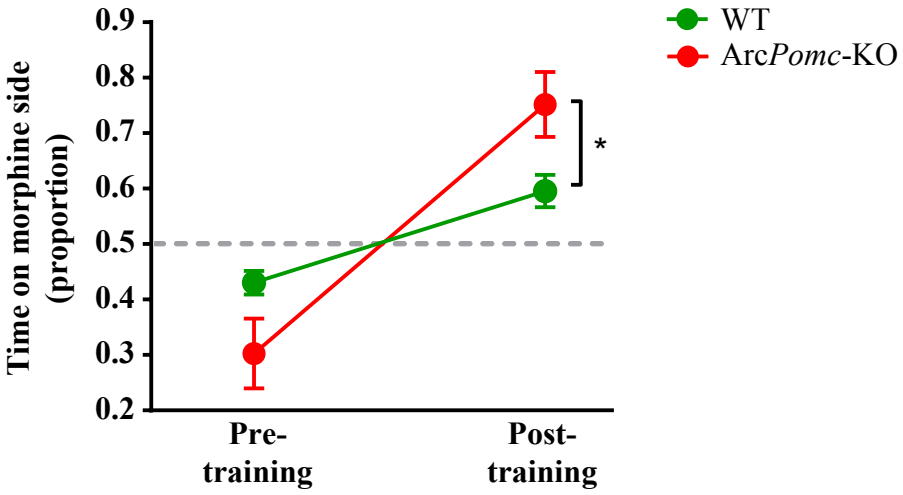

Figure 4.2: Conditioned place preference for morphine in Arc*Pomc*-KO mice. This test was performed in 6-8 month old female mice. A two-chamber conditioned place preference box was constructed with each chamber measuring 40x20 cm and a 3x5 cm opening between the two sides. One chamber had a metal grid floor and white walls and the other chamber had an acrylic floor and black walls. On day 1, mice were placed on the metal-floored side and allowed to explore freely for 30 minutes. The preferred side, determined by measuring the time spent on each side by each mouse using Med Associates software, varied between mice but there was no consistent difference between groups. On days 2-9, mice were either injected i.p. with morphine (2 mg/kg) and placed on their least preferred side or with saline and placed on their preferred side, with the opening between chambers blocked. Treatments alternated so that each mouse underwent 4 days of each treatment. On day 10, the procedure for day 1 was repeated and the place preference ratio calculated (time on morphine side / total time). Data were analyzed by RMANOVA and there was a significant effect of treatment ($F(1,11) = 39.0$, $P < 0.001$) and an interaction ($F(1,11) = 8.3$, $P < 0.05$). N = 6-7 per genotype. * $P < 0.05$ by Sidak's post hoc multiple comparisons test.

References

1. **Bertagna X**. Proopiomelanocortin-derived peptides. *Endocrinology and Metabolism Clinics of North America.* 1994;23(3):467-485.
2. **Castro MG, Morrison E**. Post-translational processing of proopiomelanocortin in the pituitary and in the brain. *Critical Reviews in Neurobiology.* 1997;11(1):35-57.
3. **Wardlaw SL**. Hypothalamic proopiomelanocortin processing and the regulation of energy balance. *European Journal of Pharmacology.* 2011;660(1):213-219.
4. **Coll AP, Challis BG, Yeo GSH, Snell K, Piper SJ, Halsall D, Thresher RR, O'Rahilly S**. The effects of proopiomelanocortin deficiency on murine adrenal development and responsiveness to adrenocorticotropin. *Endocrinology.* 2004;145(10):4721-4727.
5. **Cowley MA, Smart JL, Rubinstein M, Cordan MG, Diano S, Horvath TL, Cone RD, Low MJ**. Leptin activates anorexigenic POMC neurons through a neural network in the arcuate nucleus. *Nature.* 2001;411(6836):480-484.
6. **Cone RD**. Anatomy and regulation of the central melanocortin system. *Nature Neuroscience.* 2005;8(5):571-578.
7. **Ellacott KLJ, Cone RD**. The role of the central melanocortin system in the regulation of food intake and energy homeostasis: lessons from mouse models. *Philosophical Transactions of the Royal Society B-Biological Sciences.* 2006;361(1471):1265-1274.
8. **Dores RM, Londraville RL, Prokop J, Davis P, Dewey N, Lesinski N**. Molecular evolution of GPCRs: Melanocortin/melanocortin receptors. *Journal of Molecular Endocrinology.* 2014;52(3):T29-T42.
9. **Vallarino M, d'Amora M, Dores RM**. New insights into the neuroanatomical distribution and phylogeny of opioids and POMC-derived peptides in fish. *General and Comparative Endocrinology.* 2012;177(3):338-347.
10. **Ciofi P, Garret M, Lapirot O, Lafon P, Loyens A, Prevot V, Levine JE**. Brain-Endocrine Interactions: A Microvascular Route in the Mediobasal Hypothalamus. *Endocrinology.* 2009;150(12):5509-5519.
11. **Mullier A, Bouret SG, Prevot V, Dehouck B**. Differential Distribution of Tight Junction Proteins Suggests a Role for Tanycytes in Blood-Hypothalamus Barrier Regulation in the Adult Mouse Brain. *Journal of Comparative Neurology.* 2010;518(7):943-962.
12. **Poggioli R, Vergoni AV, Bertolini A**. ACTH-(1-24) and alpha-MSH antagonize feeding behavior stimulated by kappa opiate agonists. *Peptides.* 1986;7(5):843-848.
13. **Garfield AS, Lam DD, Marston OJ, Przydzial MJ, Heisler LK**. Role of central melanocortin pathways in energy homeostasis. *Trends in Endocrinology and Metabolism.* 2009;20(5):203-215.

14. **Xu Y, Elmquist JK, Fukuda M, Annals NYAS**. Central nervous control of energy and glucose balance: focus on the central melanocortin system. *Year in Diabetes and Obesity.* 2011;1243:1-14.
15. **De Jonghe BC, Hayes MR, Bence KK**. Melanocortin control of energy balance: evidence from rodent models. *Cellular and Molecular Life Sciences.* 2011;68(15):2569-2588.
16. **Myers MG, Jr., Olson DP**. Central nervous system control of metabolism. *Nature.* 2012;491(7424):357-363.
17. **da Silva AA, do Carmo JM, Wang Z, Hall JE**. The Brain Melanocortin System, Sympathetic Control, and Obesity Hypertension. *Physiology.* 2014;29(3):196-202.
18. **Caruso C, Carniglia L, Durand D, Scimonelli TN, Lasaga M**. Astrocytes: new targets of melanocortin 4 receptor actions. *Journal of Molecular Endocrinology.* 2013;51(2):R33-R50.
19. **Ollmann MM, Wilson BD, Yang YK, Kerns JA, Chen YR, Gantz I, Barsh GS**. Antagonism of central melanocortin receptors in vitro and in vivo by Agouti-related protein. *Science.* 1997;278(5335):135-138.
20. **Hahn TM, Breininger JF, Baskin DG, Schwartz MW**. Coexpression of Agrp and NPY in fasting-activated hypothalamic neurons. *Nature Neuroscience.* 1998;1(4):271-272.
21. **Mountjoy KG, Mortrud MT, Low MJ, Simerly RB, Cone RD**. Localization of the melanocortin-4 receptor (MC4-r) in neuroendocrine and autonomic control circuits in the brain. *Molecular Endocrinology.* 1994;8(10):1298-1308.
22. **Roselli-Rehfuss L, Mountjoy KG, Robbins LS, Mortrud MT, Low MJ, Tatro JB, Entwistle ML, Simerly RB, Cone RD**. Identification of a receptor for gamma-melanotropin and other proopiomelanocortin peptides in the hypothalamus and limbic system. *Proceedings of the National Academy of Sciences of the United States of America.* 1993;90(19):8856-8860.
23. **Yaswen L, Diehl N, Brennan MB, Hochgeschwender U**. Obesity in the mouse model of pro-opiomelanocortin deficiency responds to peripheral melanocortin. *Nature Medicine.* 1999;5(9):1066-1070.
24. **Challis BG, Coll AP, Yeo GSH, Pinnock SB, Dickson SL, Thresher RR, Dixon J, Zahn D, Rochford JJ, White A, Oliver RL, Millington G, Aparicio SA, Colledge WH, Russ AP, Carlton MB, O'Rahilly S**. Mice lacking pro-opiomelanocortin are sensitive to high-fat feeding but respond normally to the acute anorectic effects of peptide-YY3-36. *Proceedings of the National Academy of Sciences of the United States of America.* 2004;101(13):4695-4700.
25. **Huszar D, Lynch CA, FairchildHuntress V, Dunmore JH, Fang Q, Berkemeier LR, Gu W, Kesterson RA, Boston BA, Cone RD, Smith FJ, Campfield LA, Burn P, Lee F**. Targeted disruption of the melanocortin-4 receptor results in obesity in mice. *Cell.* 1997;88(1):131-141.
26. **Butler AA, Kesterson RA, Khong K, Cullen MJ, Pelleymounter MA, Dekoning J, Baetscher M, Cone RD**. A unique metabolic syndrome causes obesity in the melanocortin-3 receptor-deficient mouse. *Endocrinology.* 2000;141(9):3518-3521.
27. **Chen AS, Marsh DJ, Trumbauer ME, Frazier EG, Guan XM, Yu H, Rosenblum CI, Vongs A, Feng Y, Cao LH, Metzger JM, Strack AM, Camacho RE, Mellin TN, Nunes CN, Min W, Fisher J, Gopal-Truter S, MacIntyre DE, Chen HY, Van der**

Ploeg LHT. Inactivation of the mouse melanocortin-3 receptor results in increased fat mass and reduced lean body mass. *Nature Genetics.* 2000;26(1):97-102.

28. **Chen AS, Metzger JM, Trumbauer ME, Guan XM, Yu H, Frazier EG, Marsh DJ, Forrest MJ, Gopal-Truter S, Fisher J, Camacho RE, Strack AM, Mellin TN, MacIntyre DE, Chen HY, Van der Ploeg LHT**. Role of the melanocortin-4 receptor in metabolic rate and food intake in mice. *Transgenic Research.* 2000;9(2):145-154.
29. **Qian S, Chen H, Weingarth D, Trumbauer ME, Novi DE, Guan XM, Yu H, Shen Z, Feng Y, Frazier E, Chen AR, Camacho RE, Shearman LP, Gopal-Truter S, MacNeil DJ, Van der Ploeg LHT, Marsh DJ**. Neither agouti-related protein nor neuropeptide Y is critically required for the regulation of energy homeostasis in mice. *Molecular and Cellular Biology.* 2002;22(14):5027-5035.
30. **Schwartz MW, Seeley RJ, Woods SC, Weigle DS, Campfield LA, Burn P, Baskin DG**. Leptin increases hypothalamic pro-opiomelanocortin mRNA expression in the rostral arcuate nucleus. *Diabetes.* 1997;46(12):2119-2123.
31. **Mizuno TM, Mobbs CV**. Hypothalamic Agouti-related protein messenger ribonucleic acid is inhibited by leptin and stimulated by fasting. *Endocrinology.* 1999;140(2):814-817.
32. **van den Top M, Lee K, Whyment AD, Blanks AM, Spanswick D**. Orexigen-sensitive NPY/AgRP pacemaker neurons in the hypothalamic arcuate nucleus. *Nature Neuroscience.* 2004;7(5):493-494.
33. **Elias CF, Aschkenasi C, Lee C, Kelly J, Ahima RS, Bjorbaek C, Flier JS, Saper CB, Elmquist JK**. Leptin differentially regulates NPY and POMC neurons projecting to the lateral hypothalamic area. *Neuron.* 1999;23(4):775-786.
34. **Lam DD, Attard CA, Mercer AJ, Myers MGJ, Rubinstein M, Low MJ**. Conditional expression of Pomc in the Lepr-positive subpopulation of POMC neurons is sufficient for normal energy homeostasis and metabolism. *Endocrinology.* 2015;156(4):1292-1302.
35. **Wilson BD, Bagnol D, Kaelin CB, Ollmann MM, Gantz I, Watson SJ, Barsh GS**. Physiological and anatomical circuitry between Agouti-related protein and leptin signaling. *Endocrinology.* 1999;140(5):2387-2397.
36. **Qiu J, Fang Y, Rnnekleiv OK, Kelly MJ**. Leptin Excites Proopiomelanocortin Neurons via Activation of TRPC Channels. *Journal of Neuroscience.* 2010;30(4):1560-1565.
37. **Koch M, Horvath TL**. Molecular and cellular regulation of hypothalamic melanocortin neurons controlling food intake and energy metabolism. *Molecular Psychiatry.* 2014;19(7):752-761.
38. **Benoit SC, Air EL, Coolen LM, Strauss R, Jackman A, Clegg DJ, Seeley RJ, Woods SC**. The catabolic action of insulin in the brain is mediated by melanocortins. *Journal of Neuroscience.* 2002;22(20):9048-9052.
39. **Qu SY, Yang YK, Li JY, Zeng Q, Gantz L**. Agouti-related protein is a mediator of diabetic hyperphagia. *Regulatory Peptides.* 2001;98(1-2):69-75.
40. **de Souza FSJ, Nasif S, Lopez-Leal R, Levi DH, Low MJ, Rubinsten M**. The estrogen receptor alpha colocalizes with proopiomelanocortin in hypothalamic neurons and binds to a conserved motif present in the neuron-specific enhancer nPE2. *European Journal of Pharmacology.* 2011;660(1):181-187.
41. **Titolo D, Cai F, Belsham DD**. Coordinate regulation of neuropeptide Y and agouti-related peptide gene expression by estrogen depends on the ratio of estrogen receptor

(ER) alpha to ER beta in clonal hypothalamic neurons. *Molecular Endocrinology.* 2006;20(9):2080-2092.

42. **Ibrahim N, Bosch MA, Smart JL, Qiu J, Rubinstein M, Ronnekleiv OK, Low MJ, Kelly MJ**. Hypothalamic proopiomelanocortin neurons are glucose responsive and express K-ATP channels. *Endocrinology.* 2003;144(4):1331-1340.
43. **Chang GQ, Karatayev O, Davydova Z, Wortley K, Leibowitz SF**. Glucose injection reduces neuropeptide Y and agouti-related protein expression in the arcuate nucleus: A possible physiological role in eating behavior. *Molecular Brain Research.* 2005;135(1-2):69-80.
44. **Parton LE, Ye CP, Coppari R, Enriori PJ, Choi B, Zhang CY, Xu C, Vianna CR, Balthasar N, Lee CE, Elmquist JK, Cowley MA, Lowell BB**. Glucose sensing by POMC neurons regulates glucose homeostasis and is impaired in obesity. *Nature.* 2007;449(7159):228-U227.
45. **Jo Y-H, Su Y, Gutierrez-Juarez R, Chua S, Jr.** Oleic Acid Directly Regulates POMC Neuron Excitability in the Hypothalamus. *Journal of Neurophysiology.* 2009;101(5):2305-2316.
46. **Lam TKT, Schwartz GJ, Rossetti L**. Hypothalamic sensing of fatty acids. *Nature Neuroscience.* 2005;8(5):579-584.
47. **Balthasar N, Coppari R, McMinn J, Liu SM, Lee CE, Tang V, Kenny CD, McGovern RA, Chua SC, Elmquist JK, Lowell BB**. Leptin receptor signaling in POMC neurons is required for normal body weight homeostasis. *Neuron.* 2004;42(6):983-991.
48. **Tong QC, Ye CP, Jones JE, Elmquist JK, Lowell BB**. Synaptic release of GABA by AgRP neurons is required for normal regulation of energy balance. *Nature Neuroscience.* 2008;11(9):998-1000.
49. **Xu Y, Nedungadi TP, Zhu LR, Sobhani N, Irani BG, Davis KE, Zhang XR, Zou F, Gent LM, Hahner LD, Khan SA, Elias CF, Elmquist JK, Clegg DJ**. Distinct Hypothalamic Neurons Mediate Estrogenic Effects on Energy Homeostasis and Reproduction. *Cell Metabolism.* 2011;14(4):453-465.
50. **Xu Y, Jones JE, Kohno D, Williams KW, Lee CE, Choi MJ, Anderson JG, Heisler LK, Zigman JM, Lowell BB, Elmquist JK**. 5-HT(2C)Rs Expressed by Pro-Opiomelanocortin Neurons Regulate Energy Homeostasis. *Neuron.* 2008;60(4):582-589.
51. **Padilla SL, Carmody JS, Zeltser LM**. Pomc-expressing progenitors give rise to antagonistic neuronal populations in hypothalamic feeding circuits. *Nature Medicine.* 2010;16(4):403-405.
52. **Padilla SL, Reef D, Zeltser LM**. Defining POMC Neurons Using Transgenic Reagents: Impact of Transient Pomc Expression in Diverse Immature Neuronal Populations. *Endocrinology.* 2012;153(3):1219-1231.
53. **Sanz E, Quintana A, Deem JD, Steiner RA, Palmiter RD, McKnight GS**. Fertility-regulating Kiss1 neurons arise from hypothalamic Pomc-expressing progenitors. *Journal of Neuroscience.* 2015;35(14):5549-5556.
54. **Warne JP, Xu AW**. Metabolic transceivers: in tune with the central melanocortin system. *Trends in Endocrinology and Metabolism.* 2013;24(2):68-75.
55. **Mountjoy KG**. Pro-Opiomelanocortin (POMC) neurones, POMC-derived peptides, melanocortin receptors and obesity: How understanding of this system has changed over the last decade. *Journal of Neuroendocrinology.* 2015;27(6):406-418.

56. **Sternson SM, Atasoy D**. Agouti-Related Protein Neuron Circuits That Regulate Appetite. *Neuroendocrinology.* 2014;100(2-3):95-102.
57. **Chen YM, Lin YC, Kuo TW, Knight ZA**. Sensory Detection of Food Rapidly Modulates Arcuate Feeding Circuits. *Cell.* 2015;160(5).
58. **Betley JN, Xu S, Cao ZFH, Gong R, Magnus CJ, Sternson SM**. Neurons for hunger and thirst transmit a negative-valence teaching signal. *Nature.* 2015.
59. **Bagnol D, Lu XY, Kaelin CB, Day HEW, Ollmann M, Gantz I, Akil H, Barsh GS, Watson SJ**. Anatomy of an endogenous antagonist: Relationship between Agouti-related protein and proopiomelanocortin in brain. *Journal of Neuroscience.* 1999;19(18).
60. **Wang DQ, He XB, Zhao Z, Feng QR, Lin R, Sun Y, Ding T, Xu FQ, Luo MM, Zhan C**. Whole-brain mapping of the direct inputs and axonal projections of POMC and AgRP neurons. *Frontiers in Neuroanatomy.* 2015;9.
61. **Low MJ**. Agnostic about in vivo enverse agonism of Agouti-related peptide. *Endocrinology.* 2011;152(5):1731-1733.
62. **Ghamari-Langroudi M, Digby GJ, Sebag JA, Millhauser GL, Palomino R, Matthews R, Gillyard T, Panaro BL, Tough IR, Cox HM, Denton JS, Cone RD**. G-protein-independent coupling of MC4R to Kir7.1 in hypothalamic neurons. *Nature.* 2015;520(7545):94-U223.
63. **Tao Y-X**. Constitutive activity in melanocortin-4 receptor: biased signaling of inverse agonists. *Advances in pharmacology (San Diego, Calif).* 2014;70:135-154.
64. **Gropp E, Shanabrough M, Borok E, Xu AW, Janoschek R, Buch T, Plum L, Balthasar N, Hampel B, Waisman A, Barsh GS, Horvath TL, Bruning JC**. Agouti-related peptide-expressing neurons are mandatory for feeding. *Nature Neuroscience.* 2005;8(10):1289-1291.
65. **Luquet S, Perez FA, Hnasko TS, Palmiter RD**. NPY/AgRP neurons are essential for feeding in adult mice but can be ablated in neonates. *Science.* 2005;310(5748):683-685.
66. **Wu Q, Howell MP, Cowley MA, Palmiter RD**. Starvation after AgRP neuron ablation is independent of melanocortin signaling. *Proceedings of the National Academy of Sciences of the United States of America.* 2008;105(7):2687-2692.
67. **Wu Q, Boyle MP, Palmiter RD**. Loss of GABAergic Signaling by AgRP Neurons to the Parabrachial Nucleus Leads to Starvation. *Cell.* 2009;137(7):1225-1234.
68. **Wu Q, Clark MS, Palmiter RD**. Deciphering a neuronal circuit that mediates appetite. *Nature.* 2012;483(7391):594-U112.
69. **Aponte Y, Atasoy D, Sternson SM**. AGRP neurons are sufficient to orchestrate feeding behavior rapidly and without training. *Nature Neuroscience.* 2011;14(3):351-355.
70. **Krashes MJ, Koda S, Ye CP, Rogan SC, Adarns AC, Cusher DS, Maratos-Flier E, Roth BL, Lowell BB**. Rapid, reversible activation of AgRP neurons drives feeding behavior in mice. *Journal of Clinical Investigation.* 2011;121(4):1424-1428.
71. **Krashes MJ, Shah BP, Koda S, Lowell BB**. Rapid versus delayed stimulation of feeding by the endogenously released AgRP neuron mediators GABA, NPY, and AgRP. *Cell Metabolism.* 2013;18(4):588-595.
72. **Atasoy D, Betley JN, Su HH, Sternson SM**. Deconstruction of a neural circuit for hunger. *Nature.* 2012;488(7410):172-+.
73. **Garfield AS, Li C, Madara JC, Shah BP, Webber E, Steger JS, Campbell JN, Gavrilova O, Lee CE, Olson DP, Elmquist JK, Tannous BA, Krashes MJ, Lowell**

BB. A neural basis for melanocortin-4 receptor-regulated appetite. *Nature Neuroscience.* 2015.

74. **Zhan C, Zhou JF, Feng QR, Zhang JE, Lin SL, Bao JH, Wu P, Luo MM**. Acute and Long-Term Suppression of Feeding Behavior by POMC Neurons in the Brainstem and Hypothalamus, Respectively. *Journal of Neuroscience.* 2013;33(8):3624-3632.
75. **Hentges ST, Otero-Corchon V, Pennock RL, King CM, Low MJ**. Proopiomelanocortin Expression in both GABA and Glutamate Neurons. *Journal of Neuroscience.* 2009;29(43):13684-13690.
76. **Jarvie BC, Hentges ST**. Expression of GABAergic and Glutamatergic Phenotypic Markers in Hypothalamic Proopiomelanocortin Neurons. *Journal of Comparative Neurology.* 2012;520(17):3863-3876.
77. **Atasoy D, Betley JN, Li WP, Su HH, Sertel SM, Scheffer LK, Simpson JH, Fetter RD, Sternson SM**. A genetically specified connectomics approach applied to long-range feeding regulatory circuits. *Nature Neuroscience.* 2014;17(12):1830-1839.
78. **Novak CM, Levine JA**. Central neural and endocrine mechanisms of non-exercise activity thermogenesis and their potential impact on obesity. *Journal of Neuroendocrinology.* 2007;19(12):923-940.
79. **Dishman RK**. Gene-Physical Activity Interactions in the Etiology of Obesity: Behavioral Considerations. *Obesity.* 2008;16:S60-S65.
80. **Garland T, Schutz H, Chappell MA, Keeney BK, Meek TH, Copes LE, Acosta W, Drenowatz C, Maciel RC, van Dijk G, Kotz CM, Eisenmann JC**. The biological control of voluntary exercise, spontaneous physical activity and daily energy expenditure in relation to obesity: human and rodent perspectives. *Journal of Experimental Biology.* 2011;214(2):206-229.
81. **Tou JCL, Wade CE**. Determinants affecting physical activity levels in animal models. *Experimental Biology and Medicine.* 2002;227(8):587-600.
82. **Novak CM, Burghardt PR, Levine JA**. The use of a running wheel to measure activity in rodents: Relationship to energy balance, general activity, and reward. *Neuroscience and Biobehavioral Reviews.* 2012;36(3):1001-1014.
83. **Koo BB, Feng P, Dostal J, Strohl KP**. alpha-melanocyte stimulating hormone and adrenocorticotropic hormone: An alternative approach when thinking about restless legs syndrome? *Movement Disorders.* 2008;23(9):1234-1242.
84. **Tang-Christensen M, Vrang N, Ortmann S, Bidlingmaier M, Horvath TL, Tschop M**. Central administration of ghrelin and Agouti-related protein (83-132) increases food intake and decreases spontaneous locomotor activity in rats. *Endocrinology.* 2004;145(10):4645-4652.
85. **Adage T, Scheurink AJW, de Boer SF, de Vries K, Konsman JP, Kuipers F, Adan RAH, Baskin DG, Schwartz MW, van Dijk G**. Hypothalamic, metabolic, and behavioral responses to pharmacological inhibition of CNS melanocortin signaling in rats. *Journal of Neuroscience.* 2001;21(10):3639-3645.
86. **Bumaschny VF, Yamashita M, Casas-Cordero R, Otero-Corchon V, de Souza FSJ, Rubinstein M, Low MJ**. Obesity-programmed mice are rescued by early genetic intervention. *Journal of Clinical Investigation.* 2012;122(11):4203-4212.
87. **Sutton GM, Perez-Tilve D, Nogueiras R, Fang JD, Kim JK, Cone RD, Gimble JM, Tschop MH, Butler AA**. The Melanocortin-3 Receptor Is Required for Entrainment to Meal Intake. *Journal of Neuroscience.* 2008;28(48):12946-12955.

88. **Girardet C, Mavrikaki M, Southern MR, Smith RG, Butler AA**. Assessing Interactions Between Ghsr and Mc3r Reveals a Role for AgRP in the Expression of Food Anticipatory Activity in Male Mice. *Endocrinology.* 2014;155(12):4843-4855.
89. **Begriche K, Levasseur PR, Zhang JY, Rossi J, Skorupa D, Solt LA, Young B, Burris TP, Marks DL, Mynatt RL, Butler AA**. Genetic Dissection of the Functions of the Melanocortin-3 Receptor, a Seven-transmembrane G-protein-coupled Receptor, Suggests Roles for Central and Peripheral Receptors in Energy Homeostasis. *Journal of Biological Chemistry.* 2011;286(47):40771-40781.
90. **Tucker K, Overton JM, Fadool DA**. Kv1.3 gene-targeted deletion alters longevity and reduces adiposity by increasing locomotion and metabolism in melanocortin-4 receptor-null mice. *International Journal of Obesity.* 2008;32(8):1222-1232.
91. **Rossi J, Balthasar N, Olson D, Scott M, Berglund E, Lee CE, Choi MJ, Lauzon D, Lowell BB, Elmquist JK**. Melanocortin-4 Receptors Expressed by Cholinergic Neurons Regulate Energy Balance and Glucose Homeostasis. *Cell Metabolism.* 2011;13(2):195-204.
92. **Wortley KE, Anderson KD, Yasenchak J, Murphy A, Valenzuela D, Diano S, Yancopoulos GD, Wiegand SJ, Sleeman MW**. Agouti-related protein-deficient mice display an age-related lean phenotype. *Cell Metabolism.* 2005;2(6):421-427.
93. **Dietrich MO, Zimmer MR, Bober J, Horvath TL**. Hypothalamic Agrp Neurons Drive Stereotypic Behaviors beyond Feeding. *Cell.* 2015;160(6):1222-1232.
94. **Morton GJ, Kaiyala KJ, Fisher JD, Ogimoto K, Schwartz MW, Wisse BE**. Identification of a physiological role for leptin in the regulation of ambulatory activity and wheel running in mice. *American Journal of Physiology-Endocrinology and Metabolism.* 2011;300(2):E392-E401.
95. **Ribeiro AC, Ceccarini G, Dupre C, Friedman JM, Pfaff DW, Mark AL**. Contrasting Effects of Leptin on Food Anticipatory and Total Locomotor Activity. *Plos One.* 2011;6(8).
96. **Coppari R, Ichinose M, Lee CE, Pullen AE, Kenny CD, McGovern RA, Tang V, Liu SM, Ludwig T, Chua SC, Lowell BB, Elmquist JK**. The hypothalamic arcuate nucleus: A key site for mediating leptin's effects on glucose homeostasis and locomotor activity. *Cell Metabolism.* 2005;1(1):63-72.
97. **Huo L, Gamber K, Greeley S, Silva J, Huntoon N, Leng X-H, Bjorbaek C**. Leptin-Dependent Control of Glucose Balance and Locomotor Activity by POMC Neurons. *Cell Metabolism.* 2009;9(6):537-547.
98. **van de Wall E, Leshan R, Xu AW, Balthasar N, Coppari R, Liu SM, Jo YH, MacKenzie RG, Allison DB, Dun NJ, Elmquist J, Lowell BB, Barsh GS, de Luca C, Myers MG, Schwartz GJ, Chua SC**. Collective and individual functions of leptin receptor modulated neurons controlling metabolism and ingestion. *Endocrinology.* 2008;149(4):1773-1785.
99. **Mesaros A, Koralov SB, Rother E, Wunderlich FT, Ernst MB, Barsh GS, Rajewsky K, Bruening JC**. Activation of stat3 signaling in AgRP neurons promotes locomotor activity. *Cell Metabolism.* 2008;7(3):236-248.
100. **Lin HV, Plum L, Ono H, Gutierrez-Juarez R, Shanabrough M, Borok E, Horvath TL, Rossetti L, Accili D**. Divergent Regulation of Energy Expenditure and Hepatic Glucose Production by Insulin Receptor in Agouti-Related Protein and POMC Neurons. *Diabetes.* 2010;59(2):337-346.

101. **de Visser L, van den Bos R, Spruijt BM**. Automated home cage observations as a tool to measure the effects of wheel running on cage floor locomotion. *Behavioural Brain Research.* 2005;160(2):382-388.
102. **Meijer JH, Robbers Y**. Wheel running in the wild. *Proceedings of the Royal Society B-Biological Sciences.* 2014;281(1786).
103. **Knab AM, Lightfoot JT**. Does the difference between physically active and couch potato lie in the dopamine system? *International Journal of Biological Sciences.* 2010;6(2):133-150.
104. **Lippert RN, Ellacott KLJ, Cone RD**. Gender-Specific Roles for the Melanocortin-3 Receptor in the Regulation of the Mesolimbic Dopamine System in Mice. *Endocrinology.* 2014;155(5):1718-1727.
105. **Pandit R, van der Zwaal EM, Luijendijk MCM, Brans MAD, van Rozen AJ, Oude Ophuis RJA, Vanderschuren LJMJ, Adan RAH, la Fleur SE**. Central melanocortins regulate the motivation for sucrose reward. *PloS one.* 2015;10(3):e0121768-e0121768.
106. **Richard CD, Tolle V, Low MJ**. Meal pattern analysis in neural-specific proopiomelanocortin-deficient mice. *European Journal of Pharmacology.* 2011;660(1):131-138.
107. **Butler AA, Marks DL, Fan W, Kuhn CM, Bartolome M, Cone RD**. Melanocortin-4 receptor is required for acute homeostatic responses to increased dietary fat. *Nature Neuroscience.* 2001;4(6):605-611.
108. **Irani BG, Xiang Z, Moore MC, Mandel RJ, Haskell-Luevano C**. Voluntary exercise delays monogenetic obesity and overcomes reproductive dysfunction of the melanocortin-4 receptor knockout mouse. *Biochemical and Biophysical Research Communications.* 2005;326(3):638-644.
109. **Haskell-Luevano C, Schaub JW, Andreasen A, Haskell KR, Moore MC, Koerper LM, Rouzaud F, Baker HV, Millard WJ, Walter G, Litherland SA, Xiang ZM**. Voluntary exercise prevents the obese and diabetic metabolic syndrome of the melanocortin-4 receptor knockout mouse. *Faseb Journal.* 2009;23(2):642-655.
110. **Zhang Y, Rodrigues E, Li G, Gao Y, King M, Carter CS, Tumer N, Cheng K-Y, Scarpace PJ**. Simultaneous POMC gene transfer to hypothalamus and brainstem increases physical activity, lipolysis and reduces adult-onset obesity. *European Journal of Neuroscience.* 2011;33(8):1541-1550.
111. **Stephan FK**. The "other" circadian system: Food as a zeitgeber. *Journal of Biological Rhythms.* 2002;17(4):284-292.
112. **Patton DF, Mistlberger RE**. Circadian adaptations to meal timing: neuroendocrine mechanisms. *Frontiers in Neuroscience.* 2013;7.
113. **Begriche K, Marston OJ, Rossi J, Burke LK, McDonald P, Heisler LK, Butler AA**. Melanocortin-3 receptors are involved in adaptation to restricted feeding. *Genes Brain and Behavior.* 2012;11(3):291-302.
114. **Smith SM, Vale WW**. The role of the hypothalamic-pituitary-adrenal axis in neuroendocrine responses to stress. *Dialogues in clinical neuroscience.* 2006;8(4):383-395.
115. **Gold PW, Chrousos GP**. Organization of the stress system and its dysregulation in melancholic and atypical depression: high vs low CRH/NE states. *Molecular Psychiatry.* 2002;7(3):254-275.

116. **Chan O, Inouye K, Riddell MC, Vranic M, Matthews SG**. Diabetes and the hypothalamo-pituitary-adrenal (HPA) axis. *Minerva Endocrinologica.* 2003;28(2):87-102.
117. **de Kloet ER, Joels M, Holsboer F**. Stress and the brain: From adaptation to disease. *Nature Reviews Neuroscience.* 2005;6(6):463-475.
118. **Ulrich-Lai YM, Herman JP**. Neural regulation of endocrine and autonomic stress responses. *Nature Reviews Neuroscience.* 2009;10(6):397-409.
119. **Joels M, Baram TZ**. The neuro-symphony of stress. *Nature Reviews Neuroscience.* 2009;10(6):459-U484.
120. **Bazhan N, Zelena D**. Food-intake regulation during stress by the hypothalamo-pituitary-adrenal axis. *Brain Research Bulletin.* 2013;95:46-53.
121. **la Fleur SE**. The effects of glucocorticoids on feeding behavior in rats. *Physiology & Behavior.* 2006;89(1):110-114.
122. **Ohata H, Shibasaki T**. Involvement of CRF2 receptor in the brain regions in restraint-induced anorexia. *Neuroreport.* 2011;22(10):494-498.
123. **Liu J, Garza JC, Truong HV, Henschel J, Zhang W, Lu X-Y**. The melanocortinergic pathway is rapidly recruited by emotional stress and contributes to stress-induced anorexia and anxiety-like behavior. *Endocrinology.* 2007;148(11):5531-5540.
124. **Yamano Y, Yoshioka M, Toda Y, Oshida Y, Chaki S, Hamamoto K, Morishima I**. Regulation of CRF, POMC and MC4R gene expression after electrical foot shock stress in the rat amygdala and hypothalamus. *Journal of Veterinary Medical Science.* 2004;66(11):1323-1327.
125. **Wachira SJ, Hughes-Darden CA, Nicholas HB, Taylor CV, Robinson TJ**. Neural melanocortin receptors are differentlally expressed and regulated by stress in rat hypothalamic-pituitary-adrenal axis. *Cellular and Molecular Biology.* 2004;50(6):703-713.
126. **Vergoni AV, Bertolini A, Wikberg JES, Schioth HB**. Selective melanocortin MC4 receptor blockage reduces immobilization stress-induced anorexia in rats. *European Journal of Pharmacology.* 1999;369(1):11-15.
127. **Chaki S, Ogawa S, Toda Y, Funakoshi T, Okuyama S**. Involvement of the melanocortin MC4 receptor in stress-related behavior in rodents. *European Journal of Pharmacology.* 2003;474(1):95-101.
128. **Liu J, Garza JC, Li W, Lu XY**. Melanocortin-4 receptor in the medial amygdala regulates emotional stress-induced anxiety-like behaviour, anorexia and corticosterone secretion. *International Journal of Neuropsychopharmacology.* 2013;16(1):105-120.
129. **Chen PL, Vaughan J, Donaldson C, Vale W, Li C**. Injection of Urocortin 3 into the ventromedial hypothalamus modulates feeding, blood glucose levels, and hypothalamic POMC gene expression but not the HPA axis. *American Journal of Physiology-Endocrinology and Metabolism.* 2010;298(2):E337-E345.
130. **De Souza J, Butler AA, Cone RD**. Disproportionate inhibition of feeding in A(y) mice by certain stressors: A cautionary note. *Neuroendocrinology.* 2000;72(2):126-132.
131. **Green PK, Wilkinson CW, Woods SC**. Intraventricular corticosterone increases the rate of body weight gain in underweight adrenalectomized rats. *Endocrinology.* 1992;130(1):269-275.

132. **Zakrzewska KE, Cusin I, Stricker-Krongrad A, Boss O, Ricquier D, Jeanrenaud B, Rohner-Jeanrenaud F**. Induction of obesity and hyperleptinemia by central glucocorticoid infusion in the rat. *Diabetes.* 1999;48(2):365-370.
133. **Bray GA, York DA**. Hypothalamic and genetic obesity in experimental animals: Autonomic and endocrine hypothesis. *Physiological Reviews.* 1979;59(3):719-809.
134. **Zhang YY, Proenca R, Maffei M, Barone M, Leopold L, Friedman JM**. Positional cloning of the mouse obese gene and its human homolog. *Nature.* 1994;372(6505):425-432.
135. **Naeser P**. Function of adrenal cortex in obese-hyperglycemic mice (Gene symbol Ob). *Diabetologia.* 1974;10(5):449-453.
136. **Edwardson JA, Hough CAM**. Pituitary-adrenal system of genetically obese (ob/ob) mouse. *Journal of Endocrinology.* 1975;65(1):99-107.
137. **McGinnis R, Walker J, Margules D, Aird F, Redei E**. Dysregulation of the hypothalamus-pituitary-adrenal axis in male and female, genetically obese (ob/ob) mice. *Journal of Neuroendocrinology.* 1992;4(6):765-771.
138. **Makimura H, Mizuno TM, Roberts J, Silverstein J, Beasley J, Mobbs CV**. Adrenalectomy reverses obese phenotype and restores hypothalamic melanocortin tone in leptin-deficient ob/ob mice. *Diabetes.* 2000;49(11):1917-1923.
139. **Solomon J, Mayer J**. Effect of adrenalectomy on development of obese hyperglycemic syndrome in ob/ob mice. *Endocrinology.* 1973;93(2):510-513.
140. **Debons AF, Zurek LD, Tse CS, Abrahamsen S**. Central nervous system control of hyperphagia in hypothalamic obesity: Dependence on adrenal glucocorticoids. *Endocrinology.* 1986;118(4):1678-1681.
141. **Sainsbury A, Cusin I, RohnerJeanrenaud F, Jeanrenaud B**. Adrenalectomy prevents the obesity syndrome produced by chronic central neuropeptide Y infusion in normal rats. *Diabetes.* 1997;46(2):209-214.
142. **Nakayama S, Nishiyama M, Iwasaki Y, Shinahara M, Okada Y, Tsuda M, Okazaki M, Tsugita M, Taguchi T, Makino S, Stenzel-Poore MP, Hashimoto K, Terada Y**. Corticotropin-releasing hormone (CRH) transgenic mice display hyperphagia with increased Agouti-related protein mRNA in the hypothalamic arcuate nucleus. *Endocrine Journal.* 2011;58(4):279-286.
143. **Savontaus E, Conwell IM, Wardlaw SL**. Effects of adrenalectomy on AGRP, POMC, NPY and CART gene expression in the basal hypothalamus of fed and fasted rats. *Brain Research.* 2002;958(1):130-138.
144. **Lu XY, Shieh KR, Kabbaj M, Barsh GS, Akil H, Watson SJ**. Diurnal rhythm of agouti-related protein and its relation to corticosterone and food intake. *Endocrinology.* 2002;143(10):3905-3915.
145. **Coll AP, Challis BG, Lopez M, Piper S, Yeo GSH, O'Rahilly S**. Proopiomelanocortin-deficient mice are hypersensitive to the adverse metabolic effects of glucocorticoids. *Diabetes.* 2005;54(8):2269-2276.
146. **Uchoa ET, Silva LECM, de Castro M, Antunes-Rodrigues J, Elias LLK**. Glucocorticoids are required for meal-induced changes in the expression of hypothalamic neuropeptides. *Neuropeptides.* 2012;46(3):119-124.
147. **Gyengesi E, Liu ZW, D'Agostino G, Gan GL, Horvath TL, Gao XB, Diano S**. Corticosterone Regulates Synaptic Input Organization of POMC and NPY/AgRP Neurons in Adult Mice. *Endocrinology.* 2010;151(11):5395-5402.

148. **Tong Y, Couet J, Simard J, Pelletier G**. Glucocorticoid regulation of proopiomelanocortin mRNA levels in rat arcuate nucleus. *Molecular and Cellular Neuroscience.* 1990;1(1):78-83.
149. **Pelletier G**. Regulation of proopiomelanocortin gene expression in rat brain and pituitary as studied by in situ hybridization. *Annals of the New York Academy of Sciences.* 1993;680:246-259.
150. **Wardlaw SL, McCarthy KC, Conwell IM**. Glucocorticoid regulation of hypothalamic proopiomelanocortin. *Neuroendocrinology.* 1998;67(1):51-57.
151. **Birnberg NC, Lissitzky JC, Hinman M, Herbert E**. Glucocorticoids regulate proopiomelanocortin gene expression in vivo at the levels of transcription and secretion. *Proceedings of the National Academy of Sciences of the United States of America-Biological Sciences.* 1983;80(22):6982-6986.
152. **Bray GA, York DA**. Genetically transmitted obesity in rodents. *Physiological Reviews.* 1971;51(3):598-&.
153. **la Fleur SE, Akana SF, Manalo SL, Dallman MF**. Interaction between corticosterone and insulin in obesity: Regulation of lard intake and fat stores. *Endocrinology.* 2004;145(5):2174-2185.
154. **King BM, Smith RL**. Hypothalamic obesity after hypophysectomy or adrenalectomy - dependence on corticosterone. *American Journal of Physiology.* 1985;249(5):R522-R526.
155. **Cintra A, Bortolotti F**. Presence of strong glucocorticoid receptor immunoreactivity within hypothalamic and hypohyseal cells containing proopiomelanocortic peptides. *Brain Research.* 1992;577(1):127-133.
156. **Lee B, Kim SG, Kim J, Choi KY, Lee S, Lee SK, Lee JW**. Brain-Specific Homeobox Factor as a Target Selector for Glucocorticoid Receptor in Energy Balance. *Molecular and Cellular Biology.* 2013;33(14):2650-2658.
157. **Nieuwenhuizen AG, Rutters F**. The hypothalamic-pituitary-adrenal-axis in the regulation of energy balance. *Physiology & Behavior.* 2008;94(2):169-177.
158. **Olney JW**. Brain lesions, obesity, and other disturbances in mice treated with monosodium glutamate. *Science.* 1969;164(3880):719-&.
159. **Spinedi E, Johnston C, Negrovilar A**. Increased responsiveness of the hypothalamic-pituitary axis after neurotoxin-induced hypothalamic denervation. *Endocrinology.* 1984;115(1):267-272.
160. **Magarinos AM, Estivariz F, Morado MI, Denicola AF**. Regulation of the central nervous system pituitary adrenal axis in rats after neonatal treatment with monosodium glutamate. *Neuroendocrinology.* 1988;48(2):105-111.
161. **Motta M, Mangili G, Martini L**. A short feedback loop in control of ACTH secretion. *Endocrinology.* 1965;77(2):392-&.
162. **Suda T, Yajima F, Tomori N, Sumitomo T, Nakagami Y, Ushiyama T, Demura H, Shizume K**. Inhibitory effect of adrenocorticotropin on corticotropin-releasing factor release from rat hypothalamus in vitro. *Endocrinology.* 1986;118(1):459-461.
163. **Calogero AE, Gallucci WT, Gold PW, Chrousos GP**. Multiple feedback regulatory loops upon rat hypothalamic corticotropin-releasing hormone secretion: Potential clinical implications. *Journal of Clinical Investigation.* 1988;82(3):767-774.
164. **Papadopoulos AD, Wardlaw SL**. Endogenous alpha-MSH modulates the hypothalamic-pituitary-adrenal response to the cytokine interleukin-1 beta. *Journal of Neuroendocrinology.* 1999;11(4):315-319.

165. **Cragnolini AB, Perello M, Schioth HB, Scimonelli TN**. alpha-MSH and gamma-MSH inhibit IL-1 beta induced activation of the hypothalamic-pituitary-adrenal axis through central melanocortin receptors. *Regulatory Peptides.* 2004;122(3):185-190.
166. **Meek TH, Matsen ME, Damian V, Cubelo A, Chua SC, Jr., Morton GJ**. Role of Melanocortin Signaling in Neuroendocrine and Metabolic Actions of Leptin in Male Rats With Uncontrolled Diabetes. *Endocrinology.* 2014;155(11):4157-4167.
167. **Wiegant VM, Jolles J, Colbern DL, Zimmermann E, Gispen WH**. Intracerebroventricular ACTH activates the pituitary-adrenal system: Dissociation from a behavioral response. *Life Sciences.* 1979;25(21):1791-1796.
168. **Ludwig DS, Mountjoy KG, Tatro JB, Gillette JA, Frederich RC, Flier JS, Maratos-Flier E**. Melanin-concentrating hormone: a functional melanocortin antagonist in the hypothalamus. *American Journal of Physiology-Endocrinology and Metabolism.* 1998;274(4):E627-E633.
169. **Von Frijtag JC, Croiset G, Gispen WH, Adan RAH, Wiegant VM**. The role of central melanocortin receptors in the activation of the hypothalamus-pituitary-adrenal-axis and the induction of excessive grooming. *British Journal of Pharmacology.* 1998;123(8):1503-1508.
170. **Lu XY, Barsh GS, Akil H, Watson SJ**. Interaction between alpha-melanocyte-stimulating hormone and corticotropin-releasing hormone in the regulation of feeding and hypothalamo-pituitary-adrenal responses. *Journal of Neuroscience.* 2003;23(21):7863-7872.
171. **Kas MJH, Bruijnzeel AW, Haanstra JR, Wiegant VM, Adan RAH**. Differential regulation of agouti-related protein and neuropeptide Y in hypothalamic neurons following a stressful event. *Journal of Molecular Endocrinology.* 2005;35(1):159-164.
172. **Fekete C, Legradi G, Mihaly E, Tatro JB, Rand WM, Lechan RM**. alpha-melanocyte stimulating hormone prevents fasting-induced suppression of corticotropin-releasing hormone gene expression in the rat hypothalamic paraventricular nucleus. *Neuroscience Letters.* 2000;289(2):152-156.
173. **Serova LI, Laukova M, Alaluf LG, Sabban EL**. Blockage of melanocortin-4 receptors by intranasal HS014 attenuates single prolonged stress-triggered changes in several brain regions. *Journal of Neurochemistry.* 2014;131(6):825-835.
174. **Dhillo WS, Small CJ, Seal LJ, Kim MS, Stanley SA, Murphy KG, Ghatei MA, Bloom SR**. The hypothalamic melanocortin system stimulates the hypothalamo-pituitary-adrenal axis in vitro and in vivo in male rats. *Neuroendocrinology.* 2002;75(4):209-216.
175. **Miyabo S, Yamamura I, Ooya E, Aoyagi N, Horikawa Y, Hayashi S**. Effects of neonatal treatment with monosodium glutamate on circadian locomotor rhythm in the rat. *Brain Research.* 1985;339(2):201-208.
176. **Dutia R, Kim AJ, Mosharov E, SavontausC E, Chua SC, Wardlaw SL**. Regulation of prolactin in mice with altered hypothalamic melanocortin activity. *Peptides.* 2012;37(1):6-12.
177. **Ryan KK, Mul JD, Clemmensen C, Egan AE, Begg DP, Halcomb K, Seeley RJ, Herman JP, Ulrich-Lai YM**. Loss of melanocortin-4 receptor function attenuates HPA responses to psychological stress. *Psychoneuroendocrinology.* 2014;42:98-105.
178. **Lee M, Kim A, Chua SC, Obici S, Wardlaw SL**. Transgenic MSH overexpression attenuates the metabolic effects of a high-fat diet. *American Journal of Physiology-Endocrinology and Metabolism.* 2007;293(1):E121-E131.

179. **Karpac J, Ostwald D, Bui S, Hunnewell P, Shankar M, Hochgeschwender U**. Development, maintenance, and function of the adrenal gland in early postnatal proopiomelanocortin-null mutant mice. *Endocrinology.* 2005;146(6):2555-2562.
180. **Greenman Y, Kuperman Y, Drori Y, Asa SL, Navon I, Forkosh O, Gil S, Stern N, Chen A**. Postnatal Ablation of POMC Neurons Induces an Obese Phenotype Characterized by Decreased Food Intake and Enhanced Anxiety-Like Behavior. *Molecular Endocrinology.* 2013;27(7):1091-1102.
181. **Smart JL, Tolle V, Low MJ**. Glucocorticoids exacerbate obesity and insulin resistance in neuron-specific proopiomelanocortin-deficient mice. *Journal of Clinical Investigation.* 2006;116(2):495-505.
182. **Smart JL, Tolle V, Otero-Corchon V, Low MJ**. Central dysregulation of the hypothalamic-pituitary-adrenal axis in neuron-specific proopiomelanocortin-deficient mice. *Endocrinology.* 2007;148(2):647-659.
183. **Przewlocki R**. Stress, Opioid Peptides, and Their Receptors. *Hormones, Brain and Behavior, Vols 1-5, 2nd Edition.* 2009:289-331.
184. **Rubinstein M, Mogil JS, Japon M, Chan EC, Allen RG, Low MJ**. Absence of opioid stress-induced analgesia in mice lacking beta-endorphin by site-directed mutagenesis. *Proceedings of the National Academy of Sciences of the United States of America.* 1996;93(9):3995-4000.
185. **de Souza FSJ, Santangelo AM, Bumaschny V, Avale ME, Smart JL, Low MJ, Rubinstein M**. Identification of neuronal enhancers of the proopiomelanocortin gene by transgenic mouse analysis and phylogenetic footprinting. *Molecular and Cellular Biology.* 2005;25(8):3076-3086.
186. **Lam DD, de Souza FJS, Nasif S, Yamashita M, Lopez-Leal R, Otero-Corchon V, Meece K, Sampath H, Mercer AJ, Wardlaw SL, Rubinstein M, Low MJ**. Partially redundant enhancers cooperatively maintain mammalian Pomc expression above a critical functional threshold. *PLoS Genetics.* 2015;11(2).
187. **Rozen S, Skaletsky HJ**. Primer3. Code available at http://www-genome.wi.mit.edu/genome_software/other/primer3.html. 1998.
188. **Franklin KB, Paxinos G**. *The Mouse Brain in Stereotaxic Coordinates, Compact.* 3rd ed. Philadelphia, PA: Elsevier; 2008.
189. **van de Wall E, Leshan R, Xu AW, Balthasar N, Coppari R, Liu SM, Jo YH, MacKenzie RG, Allison DB, Dun NJ, Elmquist J, Lowell BB, Barsh GS, de Luca C, Myers MG, Jr., Schwartz GJ, Chua SC, Jr.** Collective and individual functions of leptin receptor modulated neurons controlling metabolism and ingestion. *Endocrinology.* 2008;149(4):1773-1785.
190. **Ernst MB, Wunderlich CM, Hess S, Paehler M, Mesaros A, Koralov SB, Kleinridders A, Husch A, Muenzberg H, Hampel B, Alber J, Kloppenburg P, Bruening JC, Wunderlich FT**. Enhanced Stat3 Activation in POMC Neurons Provokes Negative Feedback Inhibition of Leptin and Insulin Signaling in Obesity. *Journal of Neuroscience.* 2009;29(37):11582-11593.
191. **Mayer J**. Decreased activity and energy balance in the hereditary obesity-diabetes syndrome of mice. *Science.* 1953;117(3045):504-505.
192. **Colt EWD, Wardlaw SL, Frantz AG**. The effect of running on plastma beta-endorphin. *Life Sciences.* 1981;28(14):1637-1640.

193. **Carr DB, Bullen BA, Skrinar GS, Arnold MA, Rosenblatt M, Beitins IZ, Martin JB, McArthur JW**. Physical conditioning facilitates the exercise-induced secretion of beta-endorphin and beta-lipotropin in women. *New England Journal of Medicine.* 1981;305(10):560-563.
194. **Hoffmann P, Terenius L, Thoren P**. Cerebrospinal fluid immunoreactive beta-endorphin concentration is increased by voluntary exercise in the spontaneously hypertensive rat. *Regulatory Peptides.* 1990;28(2):233-239.
195. **Koehl M, Meerlo P, Gonzales D, Rontal A, Turek FW, Abrous DN**. Exercise-induced promotion of hippocampal cell proliferation requires beta-endorphin. *Faseb Journal.* 2008;22(7):2253-2262.
196. **Li G, Rhodes JS, Girard I, Gammie SC, Garland T**. Opioid-mediated pain sensitivity in mice bred for high voluntary wheel running. *Physiology & Behavior.* 2004;83(3):515-524.
197. **Vargas-Perez H, Sellings LHL, Peredes RG, Prado-Alcala RA, Diaz J-L**. Reinforcement of Wheel Running in Balb/c Mice: Role of Motor Activity and Endogenous Opioids. *Journal of Motor Behavior.* 2008;40(6):587-593.
198. **Lightfoot JT**. Sex hormones' regulation of rodent physical activity: A review. *International Journal of Biological Sciences.* 2008;4(3):126-132.
199. **Ogawa S, Chan J, Gustafsson JA, Korach KS, Pfaff DW**. Estrogen increases locomotor activity in mice through estrogen receptor alpha: Specificity for the type of activity. *Endocrinology.* 2003;144(1):230-239.
200. **Li Z, Wang Y, Sun KK, Wang K, Sun ZS, Zhao M, Wang J**. Sex-related difference in food-anticipatory activity of mice. *Hormones and Behavior.* 2015;70:38-46.
201. **Chowen JA, Argente J, Vician L, Clifton DK, Steiner RA**. Proopiomelanocortin messenger RNA in hypothalamic neurons is increased by testosterone through aromatization to estradiol. *Neuroendocrinology.* 1990;52(6):581-588.
202. **Raffin-Sanson ML, de Keyzer Y, Bertagna X**. Proopiomelanocortin, a polypeptide precursor with multiple functions: from physiology to pathological conditions. *European Journal of Endocrinology.* 2003;149(2):79-90.
203. **Tanoue A, Ito S, Honda K, Oshikawa S, Kitagawa Y, Koshimizu T, Mori T, Tsujimoto G**. The vasopressin V1b receptor critically regulates hypothalamic-pituitary-adrenal aids activity under both stress and resting conditions. *Journal of Clinical Investigation.* 2004;113(2):302-309.
204. **Schneider CA, Rasband WS, Eliceiri KW**. NIH Image to ImageJ: 25 years of image analysis. *Nature Methods.* 2012;9(7):671-675.
205. Franklin KB, Paxinos G. *The Mouse Brain in Stereotaxic Coordinates.* 3rd ed. Amsterdam: Elsevier Academic Press; 2008.
206. **Seasholtz AF, Bourbonais FJ, Harnden CE, Camper SA**. Nucleotide sequence and expression of the mouse corticotropin-releasing hormone gene. *Molecular and Cellular Neuroscience.* 1991;2(3):266-273.
207. **Burrows HL, Nakajima M, Lesh JS, Goosens KA, Samuelson LC, Inui A, Camper SA, Seasholtz AF**. Excess corticotropin releasing hormone-binding protein in the hypothalamic-pituitary-adrenal axis in transgenic mice. *Journal of Clinical Investigation.* 1998;101(7):1439-1447.

208. **Kesterson RA, Huszar D, Lynch CA, Simerly RB, Cone RD**. Induction of neuropeptide Y gene expression in the dorsal medial hypothalamic nucleus in two models of the Agouti obesity syndrome. *Molecular Endocrinology.* 1997;11(5):630-637.
209. Levine S. The ontogeny of the hypothalamic-pituitary-adrenal axis - The influence of maternal factors. In: de Kloet ER, Azmitia EC, Landfield PW, eds. *Brain Corticosteroid Receptors: Studies on the Mechanism, Function, and Neurotoxicity of Corticosteroid Action.* Vol 7461994:275-288.
210. **Schmidt M, Oitzl MS, Levine S, de Kloet ER**. The HPA system during the postnatal development of CD1 mice and the effects of maternal deprivation. *Developmental Brain Research.* 2002;139(1):39-49.
211. **Goel N, Workman JL, Lee TT, Innala L, Viau V**. Sex Differences in the HPA Axis. *Comprehensive Physiology.* 2014;4(3):1121-1155.
212. **Panagiotakopoulos L, Neigh GN**. Development of the HPA axis: Where and when do sex differences manifest? *Frontiers in Neuroendocrinology.* 2014;35(3):285-302.
213. **Seale JV, Wood SA, Atkinson HC, Lightman SL, Harbuz MS**. Organizational role for testosterone and estrogen on adult hypothalamic-pituitary-adrenal axis activity in the male rat. *Endocrinology.* 2005;146(4):1973-1982.
214. **Bielohuby M, Herbach N, Wanke R, Maser-Gluth C, Beuschlein F, Wolf E, Hoeflich A**. Growth analysis of the mouse adrenal gland from weaning to adulthood: time- and gender-dependent alterations of cell size and number in the cortical compartment. *American Journal of Physiology-Endocrinology and Metabolism.* 2007;293(1):E139-E146.
215. **Seale JV, Wood SA, Atkinson HC, Bate E, Lightman SL, Ingram CD, Jessop DS, Harbuz MS**. Gonadectomy reverses the sexually diergic patterns of circadian and stress-induced hypothalamic-pituitary-adrenal axis activity in male and female rats. *Journal of Neuroendocrinology.* 2004;16(6):516-524.
216. **Juntti SA, Tollkuhn J, Wu MV, Fraser EJ, Soderborg T, Tan S, Honda S-i, Harada N, Shah NM**. The Androgen Receptor Governs the Execution, but Not Programming, of Male Sexual and Territorial Behaviors. *Neuron.* 2010;66(2):260-272.
217. **Chowen-Breed JA, Clifton DK, Steiner RA**. Regional specificity of testosterone regulation of proopiomelanocortin gene expression in the arcuate nucleus of the male rat brain. *Endocrinology.* 1989;124(6):2875-2881.
218. **Chaki S, Okubo T**. Melanocortin-4 receptor antagonists for the treatment of depression and anxiety disorders. *Current Topics in Medicinal Chemistry.* 2007;7(11):1145-1151.
219. **Rakieten N, Rakieten ML, Nadkarni MV**. Studies on the diabetogenic action of streptozotocin (NSC-37917). *Cancer Chemotherapy Reports.* 1963(29):91-98.
220. **De Nicola AF, Fridman O, Delcastillo EJ, Foglia VG**. Abnormal regulation of adrenal function in rats with streptozotocin diabetes. *Hormone and Metabolic Research.* 1977;9(6):469-473.
221. **Tornello S, Coirini H, De Nicola AF**. Effects of experimental diabetes on the concentration of corticosterone in central nervous system, serum and adrenal glands. *Journal of Steroid Biochemistry and Molecular Biology.* 1981;14(12):1279-1284.
222. **Chan O, Chan S, Inouye K, Vranic M, Matthews SG**. Molecular regulation of the hypothalamo-pituitary-adrenal axis in streptozotocin-induced diabetes: Effects of insulin treatment. *Endocrinology.* 2001;142(11):4872-4879.

223. **Chan O, Inouye K, Vranic M, Matthews SG**. Hyperactivation of the hypothalamo-pituitary-adrenocortical axis in streptozotocin-diabetes is associated with reduced stress responsiveness and decreased pituitary and adrenal sensitivity. *Endocrinology.* 2002;143(5):1761-1768.
224. **Scribner KA, Walker CD, Cascio CS, Dallman MF**. Chronic streptozotocin diabetes in rats facilitates the acute stress response without altering pituitary or adrenal responsiveness to secretagogues. *Endocrinology.* 1991;129(1):99-108.
225. **Marshall NB, Andrus SB, Mayer J**. Organ weights in 3 forms of experimental obesity in the mouse. *American Journal of Physiology.* 1957;189(2):343-346.
226. **Hellerstrom C, Hellman B, Larsson S**. Some aspects of structure and histochemistry of adrenals in obese-hyperglycemic mice. *Acta Pathologica Et Microbiologica Scandinavica.* 1962;54(4):365-&.
227. **Naeser P**. Structure of adrenal glands in mice with obese-hyperglycemic syndrome (Gene symbol Ob). *Acta Pathologica Et Microbiologica Scandinavica Section a-Pathology.* 1975;A 83(1):120-126.
228. **Garthwaite TL, Martinson DR, Tseng LF, Hagen TC, Menahan LA**. A longitudinal hormonal profile of the genetically obese mouse. *Endocrinology.* 1980;107(3):671-676.
229. **Huang QL, Rivest R, Richard D**. Effects of leptin on corticotropin-releasing factor (CRF) synthesis and CRF neuron activation in the paraventricular hypothalamic nucleus of obese (ob/ob) mice. *Endocrinology.* 1998;139(4):1524-1532.
230. **Stephens TW, Basinski M, Bristow PK, Buevalleskey JM, Burgett SG, Craft L, Hale J, Hoffmann J, Hsiung HM, Kriauciunas A, Mackellar W, Rosteck PR, Schoner B, Smith D, Tinsley FC, Zhang XY, Heiman M**. The role of neuropeptide y in the antiobesity action of the obese gene product. *Nature.* 1995;377(6549):530-532.
231. **Ahima RS, Prabakaran D, Mantzoros C, Qu DQ, Lowell B, MaratosFlier E, Flier JS**. Role of leptin in the neuroendocrine response to fasting. *Nature.* 1996;382(6588):250-252.
232. **Heiman ML, Ahima RS, Craft LS, Schoner B, Stephens TW, Flier JS**. Leptin inhibition of the hypothalamic-pituitary-adrenal axis in response to stress. *Endocrinology.* 1997;138(9):3859-3863.
233. **Chan O, Inouye K, Akirav EM, Park E, Riddell MC, Matthews SG, Vranic M**. Hyperglycemia does not increase basal hypothalamo-pituitary-adrenal activity in diabetes but it does impair the HPA response to insulin-induced hypoglycemia. *American Journal of Physiology-Regulatory Integrative and Comparative Physiology.* 2005;289(1):R235-R246.
234. **Koenner AC, Janoschek R, Plum L, Jordan SD, Rother E, Ma XS, Xu C, Enriori P, Hampel B, Barsh GS, Kahn CR, Cowley MA, Ashcroft FM, Bruning JC**. Insulin action in AgRP-expressing neurons is required for suppression of hepatic glucose production. *Cell Metabolism.* 2007;5(6):438-449.
235. **Hill JW, Elias CF, Fukuda M, Williams KW, Berglund ED, Holland WL, Cho YR, Chuang JC, Xu Y, Choi M, Lauzon D, Lee CE, Coppari R, Richardson JA, Zigman JM, Chua S, Scherer PE, Lowell BB, Bruning JC, Elmquist JK**. Direct Insulin and Leptin Action on Pro-opiomelanocortin Neurons Is Required for Normal Glucose Homeostasis and Fertility. *Cell Metabolism.* 2010;11(4):286-297.

236. **Chong ACN, Vogt MC, Hill AS, Bruening JC, Zeltser LM**. Central insulin signaling modulates hypothalamuc-pituitary-adrenal axis responsiveness. *Molecular Metabolism.* 2015;4:83-92.
237. **Schwartz MW, Seeley RJ, Campfield LA, Burn P, Baskin DG**. Identification of targets of leptin action in rat hypothalamus. *Journal of Clinical Investigation.* 1996;98(5):1101-1106.
238. **Krysiak R, Obuchowicz E, Herman ZS**. Interactions between the neuropeptide Y system and the hypothalamic-pituitary-adrenal axis. *European Journal of Endocrinology.* 1999;140(2):130-136.
239. **Schwartz MW, Sipols AJ, Marks JL, Sanacora G, White JD, Scheurink A, Kahn SE, Baskin DG, Woods SC, Figlewicz DP, Porte D**. Inhibition of hypothalamic neuropeptide Y gene expression by insulin. *Endocrinology.* 1992;130(6):3608-3616.
240. **Wilding JPH, Gilbey SG, Bailey CJ, Batt RAL, Williams G, Ghatei MA, Bloom SR**. Increased neuropeptide Y messenger ribonucleic acid (messenger RNA) and decreased neurotension messenger RNA in the hypothalamus of the obese (ob/ob) mouse. *Endocrinology.* 1993;132(5):1939-1944.
241. **Sahu A, Sninsky CA, Phelps CP, Dube MG, Kalra PS, Kalra SP**. Neuropeptide Y release from the paraventricular nucleus increases in association with hyperphagia in streptozotocin-induced diabetic rats. *Endocrinology.* 1992;131(6):2979-2985.
242. **Abe M, Saito M, Ikeda H, Shimazu T**. Increased neuropeptide Y content in the arcuato-paraventricular hypothalamic neuronal system in both insulin-dependent and non-insulin-dependent diabetic rats. *Brain Research.* 1991;539(2):223-227.
243. **Thornton JE, Cheung CC, Clifton DK, Steiner RA**. Regulation of hypothalamic proopiomelanocortin mRNA by leptin in ob/ob mice. *Endocrinology.* 1997;138(11):5063-5066.
244. **Kim EM, Grace MK, Welch CC, Billington CJ, Levine AS**. STZ-induced diabetes decreases and insulin normalizes POMC mRNA in arcuate nucleus and pituitary in rats. *American Journal of Physiology-Regulatory Integrative and Comparative Physiology.* 1999;276(5):R1320-R1326.
245. **Erickson JC, Clegg KE, Palmiter RD**. Sensitivity to leptin and susceptibility to seizures of mice lacking neuropeptide Y. *Nature.* 1996;381(6581):415-418.
246. **Erickson JC, Ahima RS, Hollopeter G, Flier JS, Palmiter RD**. Endocrine function of neuropeptide Y knockout mice. *Regulatory Peptides.* 1997;70(2-3):199-202.
247. **Sainsbury A, Schwarzer C, Couzens M, Herzog H**. Y2 receptor deletion attenuates the type 2 diabetic syndrome of ob/ob mice. *Diabetes.* 2002;51(12):3420-3427.
248. **Chowdrey HS, Larsen PJ, Harbuz MS, Jessop DS, Aguilera G, Eckland DJA, Lightman SL**. Evidence for arginine vasopressin as the primary activator of the HPA axis during adjuvant-induced arthritis. *British Journal of Pharmacology.* 1995;116(5):2417-2424.
249. **Zhou Y, Leri F, Cummins E, Hoeschele M, Kreek MJ**. Involvement of arginine vasopressin and VIb receptor in heroin withdrawal and heroin seeking precipitated by stress and by heroin. *Neuropsychopharmacology.* 2008;33(2):226-236.
250. **Serino R, Ueta Y, Tokunaga M, Hara Y, Nomura M, Kabashima N, Shibuya I, Hattori Y, Yamashita H**. Upregulation of hypothalamic nitric oxide synthase gene expression in streptozotocin-induced diabetic rats. *Diabetologia.* 1998;41(6):640-648.

251. **Duan J, Choi YH, Hartzell D, Della-Fera MA, Hamrick M, Baile CA**. Effects of subcutaneous leptin injections on hypothalamic gene profiles in lean and ob/ob mice. *Obesity.* 2007;15(11):2624-2633.
252. **Zelena D, Filaretova L, Mergl Z, Barna I, Toth ZE, Makara GB**. Hypothalamic paraventricular nucleus, but not vasopressin, participates in chronic hyperactivity of the HPA axis in diabetic rats. *American Journal of Physiology-Endocrinology and Metabolism.* 2006;290(2):E243-E250.
253. **Speert DB, McClennen SJ, Seasholtz AF**. Sexually dimorphic expression of corticotropin-releasing hormone-binding protein in the mouse pituitary. *Endocrinology.* 2002;143(12):4730-4741.
254. **van de Stolpe A, Slycke AJ, Reinders MO, Zomer AWM, Goodenough S, Behl C, Seasholtz AF, van der Saag PT**. Estrogen receptor (ER)-mediated transcriptional regulation of the human corticotropin-releasing hormone-binding protein promoter: Differential effects of ER alpha and ER beta. *Molecular Endocrinology.* 2004;18(12):2908-2923.
255. **Crestani CC, Alves FHF, Gomes FV, Resstel LBM, Correa FMA, Herman JP**. Mechanisms in the Bed Nucleus of the Stria Terminalis Involved in Control of Autonomic and Neuroendocrine Functions: A Review. *Current Neuropharmacology.* 2013;11(2):141-159.
256. **Opland DM, Leinninger GM, Myers MG**. Modulation of the mesolimbic dopamine system by leptin. *Brain Research.* 2010;1350:65-70.
257. **Geiger BM, Haburcak M, Avena NM, Moyer MC, Hoebel BG, Pothos EN**. Deficits of mesolimbic dopamine neurotransmission in rat dietary obesity. *Neuroscience.* 2009;159(4):1193-1199.
258. **Berridge KC, Ho CY, Richard JM, DiFeliceantonio AG**. The tempted brain eats: Pleasure and desire circuits in obesity and eating disorders. *Brain Research.* 2010;1350:43-64.
259. **Sturm M, Becker A, Schroeder A, Bilkei-Gorzo A, Zimmer A**. Effect of chronic corticosterone application on depression-like behavior in C57BL/6N and C57BL/6J mice. *Genes Brain and Behavior.* 2015;14(3):292-300.
260. **Karatsoreos IN, Bhagat SM, Bowles NP, Weil ZM, Pfaff DW, McEwen BS**. Endocrine and Physiological Changes in Response to Chronic Corticosterone: A Potential Model of the Metabolic Syndrome in Mouse. *Endocrinology.* 2010;151(5):2117-2127.